CHEMICAL ENGINEERING SCIENCE
GENIE CHIMIQUE

VOL. 11 1959 No. 1

The degree of mixing in continuous flow systems

TH. N. ZWIETERING
Staatsmijnen in Limburg, Centraal Laboratorium, Geleen, The Netherlands

(*Received* 1 *August* 1958)

Abstract—The concepts of DANCKWERTS about the degrees of mixing and segregation are extended to the case of a continuous flow system with an arbitrary but known residence time distribution. For this purpose a life-expectation distribution is defined in addition to the age distribution. Further, a condition of maximum mixedness (minimum segregation) is defined for such a system. This condition, and the condition of complete segregation introduced by DANCKWERTS, are two opposite extremes. When the system is a reactor in which a chemical reaction of an arbitrary order takes place, the conversion can be calculated for both cases; thus two limits are obtained between which the conversion must lie.

Résumé—Les concepts de DANCKWERTS relatifs aux degrés de mélange et de ségrégation, sont étendus au cas d'un système à écoulement continu avec une répartition de temps de séjour arbitrairement choisie, mais connue. Dans ce but une distribution de durée de vie probable est définie en plus d'une distribution d'âge. De plus l'auteur définit pour ce système, une condition de mélange maximum (ségrégation minimum). Cette condition est l'opposé extrême de la ségrégation complète introduite par DANCKWERTS. Quand le système est un réacteur dans lequel se produit une réaction chimique d'ordre arbitraire la conversion peut être calculée pour les deux cas. L'auteur obtient ainsi deux limites entre lesquelles se situe la conversion.

Zusammenfassung—Die Auffassung von DANCKWERTS über die Grade der Mischung und Entmischung wird auf den Fall eines kontinuierlich durchflossenen Systems mit beliebiger aber bekannter Verweilzeitverteilung ausgedehnt. Hierzu wird eine Verteilung der Lebenserwartung zusätzlich zu der Altersverteilung definiert. Weiterhin wird eine Bedingung für die maximale Mischung (minimale Entmischung) für ein derartiges System definiert. Diese Bedingung und die Bedingung vollständigen Entmischung, wie sie von DANCKWERTS eingeführt wurde, sind zwei entgegengesetzte Extreme. Wenn das System ein Reaktor ist, in dem eine chemische Reaktion von willkürlicher Ordnung stattfindet, so kann für beide Fälle der Umsatz berechnet werden. Man erhält so zwei Grenzen, zwischen denen der Umsatz leigen muss.

1. INTRODUCTION

A PROBLEM frequently encountered in the design of continuous reactors for homogeneous reactions is the computation of the conversion from kinetic data obtained in batch experiments. For a number of simple cases, e.g. an ideal piston flow reactor, an ideal mixer or a series of ideal mixers, computation is possible and straightforward. In many cases, however, the reactor cannot be considered to fall exactly into one of these idealized categories. Then it is necessary to know more about the mixing within the system. A great deal of information about the state of mixing of the system can be obtained from the residence time distribution, which can often be found experimentally. For first order reactions knowledge of the residence time distribution suffices to compute the conversion, but with reactions of an order different from one, the residence time distribution does not determine

the conversion unambiguously. DANCKWERTS [1] elucidates the effect of the state of mixing on the average rate of reaction for a second order reaction. He considers a "well-stirred" tank reactor in which the elements of fluid entering the reactor are uniformly dispersed through its volume in a time much less than the average residence time τ. In such a reactor the distribution of residence times is that of an ideal mixed system. He then assumes two limiting circumstances.

(a) The incoming fluid is broken up into discrete fragments or streaks which are small compared to the tank and are uniformly dispersed through it, whereas the molecules of the fragments, which have entered together, remain together indefinitely. This is described by saying that the fluid remains completely segregated.

(b) The inflowing material is dispersed on the molecular scale in a time much less than τ; the environment of any particular molecule does not tend to contain an excess of molecules which entered at the same time as that molecule and the mixture is chemically uniform.

The reactor output can be calculated for both cases, and the results show that the average rate of reaction of a second order reaction is greater when the fluid remains segregated.

In general, mixing on the molecular scale between portions of reactant mixture which have been in the reactor for different lengths of time will render the output of the reactor less than if the material were completely segregated when the order of reaction is greater than unity, and vice versa.

To describe the degree of mixing in a fluid, DANCKWERTS uses the concepts of "concentration at a point" and "age of the fluid at a point." These imply the concentration or the age averaged over a region small compared to the whole system, and even small compared to the scale of segregation, but large enough to contain many molecules.

If the age α of a molecule is defined as the time which has elapsed since the molecule entered the system, it is possible to calculate the variance of the ages of all the molecules in the system:

$$\text{var } \alpha = \overline{(\alpha - \bar{\alpha})^2}$$

in which $\bar{\alpha}$ is the mean age of all molecules which are at some particular moment in the system. The variance of the ages is the same as the mean square deviation of the ages of the molecules from the mean age.

When for each "point," (defined as outlined above) the mean age of the molecules at that point is given by α_p, the variance of this quantity can be used as a measure of the degree of segregation. This variance is:

$$\text{var } \alpha_p = \overline{(\alpha_p - \bar{\alpha})^2}$$

in which the upper bar indicates an average over all "points." In the former formula for var α, the upper bar indicates an average over all molecules.

Referring to the two cases outlined above, when in a well-stirred system the mixing is uniform on the molecular scale, the mean age of all molecules at each point is the same (and equal to the mean age of all molecules in the system) and the variance between the ages of all points is zero. When, on the other hand, the system is completely segregated, the variance in ages between the points in the system equals the variance in ages between the molecules.

Therefore, DANCKWERTS defines a quantity:

$$J = \text{var } \alpha_p / \text{var } \alpha = \overline{(\alpha_p - \bar{\alpha})^2} / \overline{(\alpha - \bar{\alpha})^2}$$

which he calls the degree of segregation. For a system which has a residence time distribution which equals that of an ideal mixer, the value of J may lie between zero (mixing on the molecular scale) and one (completely segregated case).

For systems with some other residence time distribution the upper limit of J is again one, for the concept of complete segregation is then still applicable, but a value $J = 0$ is impossible because there must be a difference in ages at various points in the system. In this paper a condition of maximum mixedness, compatible with a given residence time distribution will be defined, which renders possible the computation

of a lower limit of J, and of the minimum conversion for a reaction of an order higher than one (and equally the maximum conversion for an order of reaction smaller than one).

2. The Simultaneity of the Mixing and the Chemical Reaction

In the first paragraph it has been pointed out that two continuous reactors which have identical residence time distributions, can have different degrees of chemical conversion, when the state of mixing in these two reactors is different. Another view on the problem is explained in this paragraph with the aid of a simple example. Consider two different reactors, both consisting of a long narrow tube and an ideally mixed vessel in series. The only difference between the two reactors is the order of these two parts: in reactor I the pipe reactor precedes the mixed vessel, in reactor II the order is inversed (Fig. 1). The common residence time distribution of both systems is plotted in Fig. 1a.

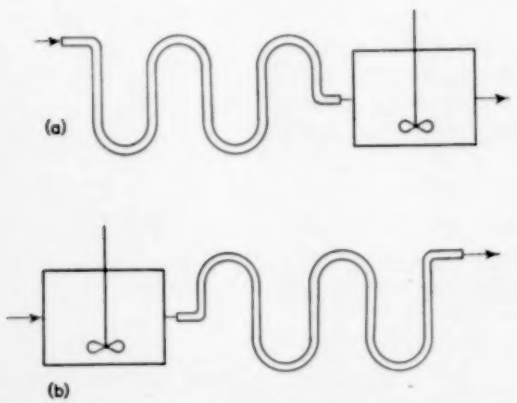

Fig. 1 (a, b). Pipe reactor and mixed tank reactor in series.

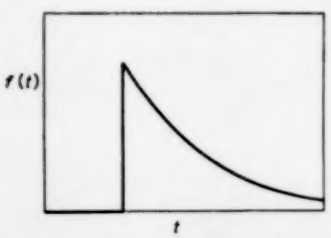

Fig. 1 (c). Total residence time distribution of pipe reactor and tank reactor in series.

It is easy to show that e.g. for a second order reaction the conversion in these two systems will be different, and that the conversion will be more complete in reactor I.

When the two systems are considered only as continuous mixing apparatus without chemical reaction (e.g. for diminishing concentration or temperature fluctuations in a steady flow of fluid) their effect will be exactly equal. The difficulty in the study of chemical reactors is that in general the mixing of the elements of the fluid occurs simultaneously with the chemical reaction. Now, although the overall mixing in both reactors I and II is, in a way, the same, this mixing occurs in reactor II in an early stage of the chemical reaction, whereas in reactor I the mixing is done at a later stage.

According to Danckwerts, reactor I has a higher degree of segregation than number II ($J_I > J_{II}$). From the considerations given above it can be seen that the difference may be expressed in another way, viz. that the mixing in reactor II is earlier than the mixing in No. I. Going back to the concept of a completely segregated system, it will be clear that such a system can be described by saying that the mixing of the fluid particles is as late as possible, i.e. at the exit of the reactor. In the following paragraphs the other extreme case will be described, which naturally must be a system in which the fluid is mixed as early as possible, where in both cases the residence time distributions are supposed to be identical. The last case is called the state of maximum mixedness. To describe these concepts in an exact way, some new quantities are defined in the next two paragraphs.

3. Residence Time Distribution and Age Distribution

Throughout this paper the residence time distribution of the steady flow system is supposed to be known. It is given by the function $F(t)$. The value of this function for a specified length of time equals the fraction of the molecules which remain shorter than a time t in the system. From this definition it is clear that $F(t)$ is monotonously non-decreasing and:

$$F(0) = 0 \qquad (1)$$

and

$$\lim_{t\to\infty} F(t) = 1 \qquad (2)$$

When $F(t)$ is differentiable, the function $f(t)$ is given by:

$$f(t) = dF(t)/dt \qquad (3)$$

The function $f(t)$ is called the residence time frequency function. From these functions one can calculate the mean residence time τ and the variance of the residence times, which are, by definition:

$$\tau = \int_0^\infty t dF \text{ or } \tau = \int_0^\infty t f(t)\, dt \qquad (4)$$

$$\text{and } \operatorname{var} t = \int_0^\infty (t-\tau)^2\, dF \text{ or}$$

$$\operatorname{var} t = \int_0^\infty (t-\tau)^2 f(t)\, dt \qquad (5)$$

The mean residence time is equal to the quotient of the volume of the system V and the volumetric flow velocity Q, which can be proved by the following reasoning.

Consider the contents of the system at time $\theta = 0$. The molecules which are then in the system have entered at some time before $\theta = 0$. Now, in the interval between $-t-\Delta t$ and $-t$ a quantity $Q\Delta t$ entered. Of this quantity a fraction $F(t)$ had a residence time shorter than t, and therefore has already left the system at the moment $\theta = 0$. So, the interval $-t-\Delta t$ to $-t$ contributes a volume $[1-F(t)]Q\,\Delta t$ to the contents of the system at the moment $\theta = 0$. Therefore, the total volume at this moment must be the sum of all these increments, or

$$V = \int_0^\infty [1-F(t)]Q dt \text{ or}$$

$$V = Q\int_0^\infty [1-F(t)]\, dt \qquad (6)$$

As this integral must be convergent, and $1-F(t)$ is monotonously non-increasing, it is easily proved that:

$$\lim_{t\to\infty} t\,[1-F(t)] = 0$$

By partial integration it is found from (6) that:

$$\frac{V}{Q} = \Big|\,[1-F(t)]\,t\,\Big|_0^\infty - \int_0^\infty t d\,[1-F(t)]$$

The first quantity to the right is zero for both limits, and therefore:

$$\frac{V}{Q} = \int_0^\infty t dF(t) \text{ and so } V/Q = \tau \qquad (7)$$

The condition for formula (7) to be true is only that the quantity entering the system, and the quantity leaving the system at any time interval Δt is exactly equal to $Q\Delta t$. It is not a necessary condition that there is only one entrance and only one exit.

The age α of a molecule which is in the system at a given moment is defined as the time which has elapsed since it entered. The distribution function of the ages, $\Phi(\alpha)$, is by definition the fraction of the molecules at a certain moment that have ages smaller than α. The age frequency function is denoted by $\phi(\alpha)$, which is equal to $d\Phi(\alpha)/d\alpha$.

The molecules which have, at time $\theta = 0$, an age between α and $\alpha+\Delta\alpha$ have necessarily entered in the time interval $-\alpha-\Delta\alpha$ to $-\alpha$. The total quantity that entered in this time interval was $Q\Delta\alpha$, but a fraction $F(\alpha)$ of these molecules have already left the system at $\theta = 0$ since this fraction has a residence time shorter than α. The quantity of molecules with an age between α and $\alpha+\Delta\alpha$ is therefore:

$$Q\Delta\alpha\,[1-F(\alpha)]$$

As the total quantity of molecules present is V, the fraction of the molecules which have ages between α and $\alpha+\Delta\alpha$ is:

$$(Q/V)\,[1-F(\alpha)]\,\Delta\alpha$$

Therefore the frequency function $\phi(\alpha)$ is found to be:

$$\phi(\alpha) = (1/\tau)\,[1-F(\alpha)] \qquad (8)$$

The age distribution function Φ is given by:

$$\Phi(\alpha) = \int_0^\alpha \phi(\alpha')\, d\alpha' \qquad (9)$$

VOL 11 1959

The formulas (8) and (9) show that the age distribution at a certain moment within the system is uniquely determined by the residence time distribution.

The mean age of the molecules is given by:

$$\bar{\alpha} = \int_0^\infty \alpha \, \phi(\alpha) \, d\alpha$$

from which it is easily found with the use of (8), (5) and (4) that:

$$\bar{\alpha} = (\overline{t^2}/2\tau) \text{ or } \bar{\alpha} = \tau/2 + (\text{var } t)/2\tau \qquad (10)$$

The variance of the ages is:

$$\text{var } \alpha = \int_0^\infty (\alpha - \bar{\alpha})^2 \, \phi(\alpha) \, d\alpha$$

and this leads to:

$$\text{var } \alpha = (\overline{t^3}/3\tau) - \left[(\overline{t^2})^2/4\tau^2\right] \qquad (11)$$

4. Life Expectation Distribution

In addition to the time which a molecule has spent already in the system, we can consider the time it will spend in the system from a specified time $\theta = 0$ until it will leave. This time is called the life expectation λ of the molecule. It must be noted that the word expectation is not used here in the statistical sense. It is the exact time which elapses between the moment $\theta = 0$ up to the moment at which the molecule which we consider will leave the system. When the residence time of a molecule is denoted by t, it follows that for each molecule:

$$t = \alpha + \lambda$$

The distribution of the life expectations of all the molecules in the system at a given moment is given by the function $\Psi(\lambda)$, which is the fraction of the molecules which are at time $\theta = 0$ in the system and will, reckoned from this moment, stay shorter than a time λ in the system. Equally, the life expectation frequency function is $\psi(\lambda) = d\Psi/d\lambda$.

The life expectation distribution is found in a manner which is exactly analogous to that of the ages.

In the interval between the times $\theta = \lambda$ and $\theta = \lambda + \Delta\lambda$ a quantity $Q\Delta\lambda$ leaves the system. A fraction $1 - F(\lambda)$ of these molecules were at time $\theta = 0$ already in the system, and therefore the quantity of molecules which had, at time $\theta = 0$, a life expectation between λ and $\lambda + \Delta\lambda$ was $Q\Delta\lambda\,[1 - F(\lambda)]$. The ratio of this quantity to the total quantity present, V, is:

$$\psi(\lambda) = (1/\tau)\,[1 - F(\lambda)] \qquad (12)$$

and

$$\Psi(\lambda) = \int_0^\lambda \psi(\lambda') \, d\lambda'$$

So the life expectation distribution has exactly the same form as the age distribution. Therefore the mean life expectation must be equal to the mean age (10):

$$\bar{\lambda} = \overline{t^2}/2\tau = \tau/2 + (\text{var } t)/2\tau \qquad (13)$$

and equally: $\text{var } \lambda = \text{var } \alpha \qquad (14)$

It must be mentioned here that the distributions of α and λ on the one hand and the distribution of the residence times on the other refer to different populations. For the first two the population consists of all the molecules which are in the system at an arbitrarily chosen moment. For the residence time distribution the population consists of the molecules entering the system in an arbitrary interval of time, or of the molecules leaving the system in an arbitrary time interval. The bar above a quantity, indicating an average over the population, must therefore be looked upon with care. As an example, for every molecule, the total residence time t must be equal to the sum of the age and the life expectation at the same moment:

$$t = \alpha + \lambda$$

By averaging over all molecules which are in the system at a given moment, it follows that:

$$\bar{t} = \bar{\alpha} + \bar{\lambda}$$

where $\bar{t}$ is the average residence time of all molecules in the system. From (10) and (13) one finds:

$$\bar{t} = \tau + (\text{var } t)/\tau$$

and therefore, in general $\bar{t} \neq \tau$

To evaluate τ, which is usually called the mean residence time, the averaging of t must not be done over all molecules present in the system, but over those that leave or enter.

5. DISTRIBUTIONS FOR A SPECIFIED POINT P

For the following considerations the fluid in the system is considered to be divided into small volume elements called "points," a concept introduced by DANCKWERTS [1]. The molecules within a point must be considered ideally mixed. Now we consider in each point at a given moment the age distribution of the molecules within this point, given by $\Phi_P(\alpha)$ and the distribution of the life expectations of these molecules $\Psi_P(\lambda)$. The corresponding frequency functions are the derivatives of these functions and are denoted $\phi_P(\alpha)$ and $\psi_P(\lambda)$. The point P is only defined at a specified moment. It does not keep its identity when time goes on. It can be divided into parts, or mixed up with others, or molecules can diffuse from it and to it. Therefore the molecules of point P can have very different life expectations.

From the definitions it follows that:

$$\phi(\alpha) = (1/V) \sum_{\substack{\text{all} \\ \text{points}}} \phi_P(\alpha)\, v_P$$

where v_P denotes the volume of point P. For convenience this can be written:

$$\phi(\alpha) = (1/V) \int_V \phi_P(\alpha) dv \qquad (15)$$

since the points are supposed to be very small compared to the total volume. In the same way:

$$\psi(\lambda) = (1/V) \cdot \int_V \psi_P(\lambda)\, dv \qquad (16)$$

Corresponding identities are valid for the distribution functions $\Phi(\alpha)$ and $\Psi(\lambda)$.

6. THE DEGREE OF MIXING OF THE CONTINUOUS FLOW SYSTEM

As outlined in the foregoing sections there is a spread between the ages of the molecules in the system. This spread can be characterized by the variance of the ages, which can be found from the residence time distribution with equation (11).

For each point P, the average age at a certain moment can be defined by:

$$\alpha_P = \int_0^\infty \alpha\, \phi_P(\alpha)\, d\alpha \qquad (17)$$

Except when the system is ideally mixed on the molecular scale, the average ages for the different points are not all equal. To describe the spread in ages between the points, the variance of α_P can be used, which is:

$$\text{var}\, \alpha_P = (1/V) \int_V (\alpha_P - \bar{\alpha})^2\, dv \qquad (17a)$$

In this equation again the summation over all points is written as an integral over the volume.

Now, DANCKWERTS has introduced as a measure for the degree of segregation, the ratio of the variance of the ages between the points and the total variance:

$$J = \text{var}\, \alpha_P / \text{var}\, \alpha \qquad (18)$$

When as a third variance is introduced the "variance in ages within the points," defined by:

$$(1/V) \int_V dv \int_{\alpha=0}^\infty (\alpha - \alpha_P)^2\, \phi_P(\alpha)\, d\alpha \qquad (19)$$

it can be proved (see appendix I) that the total variance (equation 11) is equal to the sum of the variance between points (equation 17a) and the variance within the points (equation (19)). As none of these variances can be negative, the value of J must lie between the limits 0 and 1. For a completely segregated system the variance within the points is equal to zero, since within each point the ages of the molecules are all equal, and therefore equal to α_P (see equation 19). It follows that in that case the variance between points is equal to the total variance, and $J = 1$. But a value of $J = 0$ is possible only for an ideally mixed system. In the next section the problem of finding the minimum value of J for a given residence time distribution is dealt with.

7. The Condition of Maximum Mixedness

In this paragraph a new concept is introduced, which is called the state of maximum mixedness. The significance of this concept will become clear when it is shown that it is the antithesis of the state of complete segregation, and that for this case J is minimum.

The steady flow system is said to be in a state of maximum mixedness when two conditions are fulfilled.

1. For each point, the molecules within it, will leave the system at the same moment, or:

$$\Psi_P(\lambda) = 0 \text{ for } \lambda \leqslant \lambda_P \qquad (20)$$
$$= 1 \text{ for } \lambda > \lambda_P$$

That is, the life expectation distribution function of the molecules at each point is a step function. The corresponding frequency function $\psi_P(\lambda)$ is a delta function:

$$\psi_P(\lambda) = \delta(\lambda - \lambda_P) \qquad (21)$$

2. Points with equal life expectation λ_P are mixed, or at least they have identical age distributions:

$$\Phi_P(\alpha) = \Phi(\lambda_P, \alpha) \qquad (22)$$

The first condition is analogous to the condition for complete segregation, where the molecules at each point have entered the system at the same time. These conditions together express the requirement that all molecules, which will leave at the same moment and therefore will be mixed at the outlet, are mixed already during all the time they stay in the system. So it can be seen that when these conditions are fulfilled, the mixing prescribed by the (assumed) residence time distribution is performed as early as possible*.

*Here a difficulty arises with respect to the classical example of the ideal mixer, as for this case condition 1 is not fulfilled. In appendix II it is shown that the residence time distribution of the ideal mixer is a degenerate case, where condition 1 can be dropped. The other well-known extreme case, the plug flow reactor, does indeed always conform to the conditions mentioned. In fact, the plug flow reactor is at the same time completely segregated and in the state of maximum mixedness, as this residence time distribution leaves no freedom for different degrees of segregation. The range of possible values of J has degenerated here to one value only: $J = 1$.

In appendix II it is proved that these two conditions are sufficient for the degree of segregation J being minimum. The necessary conditions for this minimum value of J are somewhat less stringent.

To show that the state of complete segregation and the here defined state of maximum mixedness are complementary we can construct two imaginary reactors which possess these characteristics.

The reactor with complete segregation is composed of a long tube, in which piston flow is supposed, with a great number of side exits, which are placed at small intervals (see Fig. 2). The flow through these side exits is controlled in such a way that the total residence time distribution of the system equals the given residence time distribution which we are studying. The volume of the side tubes is supposed to be negligible.

Fig. 2. Plug flow reactor with side exits. A case of complete segregation.

As points in this system one can consider very short lengths of the pipe. It is clear that the age distribution in each point is extremely narrow, and that there is no mixing in the system, except at the exit. So the mixing of molecules of different age is effected as late as possible, i.e. in A (see Fig. 2). The position of an arbitrary point of the pipe can be given in two ways, viz. by the age α of the molecules, or by the volume v of the piece of pipe between the entrance and this point.

Consider a small element of the pipe between α and $\alpha + \Delta\alpha$. The volume of this element is equal to the total volume of all the molecules with an age between α and $\alpha + \Delta\alpha$, and therefore equal to $V\phi(\alpha)$. So with (8):

$$\frac{\Delta v}{V} = \frac{1}{\tau}\left[1 - F(\alpha)\right]\Delta\alpha \qquad (23)$$

From this it follows that the relation between v and α is:

$$\frac{v}{V} = \frac{1}{\tau}\int_0^{\alpha} [1 - F(\alpha')]\, d\alpha' \qquad (24)$$

Further the quantity of fluid which must be drawn off in the interval between α and $\alpha + \Delta\alpha$ clearly must be $Qf(\alpha)\,\Delta\alpha$. By these relations the imaginary reactor is completely specified.

From this first flow system, which is completely segregated, the second imaginary flow system, which is a system with maximum mixedness, is simply constructed by reversal of the flow. Then there are many entrances, and one exit (Fig. 3). The life expectation at any point is exactly determined. It is supposed that radial mixing is ideal, so the incoming fluid is immediately dispersed over the width of the pipe. It is easy to see that the reversal of the flow leaves the residence time distribution unchanged. Therefore this second imaginary system fulfills both the conditions mentioned above, and has the required residence time distribution. Now here each molecule is mixed as soon as it enters with the other molecules which will leave at the same moment.

We now proceed to derive the explicit form of the function $\Phi(\lambda_p, \alpha)$ of (22), that is, the age distribution of those points which have a life expectation equal to λ_p.

Consider again the various points of the system at time $\theta = 0$. The molecules of the points which have life expectations equal to a specified λ_p will leave at time $\theta = \lambda_p$. Together with these molecules, however, other ones will leave, which enter in the time interval $0 < \theta < \lambda_p$, and have sufficiently short residence times. The fraction of the leaving molecules (at time $\theta = \lambda_p$) which were not in the system at time $\theta = 0$ equals $F(\lambda_p)$, whereas a fraction $1 - F(\lambda_p)$ of these molecules were contained in the points with expectation λ_p. Of these last ones, a fraction $1 - \Phi_p(\alpha)$ was older than α at time $\theta = 0$, and therefore older than $\alpha + \lambda_p$ at time $\theta = \lambda_p$. So the fraction of the leaving molecules which are older than $\alpha + \lambda_p$ will be $[1 - F(\lambda_p)] \times [1 - \Phi_p(\alpha)]$.

By definition, this fraction must be equal to $1 - F(\alpha + \lambda_p)$, so:

$$[1 - F(\lambda_p)][1 - \Phi_p(\alpha)] = 1 - F(\alpha + \lambda_p)$$

Solving for $\Phi_p(\alpha)$,

$$\Phi_p(\alpha) = \frac{F(\lambda_p + \alpha) - F(\lambda_p)}{1 - F(\lambda_p)} \qquad (25)$$

This formula is the explicit form of (22). It gives the common age distribution of all points which have a life expectation λ_p, for the case of maximum mixedness. When F is differentiable, Φ_p is clearly also differentiable, and:

$$\phi_p(\alpha) = \frac{f(\lambda_p + \alpha)}{1 - F(\lambda_p)} \qquad (26)$$

Using this result, it is possible to find the value of J for the case of maximum mixedness. To this end, the value of α_p, i.e. the mean age of point P, and the variance of α_p must be computed.

$$\alpha_p = \int_0^{\infty} \alpha\, \phi_p(\alpha)\, d\alpha = \int_0^{\infty} \frac{\alpha f(\lambda_p + \alpha)}{1 - F(\lambda_p)}\, d\alpha$$

By partial integration and substitution of s for $\lambda_p + \alpha$ this is found to be equal to:

$$\alpha_p = \frac{1}{1 - F(\lambda_p)} \int_{\lambda_p}^{\infty} [1 - F(s)]\, ds \qquad (27)$$

To find the numerator of J in formula (18), we use use (17a) in which the integration over the volume (summation over all points) is changed into an integration over λ_p. The volume element dv must then be replaced by $V\psi(\lambda_p)\, d\lambda_p$, which is equal to the joint volume of the points which have an expectation between λ_p and $\lambda_p + d\lambda_p$. So:

$$\text{var}\,\alpha_p = \int_{\lambda_p=0}^{\infty} \left[\frac{1}{1 - F(\lambda_p)} \int_{\lambda_p}^{\infty} \{1 - F(s)\}\, ds - \bar{\alpha}\right]^2 \times \psi(\lambda_p)\, d\lambda_p \qquad (28)$$

In this formula, $\psi(\lambda_p)$ and $\bar{\alpha}$ are known from (12) and (10); therefore (28) gives the variance of the ages between points for an arbitrary residence time distribution F, in the case of maximum mixedness. The denominator of J in (28) is given by (11), and thus the minimum value of J for every residence time distribution can be found. The

proof that this value is indeed the minimum of J, is given in appendix II.

8. The Conversion in a Chemical Reactor with Maximum Mixedness

The amount of conversion in a reactor of maximum mixedness and an arbitrary residence time distribution can be calculated when the kinetics of the chemical reaction are known. Suppose that the incoming fluid has a concentration c_0, and that the reaction velocity is given by:

$$r = R(c) \tag{29}$$

where R is a known function of c only.

Fig. 3. Plug flow reactor with side entrances. A case of maximum mixedness.

Consider now the reactor sketched in Fig. 3. Going along the reactor from the left to the right, the life expectation of the molecules λ decreases, and becomes zero at the exit. At the left of the reactor the life expectation is infinite (or equal to the maximum residence time). Analogous to (23) we have here:

$$\frac{\Delta v}{V} = -\frac{1}{\tau}\left[1 - F(\lambda)\right]\Delta\lambda \tag{30}$$

Between λ and $\lambda + \Delta\lambda$ a quantity $Qf(\lambda)\,\Delta\lambda$ is fed into the reactor by the side tubes. So the total volume flow at a point with life expectation λ is equal to:

$$Q\int_{\lambda}^{\infty} f(\lambda)\,d\lambda$$

and therefore equal to:

$$Q\left[1 - F(\lambda)\right]$$

Now consider the material balance between $\lambda + \Delta\lambda$ and λ:

Inflowing at $\lambda + \Delta\lambda$:
$Q\left[1 - F(\lambda + \Delta\lambda)\right] c(\lambda + \Delta\lambda)$
pro unit of time

Outflowing at λ:
$$Q\left[1 - F(\lambda)\right] c(\lambda)$$

Inflowing through side tubes:
$$Qf(\lambda)\, c_0\, \Delta\lambda$$

Taken away by chemical reaction:
reaction velocity times volume, equal to:
$$R(c)\,(V/\tau)\left[1 - F(\lambda)\right]\Delta\lambda$$

From this material balance one finds:

$$-f(\lambda)\,c(\lambda) + \left[1 - F(\lambda)\right] \times (dc/d\lambda) + f(\lambda)\,c_0 - R(c)\left[1 - F(\lambda)\right] = 0$$

or

$$\frac{dc}{d\lambda} = R(c) + \frac{f(\lambda)}{1 - F(\lambda)}(c - c_0) \tag{31}$$

This differential equation relates c with λ. The concentration at the outlet is the value of c for $\lambda = 0$.

The boundary condition at the left of the reactor for $\lambda = \infty$ can be found by considering that c is bounded and positive, so that for all normal cases $dc/d\lambda = 0$ for $\lambda = \infty$. The value of c at this point can be found directly from the differential equation, when the limit of $f(\lambda)/1 - F(\lambda)$ is known. When the residence time distribution is known only numerically, say from experiments with a tracer, it will appear that this boundary condition will give no difficulties, for the solution is nearly independent of the conditions at high values of λ. The reason for this is that the very small fraction of molecules which have extremely high residence times does not affect the amount of conversion perceptibly. In solving the equation numerically, it is sufficient to choose an estimated value of c for a λ which is three or four times the mean residence time, and then integrate with respect to λ (decreasing λ by small steps).

9. Solution of the Differential Equation for Some Simple Cases

a. Ideal-mixer, arbitrary reaction kinetics

When the residence time distribution is that of an ideal mixer given by:

$$f(t) = (1/\tau)\,e^{-t/\tau} \text{ and } F(t) = 1 - e^{-t/\tau},$$

the differential equation (31) becomes:

$$\frac{dc}{d\lambda} = R(c) + (1/\tau)(c - c_0)$$

The solution of this equation is $dc/d\lambda = 0$ or $c =$ constant. The value of c is found from:

$$R(c) + (1/\tau)(c - c_0) = 0$$

which is the well-known equation for a reactor which is ideally mixed on the molecular scale.

b. First order reaction, arbitrary residence time distribution

When the reaction is of the first order,

$$R(c) = kc$$

Equation (31) then reads:

$$\frac{dc}{d\lambda} = kc + \frac{f(\lambda)}{1 - F(\lambda)}(c - c_0)$$

The solution of this equation is :

$$c = \frac{c_0 e^{k\lambda}}{1 - F(\lambda)} \int_{\lambda}^{\infty} f(t)\, e^{-kt}\, dt$$

which can be verified by substitution. The concentration at the exit is found by substitution of $\lambda = 0$:

$$c_e = c_0 \int_0^{\infty} f(t)\, e^{-kt}\, dt$$

This expression is the same as that found when the system is completely segregated. In fact, for a first order reaction, the conversion is only dependent on the residence time distribution, whereas further differences in the degree of mixing have no influence.

c. Numerical solution for two explicit residence time distributions

Equation (31) has been solved for a second order reaction and two different residence time distributions, for which were chosen the functions:

$$f_1(t) = (4t/\tau^2)\, e^{-2t/\tau} \qquad (32)$$

and

$$f_2(t) = (27/2)(t^2/\tau^3)\, e^{-3t/\tau} \qquad (33)$$

These functions are the residence time frequency functions of respectively two and three well mixed vessels of equal volume, in series.

If it should be known that a given reactor has a residence time distribution according to $f_2(t)$ (see above) it would still be possible to suppose different degrees of mixing, e.g. complete segregation, or maximum mixedness, or that the reactor consists really of two well mixed vessels, in which case it is again possible to distinguish between mixing on a molecular scale in each vessel or complete segregation in each vessel. For all these cases the conversion can be calculated for a second order reaction. Of course many other intermediate cases are possible.

Let the reaction velocity be given by:

$$R(c) = kc^2 \qquad (34)$$

and let the concentration at the entrance of the reactor be c_0. Further, let:

$$K = kc_0\, \tau \text{ (where } K \text{ is dimensionless)} \qquad (35)$$

In the case of complete segregation, each fragment of fluid entering the reactor remains unmixed with other fragments in passing through the reactor, and its concentration decreases with time according to $dc/d\,\theta = -kc^2$, which gives for an element of fluid with residence time t:

$$c(t) = \frac{c_0}{1 + Kt/\tau} \qquad (36)$$

The concentration at the exit c_e is then the average concentration of all leaving fragments of fluid, which is in general:

$$c_e = \int_0^{\infty} f(t)\, c(t)\, dt \qquad (37)$$

After substitution of (32) and (36) it can be derived that:

$$\frac{c_e}{c_0} = \frac{2}{K} + \frac{4}{K^2} e^{2/K} \operatorname{Ei}\left(-\frac{2}{K}\right) \qquad (38)$$

The function $\operatorname{Ei}(x)$ is the exponential integral defined by:

$$\operatorname{Ei}(x) = -\int_{-x}^{\infty} (e^{-s}/s)\, ds$$

Tables of this function can be found in [2] and [3].

In the case of two real vessels in series, both having the residence time distribution of a well mixed vessel, but each being completely segregated, the concentration after the first vessel (in the connecting tube) is:

$$c_1 = \int_0^\infty \frac{c_0}{1 + Kt/\tau} \frac{2}{\tau} e^{-2t/\tau}\, dt$$

or:

$$\frac{c_1}{c_0} = -\frac{e^{2/K}}{\frac{1}{2}K} \operatorname{Ei}\left(-\frac{2}{K}\right) \qquad (39)$$

In the same way it is found that the concentration at the exit of the second vessel is given by:

$$\frac{c_e}{c_1} = -\frac{e^{2c_0/Kc_1}}{Kc_1/2c_0} \operatorname{Ei}\left(-\frac{2c_0}{Kc_1}\right) \qquad (40)$$

From (39) and (40) the value of c_e/c_0 can be calculated for arbitrary values of K.

For the third case, where the reactor consists of two vessels in series which are ideally mixed on the molecular scale, the conversion is determined by the equations:

$$\left.\begin{aligned} kc_1^2 &= (2/\tau)(c_0 - c_1) \\ kc_e^2 &= (2/\tau)(c_1 - c_e) \end{aligned}\right\} \qquad (41)$$

The solution for c_e is:

$$\frac{c_e}{c_0} = \frac{-1 + \sqrt{[-1 + 2\sqrt{(1 + 2K)}]}}{K} \qquad (42)$$

The fourth case is the condition of maximum mixedness. For the given residence time distribution (32) the differential equation (31) reduces to:

$$\frac{dc}{d\lambda} = kc^2 + \frac{4\lambda}{\tau + 2\lambda}(c - c_0)$$

Let $\lambda/\tau = x$ and $c/c_0 = \gamma$

$$\frac{d\gamma}{dx} = K\gamma^2 + \frac{4x}{2x + 1}(\gamma - 1)$$

The boundary condition is: for $x = \infty$, $d\gamma/dx = 0$. From this it follows that for $x = \infty$.

$$0 = K\gamma_\infty^2 + 2(\gamma_\infty - 1)$$

From this equation γ_∞ (for $x = \infty$) can be found. For large values of x the value of γ is nearly constant, and therefore one can start a numerical integration at some value of x which is so high that $f(x)$ is negligible small, say $x = 4$ or $x = 3$. The equation can then be integrated in small steps, and it appears that the solution is very nearly independent of the starting point. The value of γ for $x = 0$ (i.e. $\lambda = 0$) is the required value of c_e/c_0 which gives the concentration at the exit of the reactor.

Table 1. *The conversion in a reactor which has the residence time distribution of two well-mixed vessels in series, for different degrees of mixing, as a function* $kc_0\tau$. *Values of* c_e/c_0

$kc_0\tau$	3	5	10	20	30	50	J
Complete segregation	0·298	0·209	0·122	0·067	0·046	0·028	1·0000
2 real, segregated vessels	0·312	0·225	0·137	0·079	0·057	0·037	0·7143
2 real, ideally mixed vessels	0·326	0·242	0·155	0·096	0·071	0·049	0·1429
maximum mixedness	—	0·252	0·166	0·106	0·081	—	0·3275

Table 2. *The conversion in a reactor which has the residence time distribution of three well-mixed vessels in series, for different degrees of mixing, as a function of* $kc_0\tau$. *Values of* c_e/c_0

$kc_0\tau$	3	5	10	20	30	50	J
complete segregation	0·322	0·232	0·140	0·080	0·056	0·035	1·0000
3 real, segregated vessels	0·334	0·246	0·154	0·093	0·067	0·045	0·6250
3 real, ideally mixed vessels	0·357	0·275	0·186	0·122	0·094	0·067	0·2500
maximum mixedness	—	0·287	0·196	0·132	0·104	—	0·0831

This integration has been carried out for different values of K, viz. 5, 10, 20 and 30. The results, together with the solutions for the other cases, are given in Table 1.

Table 1 further contains the values of c_e/c_0 for $K = 3$ and $K = 50$, for the first three cases. From this table it can be seen that four different reactors, which have identical residence time distributions, show different degrees of conversion. The values of the degree of segregation, J, are given in the last column. The value $J = 0{\cdot}0275$ is the minimum value for this residence time distribution.

The same calculations have been made for the residence time distribution $f_3(t)$ (33), which is equal to the distribution for three well-mixed vessels in series. The formulae for the different cases are completely analogous (although somewhat more complicated) to those for $f_2(t)$. The results can be found in Table 2.

10. CONCLUSION

The considerations brought forward in this paper show that a knowledge of the residence time distribution of a continuous flow system, however important, is not sufficient for the description of the state of mixing.

More information is, in many cases, difficult to obtain. The conversion in a continuous reactor can be very different for different degrees of mixing. Probably this degree of mixing may have still more influence when side reactions or chain reactions occur. The condition of maximum mixedness, as defined here, may be of value in this field of study, giving one extreme of the state of mixing for every arbitrary residence time distribution.

NOTATION

c = concentration
J = degree of segregation
k = reaction velocity constant
$K = kc_0\,\tau$ for a second order reaction
Q = flow velocity through the system
t = residence time
V = volume of the flow system
v = volume of a tube reactor from the entrance up to a specified point
v_P = volume of a "point"
$\mathfrak{a}$ = age of a molecule
θ = time
λ = life expectation of a molecule
τ = mean residence time
$\mathrm{Ei}(x)$ = exponential integral function
$F(t)$ = residence time distribution
$\xi(\lambda)$ = mean age of the molecules with life expectation λ
$\Phi(\mathfrak{a})$ = age distribution
$\Psi(\lambda)$ = life expectation distribution

Suffixes:

0 = entrance
e = exit
P = for a specified point

APPENDIX I

Analysis of variance

In this appendix it is proved that the variance in ages of all molecules (which are at a given moment in the system) is equal to the sum of the variance in ages between the points and the variance in ages within the points, as defined earlier in this paper. This theorem is valid not only for the ages of the molecules, but for every characteristic of the individual molecules which can be expressed as a number, e.g. the life expectation λ or the quantity ξ which will be defined in appendix II.

When $\phi(\mathfrak{a})$ is the frequency function of the ages of the molecules which are in the system at a given moment, and $\phi_P(\mathfrak{a})$ the frequency function of the ages of the molecules of point P, the variances in question are:

$$\mathrm{var}\ \mathfrak{a} = \int_0^\infty (\mathfrak{a} - \bar{\mathfrak{a}})^2\,\phi(\mathfrak{a})\,d\mathfrak{a} \qquad \text{(I, 1)}$$

var $\mathfrak{a}$ between points:

$$(1/V)\int_V (\mathfrak{a}_P - \bar{\mathfrak{a}})^2\,dv \qquad \text{(I, 2)}$$

var $\mathfrak{a}$ with points:

$$1/V \int_V dv \int_0^\infty (\mathfrak{a} - \mathfrak{a}_P)^2\,\phi_P(\mathfrak{a})\,d\mathfrak{a} \qquad \text{(I, 3)}$$

where:

$$\int_0^\infty \phi(\mathfrak{a})\,d\mathfrak{a} = 1 \qquad \text{(I, 4)}$$

$$\int_0^\infty \phi_P(\mathfrak{a})\,d\mathfrak{a} = 1 \text{ (for every } P) \qquad \text{(I, 5)}$$

$$\bar{\mathfrak{a}} = \int_0^\infty \mathfrak{a}\,\phi(\mathfrak{a})\,d\mathfrak{a} \text{ (by definition)} \qquad \text{(I, 6)}$$

$$\mathfrak{a}_P = \int_0^\infty \mathfrak{a}\phi_P(\mathfrak{a})\,d\mathfrak{a} \text{ (by definition)} \qquad \text{(I, 7)}$$

and

$$\phi(\mathfrak{a}) = 1/V \int_V \phi_P(\mathfrak{a})\,dv \text{ (for every } \mathfrak{a}) \qquad \text{(I, 8)}$$

The last equation expresses the fact that the quantity of molecules with ages between α and $\alpha + \Delta\alpha$ of the system, which is equal to $V\phi(\alpha)\,\Delta\alpha$, is equal to the sum of the quantities of such molecules in all points of the system which is $\Sigma v_P\,\phi_P(\alpha)\,\Delta\alpha$. As mentioned earlier, a sum over all points is written for convenience as an integral over the volume. From (I, 8) it follows (by multiplication by α on both sides and then integrating over α) that:

$$\int_0^\infty \alpha\phi(\alpha)\,d\alpha = \int_0^\infty (1/V)\int_V \alpha\phi_P(\alpha)\,dv\,d\alpha$$

Interchanging the integrations on the right hand side of this equation, it is found that:

$$\bar{\alpha} = (1/V)\int_V \alpha_P\,dv \qquad \text{(I, 9)}$$

This equation states that the mean age of all molecules is equal to the weighed average of the mean ages of the points, with the volume of each point as the weight.

With the aid of the equations (I, 4) to (I, 9) we can reduce the expressions for the three variances to more simple forms:

$$\text{var}\,\alpha = \int_0^\infty (\alpha^2 - 2\alpha\bar{\alpha} + \bar{\alpha}^2)\,\phi(\alpha)\,d\alpha$$

$$= \int_0^\infty \alpha^2\phi(\alpha)\,d\alpha - 2\bar{\alpha}\int_0^\infty \alpha\phi(\alpha)\,d\alpha + \bar{\alpha}^2\int_0^\infty \phi(\alpha)\,d\alpha$$

(with I, 6 and I, 4):

$$= \int_0^\infty \alpha^2\phi(\alpha)\,d\alpha - 2\bar{\alpha}^2 + \bar{\alpha}^2$$

so $$\text{var}\,\alpha = \int_0^\infty \alpha^2\phi(\alpha)\,d\alpha - \bar{\alpha}^2. \qquad \text{(I, 10)}$$

var α between points =

$$(1/V)\int_V (\alpha_P^2 - 2\bar{\alpha}\alpha_P + \bar{\alpha}^2)\,dv$$

$$= (1/V)\int_V \alpha_P^2\,dv - \frac{\bar{\alpha}^2}{V}\int_V \alpha_P\,dv + \frac{\bar{\alpha}^2}{V}\int_V dv$$

(with I, 9) $$= (1/V)\int_V \alpha_P^2\,dv - 2\bar{\alpha}^2 + \bar{\alpha}^2$$

so var α between points $= (1/V)\int_V \alpha_P^2\,dv - \bar{\alpha}^2$. (I, 11)

var α within points =

$$(1/V)\int_V dv \int_0^\infty (\alpha^2 - 2\alpha\alpha_P + \alpha_P^2)\,\phi_P(\alpha)\,d\alpha$$

$$= (1/V)\int_V dv \left[\int_0^\infty \alpha^2\phi_P(\alpha)\,d\alpha - 2\alpha_P\int_0^\infty \alpha\phi_P(\alpha)\,d\alpha + \alpha_P^2\int_0^\infty \phi_P(\alpha)\,d\alpha\right]$$

(with I, 7 and I, 5)

$$= (1/V)\int_V dv \left[\int_0^\infty \alpha^2\phi_P(\alpha)\,d\alpha - 2\alpha_P^2 + \alpha_P^2\right]$$

Interchanging the integrations for the first term between the brackets, this gives:

var α within points =

$$\int_0^\infty \alpha^2\,d\alpha \int_V \phi_P(\alpha)\,(dv/V) - (1/V)\int_V \alpha_P^2\,dv$$

(with I, 8)

var α within points =

$$\int_0^\infty \alpha^2\phi(\alpha)\,d\alpha - (1/V)\int_V \alpha_P^2\,dv \qquad \text{(I, 12)}$$

From the equations (I, 10), (I, 11) and (I, 12) it can be seen that:

var α = var α between points + var α within points (I, 13)

Appendix II

Theorem

The quantity J reaches its minimum (for a given residence time distribution) when the conditions of paragraph 6 are true. These conditions are sufficient but not necessary.

Proof

Firstly, we prove that the residence time distribution determines uniquely the simultaneous distribution of α and λ of the molecules which are in the system.

Let the simultaneous frequency function of α and λ be denoted by $g(\alpha, \lambda)$, which means that a fraction

$$g(\alpha, \lambda)\,\Delta\alpha\,\Delta\lambda$$

of the molecules have, at moment $\theta = 0$, an age between α and $\alpha + \Delta\alpha$ and at the same time a life expectation between λ and $\lambda + \Delta\lambda$.

The quantity of molecules which have ages between α and $\alpha + \Delta\alpha$ and at the same time life expectations between λ and $\lambda + \Delta\lambda$ at time zero is the same as the quantity of molecules with ages between $\alpha + \theta$ and $\alpha + \theta + \Delta\alpha$ and life expectations between $\lambda - \theta$ and $\lambda - \theta + \Delta\lambda$ at time θ (when $\theta \ll \lambda$), for these are the same molecules, none of which has left the system. Because the flow is steady, all distributions are independent of time, therefore:

$$g(x, \lambda)\,\Delta x\,\Delta\lambda = g(x + \theta,\ \lambda - \theta)\,\Delta x\,\Delta\lambda \qquad \text{(II, 1)}$$

So, $g(x, \lambda)$ only depends on the sum of x and λ

$$g(x, \lambda) = g^*(x + \lambda) \qquad \text{(II, 2)}$$

Now the marginal distributions of g are $\phi(x)$ and $\psi(\lambda)$, so:

$$\int_0^\infty g(x, \lambda)\,d\lambda = \phi(x) \qquad \text{(II, 3)}$$

so with (8) and (II, 2):

$$\int_0^\infty g^*(x + \lambda)\,d\lambda = (1/\tau)\left[1 - F(x)\right] \qquad \text{(II, 4)}$$

or:

$$\int_x^\infty g^*(s)\,ds = (1/\tau)\left[1 - F(x)\right] \qquad \text{(II, 5)}$$

Differentiation with respect to x gives:

$$g^*(x) = 1/\tau\, f(x)$$

and so:

$$g(x, \lambda) = 1/\tau\, f(x + \lambda) \qquad \text{(II, 6)}$$

From (II, 6) it is seen that the simultaneous distribution of x and λ is completely determined by the residence time distribution, and therefore does not depend on the degree of mixing. From this it follows that also the simultaneous distribution of two quantities that are functions of x and λ is completely determined, a result that is used in the following argument.

Now consider a quantity ξ which is a function of λ, given by:

$$\xi(\lambda) = \frac{\int_0^\infty x\, g(x, \lambda)\,dx}{\int_0^\infty g(x, \lambda)\,dx} \qquad \text{(II, 7)}$$

This is the average age of the molecules having a life expectation λ.

For every molecule we define the quantity ξ as the the given function (II, 7) in which the argument λ is taken equal to the life expectation of this molecule (the age of the molecule being left out of account). For every point we define ξ_P as the average of the values of ξ for all molecules in that point.

The analysis of variance of the quantities x, ξ and $x - \xi$ can be written as:

$$\left.\begin{aligned} &\text{var } x \text{ within points} + \text{var } x \text{ between points} \\ &\quad = \text{var } x \\ &\text{var } \xi \text{ within points} + \text{var } \xi \text{ between points} \\ &\quad = \text{var } \xi \\ &\text{var } (x - \xi) \text{ within points} + \text{var } (x - \xi) \\ &\quad \text{between points} = \text{var } (x - \xi) \end{aligned}\right\} \qquad \text{(II, 8)}$$

Since the molecules within a given point are ideally mixed, the distributions of x and λ within this point must be independent. This can be expressed by:

$$g_P(x, \lambda) = \phi_P(x)\,\psi_P(\lambda)$$

Therefore also x and ξ must be distributed independently within each point. From this it follows that:

$$\text{var } (x - \xi) \text{ within points} = \text{var } x \text{ within points} + \text{var } \xi \text{ within points} \qquad \text{(II, 9)}$$

Combining (II, 8) and (II, 9):

$$\left.\begin{aligned} &\text{var } x \text{ between points} = \\ &\quad = \text{var } x - \text{var } x \text{ within points} \\ &\quad = \text{var } x - \text{var } (x - \xi) \text{ within points} + \text{var } \xi \text{ within points} \\ &\quad = \text{var } x - \text{var } (x - \xi) + \text{var } (x - \xi) \text{ between points} + \text{var } \xi \text{ within points} \end{aligned}\right\} \qquad \text{(II, 10)}$$

The quantity at the left is the numerator of J in equation (18). We must prove that this quantity is minimum. The first two quantities of the right in eq. (II, 10) only depend on the residence time distribution, and not on the degree of mixing. Therefore they can be considered constant. The last two terms of (II, 10) can reach the value zero, as will be shown below, so that the minimum value of var x between points will be reached if, and only if these two quantities are both equal to zero.

Sufficient conditions

The quantity var ξ within points (4th term of II, 10) is zero when all molecules within a point have the same ξ, which is necessarily true when they have equal life expectations, corresponding with the first condition for maximum mixedness.

The third term on the right in (II, 10) is zero when $x_P = \xi_P$ for each point. This condition can be fulfilled owing to our choice of the function $\xi(\lambda)$. When each point contains only molecules with life expectations equal to the value of λ_P of that point, and all points with the same λ_P have the same age distribution, each of these points has the same average age x_P, which must be equal to the average of all molecules with this life expectation, so equal to $\xi(\lambda)$ and therefore equal to ξ_P.

So we have proven that the two conditions for maximum mixedness are sufficient for reaching the minimum of the numerator of J, and since the denominator of J is determined by the residence time distribution, they are sufficient conditions for J being minimum.

Necessary conditions

From (II, 10) it is clear that the necessary conditions for the minimum value of J are the following.

1. All molecules within a point have equal ξ, that is,

the frequency function of ξ within each point is a δ-function. When this is true, for every point ξ_P is defined as the common value of ξ of all molecules within this point.

2. Points with equal ξ_P have equal mean ages $\bar{\alpha}_P$.

The first of these conditions is identical with the condition 1 of paragraph 7, when the inverse of the function $\xi(\lambda)$, i.e. the function $\lambda(\xi)$, is single-valued. This depends on the given residence time distribution and can be ascertained by examining a plot of:

$$\xi(\lambda) = \frac{\int_0^\infty \alpha f(\alpha+\lambda)\,d\alpha}{\int_0^\infty f(\alpha+\lambda)\,d\alpha} = \frac{\int_0^\infty \alpha f(\alpha)\,d\alpha}{1-F(\lambda)} - \lambda \qquad \text{(II, 11)}$$

An example in which the inverse $\lambda(\xi)$ is not single-valued is the case of the residence time distribution $f(t) = (1/\tau)\exp(-t/\tau)$, (which is the distribution of a well-stirred vessel). For this distribution the function $\xi(\lambda)$ is constant, viz.:

$$\xi(\lambda) = \tau \qquad \text{(II, 12)}$$

Therefore the first necessary condition (all molecules of a point have equal ξ) is always satisfied, and the second necessary condition becomes: all points have equal mean ages. In the case of a vessel which is ideally mixed on the molecular scale, the two necessary conditions are indeed satisfied, whereas the conditions of paragraph 7 are not.

The second necessary condition for minimum J, mentioned above, which only requires that points with equal ξ have equal $\bar{\alpha}_P$, is clearly somewhat less stringent than the condition of equal α-distributions. For the definition of the state of maximum mixedness the more stringent condition is to be preferred.

References

[1] Danckwerts P. V. *The Effect of Incomplete Mixing on Homogeneous Reactions.* Chemical Reaction Engineering, 12th Meeting Europ. Fed. Chem. Engng. Amsterdam 1957.

[2] Jahnke E. and Emde F. *Funktionentafeln* (3er Aufl.) Leipzig, Berlin 1938; (4th Ed.) Dover Publications, New York 1945.

[3] *Mathematical Tables, British Association* (2nd Ed.) Vol. 1 p. 31. Cambridge University Press 1946.

Chemical Engineering Science, 1959, Vol. 11, pp. 16 to 23. Pergamon Press Ltd., London. Printed in Great Britain

The packed thermal diffusion column

M. Lorenz and A. H. Emery, Jr.

School of Chemical and Metallurgical Engineering, Purdue University, Lafayette, Indiana, U.S.A.

(*Received* 27 *October* 1958)

Abstract—Equations have been developed to describe a thermal diffusion column in which fine packing material has been placed to reduce the convection currents. The separation calculated for a given column is increased when packing is introduced, in agreement with observation. Economic calculations show that the cost of performing a desired separation with a packed column is about the same as that for a column without packing.

Résumé—Les auteurs développent des équations pour décrire une colonne à diffusion thermique dans laquelle ils mettent un garnissage fin pour réduire les courants de convection. La séparation calculée pour une colonne donnée augmente avec l'introduction du garnissage comme le montre l'expérimentation. Du point de vue économique le prix de revient d'une séparation désirée est à peu près le même avec une colonne à garnissage ou sans garnissage.

Zusammenfassung—Zur Beschreibung einer Thermodiffusionssäule, in der feine Füllkörper zur Verringerung der Konvektion eingebracht wurden, sind Gleichungen abgeleitet worden. Die berechnete Trennung für eine gegebene Kolonne steigt durch das Einbringen der Füllkörper an, was in Übereinstimmung mit der Beobachtung ist. Wirtschaftlichkeitsberechnungen zeigen, dass die Kosten für eine gewünschte Trennung mit einer gefüllten Kolonne ungefähr dieselben wie für eine leere Kolonne sind.

The thermal diffusion column is a mass separation device which appears to have some commercial promise for certain types of fluid systems. The basic thermal diffusion effect, which has been known for a century, is a molecular phenomenon in which small concentration differences arise under the influence of a temperature gradient. The thermal diffusion column, which was devised by Clusius and Dickel in 1938 [1], enhances the basic separation by means of convection currents, in a manner somewhat analogous to the way a countercurrent extraction tower produces concentration differences many times those observed in a single-stage contact.

The principles of the column were discerned by a number of persons very soon after its introduction [2, 3, 4]. The first complete presentation of the theory of the "open" (as contrasted to packed) column was that of Furry *et al.* in 1939 [5]. The column consists essentially of two opposing vertical plates separated by a very narrow open space. One plate is heated and the other cooled, and the thermal diffusion effect causes one component of, say, a binary mixture to diffuse toward the hot plate. At the same time, the density gradient which arises because of the temperature gradient causes smooth laminar convection currents up the hot plate and down the cold. Because of the concentration gradient set up by the thermal diffusion, the convection currents transport one component preferentially toward the top and thus create large concentration differences between the top and the bottom of the column.

The distance between the hot and cold plates in most thermal diffusion columns using liquids lies in the range 0·015–0·060 in. Since the separation obtainable decreases rapidly with increasing plate spacing, careful construction is obviously necessary. The economically optimum plate spacing for liquid systems is even smaller than this range. However, when a column with a large plate spacing is filled with a packing material, it behaves as an open column of small plate spacing. Thus the packed column offers the advantage that it requires less precision in its

construction than the open column. The object of the work reported here was to develop the theory of the packed thermal diffusion column and to determine if the introduction of packing alters the economic picture of thermal diffusion.

Previous Work

Although there is a large body of literature on the open column, almost no work has been reported on the packed column. The earliest precursor of the packed column appears to be the indication by Brewer and Bramley [6] that separations are improved by the presence of a few baffles fastened to one plate. The first packed column is reported by Debye and Bueche [7], who used a short column packed with glass wool to fractionate polymers in solution. These authors noted the reason that packing improves the separation over that attained in the same column without packing. The separation achieved in a thermal diffusion column depends on a balance of two rates, the rate of mass flux by the basic thermal diffusion effect in the horizontal direction, and the convection velocity in the vertical direction. Anything that decreases the convection velocity, such as inclining the column from the vertical to reduce the effect of gravity [8], or baffles, or packing, increases the relative importance of the horizontal flux and thus increases the steady state separation in the batch column.

The only measurements of the effects of operating variables in a packed column that have been reported are those of Sullivan *et al.* [9], who measured the effect of plate spacing and packing density on separation, using glass wool packing. Unfortunately, not enough information was obtained to test the equations developed below.

Calculation of the Transport Equation

The calculation proceeds in several steps. First, the convection velocity, v, is calculated as a function of x. This result is used to obtain the horizontal mass flux, J_x, then from this the concentration is obtained, and finally the rate of vertical transport, τ.

The fluid in the column is subjected to four vertical forces which influence its motion. These are gravity, the vertical pressure gradient, fluid shear and the drag of the packing. It is assumed that the convection velocities are vertical only, that the pressure gradient is vertical, that there is no net flow through the column, that temperature is linear in x and that density is linear in temperature. We follow the notation of Furry *et al.*, which puts the origin of the co-ordinate system at the centre of the column. The differential equation resulting from these considerations is

$$\frac{d^2v}{dx^2} + \frac{g\,\Delta T\,\beta}{2w\,\mu}x - \frac{v}{k} = 0 \qquad (1)$$

This same equation, without the last term, is the starting point for the calculations on the open column. The last term represents the drag of the packing. It contains a permeability, k, which may be evaluated by means of isothermal flow measurements, using the equation

$$v = k\,(-\Delta p_f)/\mu L \qquad (2)$$

This differs from the more traditional definition of permeability in that v is the actual, not the superficial velocity.

The solution of equation (1), noting that the velocity is zero at the plates, and assuming that the properties of the fluid are independent of temperature, is

$$v = \frac{g\,\Delta T\,\beta\,k}{2\mu}\left(\frac{x}{w} - \frac{\sinh y}{\sinh Y}\right) \qquad (3)$$

where $y = x/\sqrt{k}$ and $Y = w/\sqrt{k}$. Some samples of the velocity profile calculated from equation (3) are shown in Fig. 1. The curve for $Y = 0$ is the case of infinite permeability, or no packing. Equation (3) has been altered by the substitution $k = w^2/Y^2$ to give an ordinate applicable to both packed and open columns. With this method of presentation, the shape and magnitude of the curves are general. To obtain velocities for a particular case, one would multiply the values of the ordinate by the properties and operating variables indicated. The same is true of Figs. 2 and 3. The presence of the packing reduces the convection velocity considerably. For this reason, the ordinate of the curve for $Y = 20$ has been multiplied by 25 before plotting, and that for

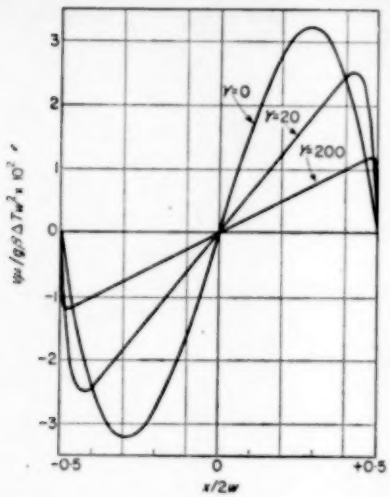

Fig. 1. Vertical convection velocity v as a function of horizontal distance for the open column ($Y = 0$) and for two conditions of packing. The cold plate is at the left edge and the hot plate is at the right edge of the plot. The ordinates for $Y = 20$ have been multiplied by 25 and those for $Y = 200$ by 1,000 before plotting, to make these two curves visible with a common ordinate scale.

$Y = 200$ has been multiplied by 1000 before plotting so that one ordinate scale could be used. Actually, the maximum dimensionless velocities involved are $3{\cdot}2 \times 10^{-2}$ for $Y = 0$, $1{\cdot}0 \times 10^{-3}$ for $Y = 20$, and $1{\cdot}2 \times 10^{-5}$ for $Y = 200$.

The horizontal mass flux rate of one constituent of the mixture is related to the velocity by the differential mass balance

$$\frac{dJ_x}{dx} + v\,\rho\epsilon\,\frac{\partial c}{\partial z} = 0 \qquad (4)$$

In writing this equation, the assumptions are made that diffusion in the vertical direction is negligible, and that the concentration at a point is independent of time. The expression for J_x obtained, assuming that $\partial c/\partial z$ is independent of x, is

$$J_x = \frac{g\,\Delta T\,\beta\rho\,k\,\epsilon}{2\mu}\,\frac{\partial c}{\partial z} \times \left(\frac{w^2 - x^2}{2w} + \frac{\sqrt{k}\cosh y}{\sinh Y} - \sqrt{k}\,\mathrm{etnh}\,Y\right) \qquad (5)$$

Examples of the mass flux distribution calculated from equation (5) are shown in Fig. 2 for the two limiting values of Y, zero for the open column and infinity for a densely packed column. The vertical concentration gradient, $\partial c/\partial z$, has been eliminated by taking the steady state value for the batch column, given by equation (9) with $\tau = 0$. The shape and magnitude of the dimensionless flux curve are relatively unaffected by the presence of packing.

Equation (5) is based on a mass balance. In addition, there is the expression for J_x in terms of the two contributions, ordinary and thermal diffusion,

$$J_x = D\rho\,\epsilon\left(-\frac{\partial c}{\partial z} + \frac{\alpha\,c\,(1-c)}{T}\,\frac{dT}{dx}\right) \qquad (6)$$

from which the concentration profile may be calculated by equating (5) and (6) and integrating. It is assumed that $c\,(1 - c)$ is independent of x.

$$c = c_0 + \frac{\alpha\,c\,(1-c)\,\Delta T}{2wT}\,x + \frac{g\,\beta\,\Delta T k}{2D\,\mu}\,\frac{\partial c}{\partial z}\left(\frac{x^3 - 3\,xw^2}{6w} - \frac{k\sinh y}{\sinh Y} + \sqrt{k}\,x\,\mathrm{etnh}\,Y\right) \qquad (7)$$

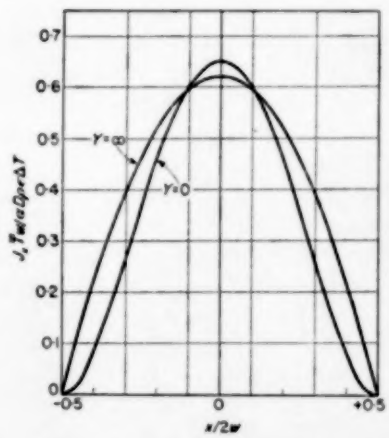

Fig. 2. Horizontal mass flux rate J_x as a function of horizontal distance for the two limiting cases $Y = 0$ and $Y = \infty$ at steady state in the batch column.

The rather odd assumption is made in this step that the T appearing in the denominator of the thermal diffusion term is independent of x, while dT/dx is replaced by $\Delta T/2w$. It can be shown that in the case of the open column this

leads to the same result as obtained by FURRY *et al.* by a later, more obvious simplification. Further, neglect of the variation of T with x is much less serious than the neglect of the variation of viscosity and diffusivity. Examples of the concentration profile are shown in Fig. 3 for the same cases as Fig. 2. The steady state batch value of $\partial c/\partial z$ has again been used. The shape and magnitude of the concentration profile are relatively unaffected by the presence of packing.

The rate of vertical transport of one component, neglecting vertical back-diffusion, is given by

$$\tau = B\rho\epsilon \int_{-w}^{w} vc\, dx \tag{8}$$

Combining (3), (7) and (8) and integrating, one obtains for zero throughput (the batch case)

$$\tau = Hc(1-c) - K\frac{\partial c}{dz} \tag{9}$$

where

$$H = \frac{gB\,\Delta T^2\, wk\,\alpha\,\beta\rho\epsilon}{6\,\mu\,T}\left[1 - \frac{3}{Y^2}(Y \operatorname{ctnh} Y - 1)\right] \tag{10}$$

$$K = K_c + K_d$$

$$K_c = \frac{g^2\,B\,\Delta T^2\, w^3k^2\,\beta^2\,\rho\epsilon}{15\,\mu^2\,D}\left[1 - \frac{15}{4Y^2} - \frac{15}{Y^4} - \right.$$

$$\left. - \frac{5}{Y}\operatorname{ctnh} Y + \frac{15}{4Y^3}\operatorname{ctnh} Y + \frac{45}{4Y^2}\operatorname{ctnh}^2 Y\right] \tag{11}$$

$$K_d = 2w\,B\rho\,D\epsilon \tag{12}$$

The term K of equation (9) is shown as consisting of two parts, K_c and K_d. The previous equations itemized here actually lead only to K_c. We follow the procedure of FURRY *et al.* of adding the term K_d, which represents back-diffusion in the vertical direction, after the other operations are completed. Although back-diffusion is negligible under ordinary operating conditions, it is important in determining the optimum conditions.

As the value of Y approaches infinity, corresponding to a fairly impermeable packing or a large plate spacing, the brackets in (10) and (11) approach the value unity, and H and K_c are given simply by the product of the properties shown. As Y approaches zero, corresponding to a loose packing or to a small plate spacing, the expressions can be shown to approach those obtained for the open column. The terms in the brackets thus account for the relative effect of the plates in imposing drag on the fluid. In a densely packed column, the drag of the plates is of no consequence, while in an open column the plates present the only drag on the fluid.

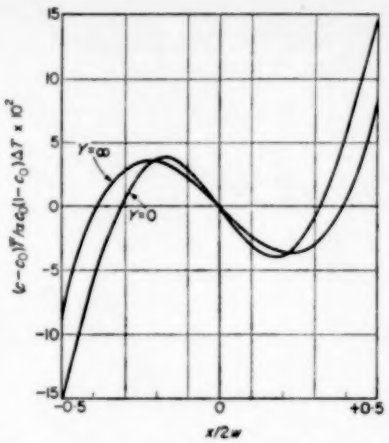

FIG. 3. Concentration c as a function of horizontal distance for $Y = 0$ and $Y = \infty$ at steady state in the batch column.

The transport equation, equation (9), is the same as the equation derived by FURRY *et al.* for the open column, except that H and K are given by different expressions. This equation has been the starting point of the development of a number of operating equations for the open column. None of these derivations involved any assumption about the nature of H and K, and no characteristic of the packed column as we picture it is contrary to these derivations. Consequently, the operating equations developed and proved for the open column should be equally valid for the packed column. However, this remains to be proved experimentally.

To demonstrate the differences between the two types of column, consider the steady state in the batch column. The solution of the transport equation for this case is [5]

$$\ln q = HL/K$$

where

$$q = \left(\frac{c}{1-c}\right)_{\text{top}} \left(\frac{1-c}{c}\right)_{\text{bottom}}$$

If back-diffusion is ignored and the permeability is assumed to be low enough for the brackets in equations (10) and (11) to equal unity, the operating equation is

$$\ln q = \frac{5\,\alpha\mu\,DL}{2g\overline{T}\,\beta\,k w^2}$$

For the open column, the corresponding expression is

$$\ln q = \frac{63\,\alpha\mu\,DL}{2g\overline{T}\,\beta\,w^4}$$

The two are quite similar and differ only in the numerical constant, the permeability, and the effect of plate spacing. The ratio of steady state separations achieved in a given column with and without packing is

$$\frac{(\ln q)_{\text{packed}}}{(\ln q)_{\text{open}}} = \frac{5\,w^2}{63\,k}$$

As an example, consider a plate spacing of $\frac{1}{8}$in. and a packing of uniform spheres of diameter 0·02in., for which the permeability is about 2×10^{-6} cm^2. The ratio of separations is 4000, which certainly is in accord with the observation that the presence of packing improves the steady state separation. Unfortunately, it also increases the time it takes to reach steady state. The ratio of the time to reach a given fraction of the steady state in the packed column to that without packing is about the square of the ratio of separations at steady state, $1{\cdot}6 \times 10^7$. In a practical application, the advantage of the former effect tends to be offset by the disadvantage of the latter, and this is undoubtedly why the economic calculations outlined below show little difference between the two types of column.

Optimum Operating Conditions

The open thermal diffusion column has received the attention of industrial workers, but it has had little use in industrial operations, reportedly because it is expensive. To investigate what effect the introduction of packing into the column has on the cost of separation, we have considered the case in which the separation and rate of throughput have been specified and it is desired to determine the optimum combination of the variables w, Y, B and L.

This problem was treated by Krasny-Ergen in 1940 [11] for the case of gaseous isotopes in the open column. He noted without demonstration that when the properties of liquid isotopes were used, the column dimensions were rather awkward. More recently, Powers and Wilke [8] performed the calculations for the case of liquids in the middle concentration range in the open column, and they too found the optimum dimensions awkward. Fortunately, they found they were able to move away from the optimum to get reasonable dimensions without increasing the cost too much. We followed the same optimization procedure. Further, we used the same system for an example as Powers and Wilke and found much the same result, namely absurd optimum dimensions and a small increase in cost on moving away from the optimum sufficiently to get reasonable dimensions.

The cost of making a separation by thermal diffusion consists essentially of two parts, a fixed charge and an operating expense. The fixed charge is roughly proportional to the equipment cost, and thus to the area of the plates, BL. The operating expense is chiefly heat, and the heat rate is obtainable from the conductivity equation, $\lambda\,BL\,\Delta T/2w$. Thus the cost of the separation per unit time is

$$\text{cost} = a_1 BL + a_2 BL/w \qquad (12)$$

where $a_2 = a_3\,\lambda\,\Delta T/2$. The constant a_1 is the fixed charge per unit area of the plates, and a_3 is the cost of heat per B.t.u.

In order that the separation be made, the variables must satisfy the appropriate operating equation. For the simplifying conditions of equal size of product streams and product compositions in the range of mole or weight fractions of 0·3–0·7, this is, for continuous operation, [10]

$$L = -\frac{2K}{\sigma} \ln\left(1 - \frac{2\sigma\,\Delta}{H}\right) \qquad (13)$$

The terms H and K are given by equations (10), (11) and (12), and are rewritten here for convenience as

$$H = H_1 H_2(Y)\, w^3 B$$

$$K_c = K_1 K_2(Y)\, w^7 B$$

$$K_d = K_3 w B$$

where

$$H_1 = g\,\Delta T^2 \alpha \beta \rho \epsilon / 6 \mu \bar{T}$$

$$H_2(Y) = \frac{1}{Y^2}\left[1 - \frac{3}{Y^2}(Y \operatorname{ctnh} Y - 1)\right]$$

$$K_1 = g^2 \Delta T^2 \beta^2 \rho \epsilon / 15 \mu^2 D$$

$$K_2(Y) = \frac{1}{Y^4}\left[1 - \frac{15}{4Y^2} - \frac{15}{Y^4} - \frac{5}{Y}\operatorname{ctnh} Y + \frac{15}{4Y^3}\operatorname{ctnh} Y + \frac{45}{4Y^2}\operatorname{ctnh}^2 Y\right]$$

$$K_3 = 2\rho \epsilon D$$

The restriction imposed by the operating equation is incorporated by replacing L in equation (12) by its value from equation (13). The partial derivative of cost with respect to each of the three remaining variables is equated to zero, and these three equations are solved simultaneously to yield the optimum values of the variables. The partial with respect to B leads to the equation

$$BH_2 w^3 = 2{\cdot}78\, \sigma \Delta / H_1 \qquad (14)$$

The equation which results from taking the partial of cost with respect to w and eliminating B by using (14) is

$$w^7 K_2 - 5\frac{K_3}{K_1} w = 6\frac{K_3}{K_1}\frac{a_2}{a_1} \qquad (15)$$

Finally, the partial with respect to Y, after elimination of B, gives

$$w^6 = 2\frac{K_3}{K_1}\frac{dH_2}{dY} \Big/ \left(H_2 \frac{dK_2}{dY} - 2K_2 \frac{dH_2}{dY}\right) \qquad (16)$$

The term w can be eliminated between (15) and (16) to give an equation which contains functions of Y only. This equation cannot be solved algebraically, but the results of several numerical solutions are plotted in Fig. 4. The optimum value of Y is a function of the group $G = (a_2/a_1)(K_1/2K_3)^{1/6}$. At higher values of Y than shown, the curve fits the equation $Y = 0{\cdot}633\, G^{6/11}$.

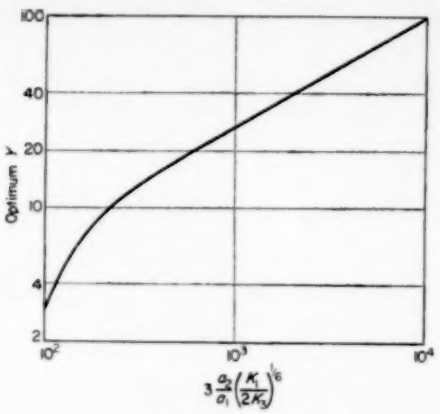

FIG. 4. Optimum Y as a function of cost variables and physical constants. Obtained from simultaneous solution of (15) and (16).

It can be seen that although the cost factors have a fairly direct effect on the optimum Y, the physical properties of the system, entering as they do only the 1/6 power, have very little to do with the optimum value of Y. Further, numerical calculations using equation (15) have shown that neither the cost factors nor the physical properties have much influence on the optimum value of w. Thus, given the cost data, most systems and desired separations will yield about the same optimum values of Y and w. The same is true of w for the open column. B and L, on the other hand, will vary from case to case.

Ostensibly, the temperature difference ΔT and average temperature $\bar{T}$ are also variables and should be included in the optimization procedure. However, one finds simply that it is best to operate at the biggest ΔT feasible, so these variables have been omitted from the above analysis for simplicity. If the viscosity and diffusivity are assumed to be the only properties that vary with temperature, the cost of operation is inversely proportional to about the square of ΔT and $\bar{T}$ to a rather large power which depends on the system. Obviously, both of these quantities are enhanced by a high hot plate temperature, but as the cold plate temperature is reduced, the ΔT is increased and the $\bar{T}$ is decreased, indicating that an optimum may exist. For aqueous systems, the optimum ratio of the absolute hot plate

temperature to that of the cold plate is a little over two, which is commercially unattainable. Thus, a practical operation would probably use tap water as a cooling agent and the highest temperature heat source available which did not decompose the material or, if liquid, vaporize it.

Numerical Example

The procedure to be followed in using these results is first to evaluate G, and then to locate the optimum Y on Fig. 4. This is then used in (15) to calculate the optimum value of w, then (14) is used to get the optimum B, and finally (13) is used to get L.

As an example, we have taken the system used by Powers and Wilke. The feed is 50 mole percent n-heptane in benzene fed at a rate of 1000 barrels per day, and equal product streams containing 30 and 70 mole per cent n-heptane are produced. The actual feed rate chosen affects only the value of B, and has no influence on the optimum values of the other variables. Using their values of system properties and cost data, we obtained an optimum plate spacing of 0·0087 in. almost the same as that for the open column. The optimum L and B are also similar in the packed and open column, as shown in Table 1. (Note that the values for B and " cost " for the packed column in Table 1 should be divided by the void fraction of the packing). The packed column requires one more parameter, of course, the optimum value of Y, which is 4·5.

Table 1. *Summary of design calculations*

	Arbitrarily fixed	*None*	w	w *and* L
*Open column**	$2w$ (in.)	0·0072	1/32	
	L	0·56 (in.)	17 (ft)	
	B (miles)	83	1·0	
	cost ($/day)	8400	10,900	
Packed column	$2w$ (in.)	0·0087	1/32	1/32
	L	0·41 (in.)	3·2 (in.)	2·5 (ft)
	ϵB (miles)	130	55	6·2
	k (cm^2 × 10^6)	6·1	2·1	26
	ϵ cost ($/day)	8100	9300	9900

* from Powers and Wilke [8]

The optimum plate spacing is too small to be practical, and it is necessary to move away from the optimum to get a more reasonable value. If the plate spacing is set at 1/32 in. while the other variables are allowed to assume their most optimum values subject to this limitation, a value of L of 3·2 in. is obtained. This is not a feasible column length. This same procedure in the open column yielded a reasonable value of 17 ft, as shown in Table 1, but with the packed column it is necessary to move farther from the optimum conditions. One way of doing this is to increase w more, but the cost is increased less if w is held constant at 1/32 in. and L is increased arbitrarily, while B and Y are allowed to assume their most optimum values subject to these limitations. As L is increased in this procedure, B and Y decrease, approaching in the limit a Y of zero, signifying no packing at all, and the L and B obtained in the open column for a w of 1/32 in. As one example, a feasible column length of 2·5 ft is shown in Table 1.

There is one interesting characteristic of the permeability k obtained in all of these cases, and that is the fact that it is high enough to restrict the type of packing that may be used. A permeability of 2×10^{-6} cm^2 may be attained with uniform spheres of diameter 0·02 in., for example, but this size sphere is much too large for the 1/32 in. plate spacing. Smaller spheres will of course have a smaller permeability, and so it is necessary to use a different type of packing, such as the glass wool used successfully by Debye [2] and Sullivan *et al.* [9].

The advantage of putting packing in a thermal diffusion column has been stated to be that one may operate at large plate spacings and get separations identical to those obtained at small plate spacings in the open column, and thus avoid the necessity of careful column construction. This is true, and for research columns is a decided advantage. However, the calculations above show that for economic operation, industrial packed columns will have to have about the same plate spacing as open columns, and therefore the constructional advantage is lost. Further, the costs are roughly equivalent. The packed column has a slight advantage if the void fraction is high,

but this is probably not worth the extra trouble of dealing with the packing. It must be concluded that for industrial operations the packed column has no advantage over the open column. This and the other conclusions above are of course tentative, for the packed column equations have not been experimentally verified.

Notation

a_1 = fixed charges per unit area of column
a_2 = operating cost factor
a_3 = cost of heat per B.t.u.
B = width of column, perpendicular to x and z directions
c = concentration of a component of a mixture, mole or weight fraction
c_0 = centreline concentration at a particular z
D = diffusion coefficient
g = acceleration of gravity
H = constant in transport equation, equation (9)
J_x = horizontal mass flux of a component of the mixture
k = permeability of packing
K = constant in transport equation
L = vertical height of column, in the z direction
ΔP_f = friction loss in packed column in isothermal flow
q = separation factor
T = absolute temperature
$\bar{T}$ = arithmetic mean of plate temperatures
ΔT = difference between plate temperatures
v = vertical convection velocity at a point
w = half the distance between the plates
x = horizontal distance co-ordinate
$y = x/\sqrt{k}$
$Y = w/\sqrt{k}$
z = vertical distance co-ordinate
α = thermal diffusion constant
$\beta = -\partial\rho/\partial T$
Δ = concentration difference between product streams in continuous column
ϵ = void fraction of packing
λ = thermal conductivity of fluid
μ = viscosity of fluid
ρ = density of fluid
σ = rate of throughput in one section of the continuous column, half the total feed rate in the example used
τ = rate of vertical transport of one component

References

[1] Clusius K. and Dickel G. *Naturwissenschaften* 1938 **26** 546.

[2] Debye P. *Ann. Phys.* 1939 **36** 284.

[3] Waldmann L. *Naturwissenschaften* 1939 **27** 230.

[4] van der Grinten W. *Naturwissenschaften* 1939 **27** 317.

[5] Furry W. H., Jones R. C. and Onsager L. *Phys. Rev.* 1939 **55** 1083.

[6] Brewer A. K. and Bramley A. *U.S. Pat.* 2258594. Oct. 14 1942.

[7] Debye P. and Bueche A. M. *High Polymer Physics* (Edited by Robinson, H. A.) p. 497. Chemical Publishing Co., Brooklyn 1948.

[8] Powers J. E. and Wilke C. R. *Amer. Inst. Chem. Engrs. J.* 1957 **3** 213.

[9] Sullivan L. J., Ruppel T. C. and Willingham C. B. *Industr. Engng. Chem.* 1957 **49** 110.

[10] Jones R. C. and Furry W. H. *Rev. Mod. Phys.* 1946 **18** 151.

[11] Krasny-Ergen W. *Phys. Rev.* 1940 **58** 1078.

Chemical Engineering Science, 1959, Vol. 11, pp. 24 to 34. Pergamon Press Ltd., London. Printed in Great Britain

Influence of the structure of a silicotungstic acid on silica gel catalyst on catalytic activity

J. M. Oelderik and H. I. Waterman
Institute of Chemical Technology, Delft

(*Received* 6 *January* 1959)

Abstract—Silicotungstic acid on silica gel is a very active solid acid catalyst.

The influence of a number of variables in the preparation of the catalyst has been studied. A simple method for determining its activity has been developed and used to investigate the effect of different pretreatments given to some silica gels as well as the influence of the percentage of silicotungstic acid and of particle size.

It was found that the silica gel with the largest average pore diameter gave the most efficient catalyst. This gel had the smallest specific surface area. The catalytic activity increased substantially as the catalyst particle size was reduced, indicating that only a minor part of the catalyst particles is accessible to the reactants. This conclusion was confirmed by the results of disproportionation experiments performed with cumene. The throughput could be increased about 10 times – the percentage of cumene conversion remaining constant – when the particle size was reduced by a factor of 7. It appeared that 90 per cent of the equilibrium conversion could still be obtained at the extremely high L.H.S.V. of 40 l/hr l., using a catalyst sieve fraction of 0·3–0·6 mm. The diameter of a silicotungstic acid molecule and the surface area of a monomolecular layer formed by 1 g of this acid as calculated from crystallographic data were found to be 10 Å and 200 m^2, respectively.

Résumé—L'acide silicotungstique sur le gel de silice constitue un catalyseur acide hétérogène très actif.

On a examiné l'influence d'un nombre de variables qui jouent dans la préparation du catalyseur. On a mis au point une méthode simple pour déterminer son activité et pour étudier l'effet de différents traitements préliminaires auxquels certains gels de silice ont été soumis et l'influence du pourcentage d'acide silicotungstique et de la taille des particules.

Il a été trouvé que le gel de silice ayant le plus grand diamètre moyen des particules a donné le catalyseur le plus efficace. Ce gel avait la surface spécifique la plus petite. L'activité catalytique augmentait considérablement à mesure que les dimensions des particules du catalyseur étaient plus petites, ce qui indique que seulement une faible partie des particules du catalyseur est accessible aux réactants. Cette conclusion a été confirmée par des résultats des expériences de disproportionnement effec uées sur le cumène. Le débit a pu être augmenté de dix fois – le pourcentage de conversion du cumène restant constant alors que les dimensions des particules ont été réduites d'un facteur de 7. Il est apparu que 90 pour cent de la conversion d'équilibre a encore pu être obtenu à une vitesse de 40 l. cumène/l. catalyseur hr avec une fraction du catalyseur obtenue sur tamis de 0·3–0·6 mm. Calculés à partir de donnes crystallographiques le diamètre d'une molécule d'acide silicotungstiqu eet la surface d'une couche monomoléculaire formée par 1 g de cet acide, sont de 10 Å et de 200 m^2 respectivement.

Zusammenfassung—Kieselwolframsäure auf Silicagel ist ein sehr wirksamer heterogener saurer Katalysator.

Der Einfluss einer Anzahl Variablen bei der Herstellung dieses Katalysators wurde untersucht. Eine einfache Methode zur Bestimmung seiner Wirksamkeit wurde entwickelt, mit deren Hilfe sowohl der Effekt verschiedener Vorbehandlungen einiger Silicagele als der Einfluss des Prozentsatzes an Kieselwolframsäure und der Korngrösse untersucht wurde.

Es stellte sich heraus, dass das Silicagel mit dem grössten durchschnittlichen Porendurchmesser den wirksamsten Katalysator lieferte. Dieses Gel besass die kleinste spezifische Oberfläche. Die katalytische Wirksamkeit zeigte eine erhebliche Steigung bei abnehmender Korngrösse des Katalysators, was darauf hindeutete, dass nur ein sehr geringer Teil der Katalysatorteilchen

für die Reaktionsteilnehmer zugänglich ist. Diese Folgerung fand ihre Bestätigung in den Ergebnissen von mit Cumol durchgeführten Disproportionierungsversuchen. Der Durchsatz liess sich – bei prozentual gleichbleibender Cumolumsetzung – auf etwa das Zehnfache steigern, wenn die Korngrösse um einen Faktor 7 verkleinert wurde. Es ergab sich, dass beim ausserordentlich hohen Durchsatz von 40 l. Cumol/l. Katalysator/St der Gleichgewichtsumsatz mit einem Katalysator-Korngrösse von 0,3–0,6 mm doch noch bis zu 90 per cent erreicht werden konnte. Aus kristallographischen Daten wurden der Durchmesser der Kieselwolframsäuremolekel und die Oberfläche einer monomolekularen Schicht aus 1 g dieser Säure ermittelt; die gefundenen Werte waren 10 Åbzw. 200 m².

Introduction

A great number of investigations carried out in the Laboratory of Chemical Technology of the University of Technology at Delft have shown that silicotungstic acid is a very active catalyst in many reactions proceeding under the influence of acid catalysts, such as polymerization of propene [1] and ethene [2], hydration of propene and ethene [3], dehydration of alcohols [4], alkylation of aromatic compounds with olefins [5], transalkylation of polyalkylbenzenes with benzene [5], etc.

Evidence has been obtained [1, 2] indicating that a given amount of silicotungstic acid acquires a greater catalytic activity when applied to a porous carrier. Verstappen [1] used Surinam bauxite for this purpose. Klinkenberg [2] has proved that increased activity can be obtained with silica gel as a carrier.

Further to these investigations we have attempted to provide some insight into the structure of the silicotungstic acid on silica gel catalyst.

The work described here is far from complete, since the study of a solid, porous catalyst has so many aspects that results can only be obtained by selecting a limited number of variables.

The main object of the investigation was to find a method of reproducibly preparing a silicotungstic acid on silica gel type of catalyst, so as to enable alkylation and transalkylation processes to be studied with the aid of a standardized catalyst.

Measuring Catalyst Activity

1. *Method*

The activity of a catalyst is measured by the rate at which it causes a certain chemical reaction to proceed. It is tested preferably in the reactions for which the catalyst is intended. In the present case these were the alkylation of benzene with propene, of cumene with propene and transalkylation of poly*iso*propylbenzenes with benzene. It has appeared, however, that a silicotungstic acid on silica gel catalyst that was active in the polymerization of olefins has a similar effect on the hydration of olefins, the dehydration of alcohols, the alkylation of aromatic compounds with olefins, etc.

The activity of a catalyst accelerating a great many reactions, is determined preferably in that reaction which combines the best indication with a minimum of experimental difficulties. Such difficulties may arise from the equipment or its operation, the availability of base materials (and the purifications involved), analysis of the reaction product and determination of the conversion, serving as a measure of the activity.

At first we determined the activity of a catalyst in the polymerization of ethene as follows:—

A steel autoclave (capacity: 250 ml) was filled with 20 g of catalyst and evacuated by means of a water jet air pump and weighed. Next, 40 g of ethene was introduced under pressure (approx. 55 atm at room temperature). The rotating autoclave was brought to a temperature of 250°C within 20 min and kept at this temperature for exactly 1 hr. After cooling down in a stream of compressed air, unconverted ethene was drawn off and the autoclave was weighed again. The ethene conversion was calculated from the ratio of ethene converted to total quantity of ethene introduced. This method does not take into account the loss—during drawing off—of any C_4-fraction formed and of volatile C_5 compounds.

A drawback of this method is that a difference in weight of 30–35 g is determined by weighing

an autoclave of 20–30 kg. The pressure drop in such a vessel cannot be measured with great accuracy either. The manometers must have a measuring range of at least 400 atm and they are subjected to temperature changes and shocks.

Prompted by a remark made by Tamele [6] and a somewhat more detailed article by Johnson [7], we decided, in order to circumvent the above difficulties, to adopt the method they propose for measuring the activity of cracking catalysts.

Johnson gives the following description of the procedure:— The polymerization rate of propene is determined in an all-glass system (capacity: 75 ml) by measuring the pressure drop with the aid of a mercury manometer. The reaction vessel is kept at 200°C, the initial propene pressure being 193 mm Hg. The experiment is carried out with a 100-mg sample of cracking catalyst (14–28 mesh) dried at 200°C for 1 hr.

No particulars are given about equipment and experimental procedure.

The apparatus we used for the activity measurements (see Fig. 1) is made entirely from pyrex glass and consists of two vertical cylinders, placed side by side, with a capacity of about 0·5 l. each; they are connected at the top by a short capillary (internal diameter: 3 mm), which can be closed by a cock.

In the left-hand vessel, at the top, there is an opening through which a small cylinder of coarse gauze, suspended from a glass hook at the ground-in stopper, can be introduced into the vessel. The right-hand vessel is connected with a closed mercury manometer, about 70 cm long, from which, by means of a vernier, the pressure in the apparatus can be read to within 0·1 mm. A cock at the top of this vessel closes the inlet to a line which, via a three-way cock, may be connected either to a vacuum pump or to a propene cylinder. The whole apparatus is immersed in a thermostatic oil bath up to the stopper and the two cocks.

The activity is measured as follows:—

The oil is brought to a temperature of 150°C. The cylinder, filled with the catalyst, is introduced into the left-hand vessel. Thereupon the apparatus is put under vacuum for 30 min to dry the catalyst. After drying the apparatus is closed. The pressure (0·01–0·1 mm of Hg) does not appreciably rise within a period of 15 min (the time generally required for one measurement). This is at the same time a check on possible leakage.

Next the cock between the two vessels is closed and propene is admitted to the right-hand

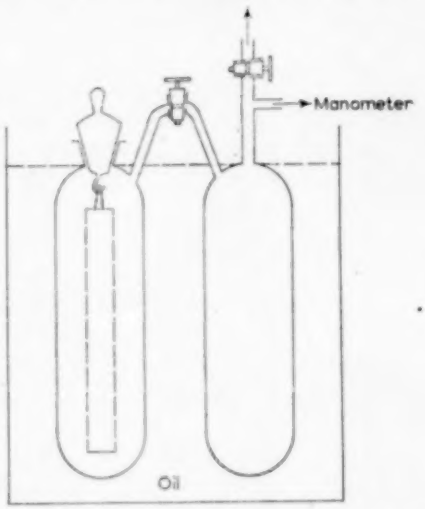

Fig. 1. Equipment for activity measurements propene cylinder and vacuum pump manometer.

vessel till the pressure has reached such a value that, after closing the supply line and opening the cock between the vessels, the pressure in the entire vessel, i.e. the initial polymerization pressure, is 200 mm Hg. The pressure required for this purpose in the right-hand vessel has been accurately determined by calibration, with a corresponding volume of inert silica gel in the small cylinder. Maximum variations in the initial pressure were only between 199·6 and 200·4 mm. As compared with the initial pressure these variations are negligible.

As the cock between the two vessels is opened, a stopwatch is started and the periods during which the pressure in the apparatus drops, e.g. 30·0, 40·0, etc. mm Hg below the initial pressure, are recorded.

The periods required to obtain equal pressure drops increase very rapidly with time, because the catalyst surface becomes covered with reaction products.

According to JOHNSON the reaction proceeds according to the equation:—

$$dx/dt = k\,(a - x)/(1 + bx)$$

where x = pressure drop in mm Hg;
t = time in sec;
a = initial pressure in mm Hg;
b = a constant;
k = activity constant in sec^{-1}.

This equation is a special version of the equation derived, among others, by LAIDLER [8] for first order reactions occuring on the surface of a solid catalyst and inhibited by reaction products formed. HINSHELWOOD and PRICHARD [9] have applied the same formula to the catalytic decomposition of N_2O at a platinum surface, giving constant values for k and b.

The latter are determined by plotting x/t against $(1/t)\log[a/(a-x)]$, according to the integral formula:—

$$\frac{x}{t} = \frac{1}{t}\left(a + \frac{1}{b}\right)\ln\left(\frac{a}{a-x}\right) - \frac{k}{b}$$

In this way a straight line is obtained with a slope of 2·3 $(a + 1/b)$, the intercept on the x/t-axis being $-k/b$. The value of b is calculated from the slope and, next, the value of k from the intercept. When plotting our values of x/t against $(1/t)\log[a/(a-x)]$, however, we did not obtain a straight line. From the observations made, no constant values could be derived for k and b either graphically or by calculation. We therefore concluded that the proposed equation for the reaction velocity was not applicable in our case. When the results obtained by JOHNSON were studied in more detail, it appeared that his observations, too, were not in conformity with the equation

$$x/t = 2{\cdot}3\,(1/t)\,(a + 1/b)\log[a/(a-x)] - k/b.$$

For, whereas according to this equation the slope of the line is at least 2·3 a, in all cases where reasonable pressure drops (e.g. down to 50 per cent of the initial pressure) occurred, JOHNSON obtained smaller slopes.

Attempts to draw up an equation for the reaction velocity in conformity with the observations and from which an activity constant could be calculated, remained unsuccessful. We are therefore unable to express the activity of a catalyst in a simple figure. It appeared, however, that a catalyst causing a rapid pressure drop in the testing apparatus, also induced a high alkylation and dehydration velocity.

For a number of catalysts Table 1 gives the periods required to reach given pressure drops.

Before considering the experimental results, we shall first discuss the base materials and the method of preparing the catalyst.

2. *Base materials and method of preparing the catalyst*

(*a*) *Silicotungstic acid.* Silicotungstic acid [10, 11] is generally considered to be represented by the formula $H_4SiW_{12}O_{40}\,n$ aq. (molecular weight in the presence of 5 molecules of crystallization water: 2969). The acid can be prepared by adding hydrochloric acid to a solution containing water glass and sodium tungstate:—

$$12\,Na_2WO_4 + Na_2SiO_3 + 26\,HCl \rightarrow H_4SiW_{12}O_{40}\,n\,H_2O + 26\,NaCl + (11-n)\,H_2O.$$

This preparation was carried out according to the directions given by BOOTH [10]. A reproducible product was obtained which, used as a catalyst under identical conditions, invariably produced the same result.

After drying at 120°C for 48 hr the acid contains about 5 molecules of crystallization water. It is a stable, non-hygroscopic substance, which can be easily dissolved in water.

At temperatures over 300°C, the acid begins to decompose into WO_3 and SiO_2; silicotungstic acid itself therefore cannot be used in reactions which require temperatures of 300°C and higher.

A survey of the very extensive literature on silicotungstic acid is given in [11].

(*b*) *Silica gel.* The structure of silica gel has been widely investigated [12]. These studies have revealed that silica gel is composed of small particles or micelles. The great porosity of silica gel indicates that these particles have only few points of contact. Thus, owing to variations in shape, dimensions and structure of the primary particles and in their packing density there are a great many different gels. Indeed, the term

Table 1. *Catalyst : method of preparation and remarks*

	x (mm)	*t* (sec)	*duplicate t* (sec)
Experiment I.	30	37	
Gel 0.	40	78	
Untreated.	50	155	
20 % wt silicotungstic acid.	60	283	
	70	496	
	80	848	
Experiment II.	30	25	24
Gel 0, for 4 × 24 hr in 4N cold HCl changed 4 times.	40	50	51
	50	97	97
Washed with distilled water.	60	171	169
20 % wt silicotungstic acid.	70	295	296
	80	498	498
Experiment III.	30	29	31
Gel. 0, 14 days on steam-bath in regularly changed 4N HCl until acid remained colourless.	40	61	63
	50	120	124
	60	219	224
	70	391	390
Washed with distilled water.	80	689	691
20 % wt silicotungstic acid.			
Experiment IV.	30	25	25
Gel 0, 4 × 24 hr (incl. 4 × 8 hr boiling) in 4N H_2SO_4 changed 4 times.	40	50	51
	50	93	94
	60	162	166
Washed with distilled water.	70	270	273
20 % wt silicotungstic acid.	80	450	458
2·0–2·8 mm.			
Experiment V.	30	30	30
Gel 0, same treatment as in exp. no. IV.	40	61	61
	50	110	110
20 % wt silicotungstic acid.	60	195	191
2·8–3·4 mm.	70	317	311
	80	—	415
Experiment VI.	30	35	35
Gel 0, same treatment as in exp. no. IV.	40	70	70
	50	131	127
20 % wt silicotungstic acid.	60	220	217
3·4–4·0 mm.	70	355	350
	80	573	580
Experiment VII.	30	31	31
Gel 0, 4 × 24 hr (incl. 4 × 8 hr boiling) in 4N HCl.	40	67	67
	50	135	132
Washed with distilled water.	60	250	244
20 % wt silicotungstic acid.	70	440	429
2·0–2·8 mm.	80	785	760
Experiment VIII.	30	52	51
Gel 0, same treatment as in exp. no. VII.	40	107	105
	50	198	193
20 % wt silicotungstic acid.	60	348	340
3·4–4·0 mm.	70	592	590
	80	1012	1005
Experiment IX.	28	63	
Gel 0, 4 × 24 hr (incl. 4 × 8 hr boiling in 4N H_2SO_4	30	95	
	32	150	
washed with distilled water.	34	234	
1 g conc. H_2SO_4 on 20 g gel.	36	420	
3·8 g sample.			
Experiment X.	30	23	24
Gel 0, 4 × 24 hr (incl. 4 × 8 hr on steam-bath) in 4N HNO_3	40	49	48
	50	89	90
washed with distilled water.	60	154	158
20 % wt silicotungstic acid.	70	268	272
	80	466	458
Experiment XI.	30	24	24
Gel 0, treated in a separate experiment as in exp. X, 3·2 g	40	48	48
	50	91	92
carrier gave a pressure drop	60	155	157
of 2·5 mm within 12 min.	70	255	260
	80	420	430
Experiment XIII.	30	18	19
Gel I, 24 hr in 4N cold HCl	40	43	42
changed once.	50	84	84
Washed with distilled water.	60	155	158
20 % wt silicotungstic acid.	70	276	281
	80	493	500
Experiment XIV.	30	17	18
Gel I, 8 × 24 hr in 4N HNO_3,	40	38	38
changed every 2nd day.	50	78	78
8 hr/day on steam-bath.	60	149	147
Extracted with distilled water;	70	270	267
(carrier not active).	80	469	471
20 % wt silicotungstic acid.			

Table 1. *Catalyst : method of preparation and remarks*—contd.

	x (mm)	*t* (sec)	*Duplicate t* (sec)
Experiment XV.	30	19	19
Gel I, 4 × 24 hr in 4N cold	40	39	39
HCl.	50	75	77
Rinsed with tap water.	60	139	143
Washed with distilled water.	70	246	253
20% silicotungstic acid.	80	427	443
2·0–2·8 mm.			
Experiment XVI.	30	24	24
Gel I, treated as in exp. XV.	40	49	48
20% wt silicotungstic acid.	50	88	89
2·8–3·4 mm.	60	155	155
	70	265	267
	80	454	—
Experiment XVII	30	27	27
Gel I, treated as in exp. XV.	40	56	55
20% wt silicotungstic acid.	50	106	106
3·4–4·0 mm.	60	187	186
	70	329	320
	80	577	546
Experiment XIX.	30	24	25
Gel II, 24 hr in 4N cold HCl.	40	49	51
changed once.	50	92	96
Washed with distilled water.	60	161	166
20% wt silicotungstic acid.	70	269	278
	80	446	455
Experiment XX.	30	24	24
Gel II, treated as in exp. XIV.	40	48	48
20% wt silicotungstic acid.	50	91	90
	60	156	160
	70	269	271
	80	449	451

	x (mm)	*t* (sec)	*Duplicate t* (sec)
Experiment XXI.	30	65	67
Gel I, 4 × 24 hr in 4N cold	40	181	186
HCl.	50	389	390
Rinsed in tap water.	60	713	716
Washed with distilled water.	70		
2 g silicotungstic acid on 20 g	80		
of gel.			
3·52 g sample (containing 3·2 g	—		
silica gel).			
Experiment XXII.	30	22	22
Gel I, treated as in exp. XXI.	40	49	49
4 g silicotungstic acid on 20 g	50	108	106
gel.	60	201	200
3.84 g sample (containing 3·2 g	70	359	359
silica gel).	80	617	618
Experiment XXIII.	30	16	16
Gel I, treated as in exp. XXI.	40	32	32
6 g silicotungstic acid on 20 g	50	60	60
gel.	60	109	109
4.16 g sample (containing 3·2 g	70	191	193
silica gel).	80	341	336
Experiment XXIV.	30	13	13
Gel I, treated as in exp. XXI.	40	26	25
10 g silicotungstic acid on 20 g	50	46	45
gel.	60	80	78
4.80 g sample (containing 3·2 g	70	136	134
silica gel).	80	236	236

"silica gel" denotes at least an equally wide range of products as the name "hydrocarbons."

Consequently, if a more detailed description is required, some characteristics have to be mentioned. The most important of these in the case of catalysts are: the specific surface area S (in m^2/g) and the pore volume V (in ml/g), from which the average pore diameter can be calculated. For cylindrical pores $d = 4\ (V/S)\ 10^4$ Å, if V and S are expressed in the terms indicated [13].

Three types of medium-porous silica gel, denoted as gel 0, gel I and gel II, were used in the present investigation.

According to information supplied by the manufacturer (N.V. "Gembo," Winschoten, Holland), the term medium-porous silica gel comprises a gel with the following properties:

bulk density	approx.	0·50 g/cm³;
actual specific weight	,,	2·20 g/cm³;
surface area	,,	500 m²/g;
pore diameter	,,	75 Å.

Table 2

Sample	*No.*	*Specific surface area* (m^2/g of sample)	*Specific surface area* (m^2 per quantity of sample containing 1 g silica gel)	*Pore volume* (ml/g of sample)	*Pore volume* (ml per quantity of sample containing 1 g silica gel)	*Average pore diameter* (Å)
Gel I Untreated.	A	396	396	0·82	0·82	83
Gel I, 24 hr in 4N cold HCl (carrier exp. XIII)	B	417	417	0·89	0·89	85
Gel I, 4 × 24 hr in 4N cold HCl. 20% wt silicotungstic acid (catalyst exp. XV).	C	345	431	0·66	0·83	77
Gel I, treated as sample C. 6 g silicotugstic acid on 20 g gel (catalyst exp. XXIII)	D	334	434	0·64	0·83	77
Gel I, treated as sample C. 2 g silicontungstic acid on 20 g gel (catalyst exp. XXI).	E	398	438	0·79	0·87	79
Gel II, untreated.	F	487	487	0·66	0·66	54
Gel II, 24 hr in 4N cold HCl (carrier exp. XIX)	G	516	516	0·64	0·64	50
Gel 0, untreated. 20% wt silicotungstic acid (catalyst exp. I).	H	307	384	0·42	0·53	55
Gel 0, 4 × 24 hr in 4N cold HCl. 20% wt silicotungstic acid (catalyst exp. II).	K	326	408	0·47	0·59	58
Gel 0, 4 × 24 hr (incl. 4 × 8 hr on steam bath) in 4N HNO_3. 20% wt silicotungstic acid (catalyst exp. X).	L	331	414	0·49	0·61	59

These figures, however, merely approximate the average properties of the product manufactured by a given method. They do not refer to a particular batch. If, therefore, silica gel is used in such investigations as are described here, the relevant specific data have to be determined.

It appeared that the silica gels we used contained components giving an alkaline reaction. For this reason they were given a pretreatment with a mineral acid, washed with water and dried at 120°C.

(*c*) *Preparation of the catalyst.* (1) Silicotungstic acid is prepared according to the method given by Booth.

(2) The acid so obtained is dried for 48 hr at 120°C.

(3) The silicotungstic acid is dissolved in such an amount of water that the required quantity of pretreated silica gel can just be immersed in it. The water is evaporated in a drying oven, with occasional stirring of the slurry.

The catalyst is dried for 48 hr at 120°C.

(4) The catalyst is sieved to remove any particles which may have been pulverized during the various treatments.

3. *Results of activity measurements*

In nine measurements made on 4 g of a certain catalyst, although conditions were identical, the periods required to reach given pressure drops showed variations of 15 per cent. These were found to be due to the difference in particle size during sampling. In one sample small particles, in another large ones were predominant. After the sample had been divided into 3 fractions (2·0–2·8 mm, 2·8–3·4 mm and 3·4–4·0 mm), each sieve fraction gave duplicate determinations in which variations in time averaged 2 per cent, with a maximum of 4 per cent.

Table 1 gives a summary of the principal experimental results. Unless stated otherwise, in all cases 4 g of the sieve fraction 2·0–2·8 mm was used in the activity measurements.

4. *Specific surface area and pore volume of some carriers and catalysts*

In order to ascertain whether the structure of the silica gel is modified by the acid treatment and how its surface area and pore volume are affected by the application of silicotungstic acid, we had to gain information concerning the specific surface area and the pore volume of the silica gel used and the catalysts prepared with it.

Of a few samples these data were determined for us at Koninklijke/Shell-Laboratorium, Amsterdam, by means of nitrogen adsorption, using the B.E.T.-method.

The results of these measurements are summarized in Table 2.

5. *Discussions and conclusions*

The data given in Table 1 permit of drawing the following conclusions.

(1) It has once again been proved that the silica gel should be pretreated with a mineral acid (cf. exp. I and II).

(2) When the silica gel is treated with hydrochloric acid (exp. II), sulphuric acid (exp. IV) or nitric acid (exp. X), almost identical results are obtained when, starting from a given gel, a treatment with 4N acid, repeated four times, is applied. The effect of nitric acid seems to be slightly better than that of the other acids. Experiment XIII shows that soaking of the silica gel in cold 4N mineral acid for 24 hr is sufficient; a prolonged acid treatment or a rise in temperature do not result in an increased activity of the catalyst.

(3) Gel I, after being given the same treatment as gel 0 sample and gel II, provides the most active catalyst. The behaviour of gel II and gel 0 as carriers is about the same.

(4) Mineral acid that has remained behind in the gel hardly contributes to the activity of the catalyst. From exp. IX it appears that when adding 1 g of concentrated sulphuric acid to 20 g of gel, the resulting pressure drop is only a fraction of that caused by the addition of 4 g of silicotungstic acid to 20 g of gel.

In many experiments, among them exp. XIV, the carrier was found to be entirely inactive.

(5) *The smaller the particles, the greater the rate at which the pressure decreases.* The considerable influence of the particle diameter indicates that only a small part of the catalyst particle is accessible to propene.

(6) *The higher the percentage of silicotungstic acid, the greater the activity of the catalyst.* The catalyst with 33% of acid (cf. exp. XXIV) appears to possess the greatest activity.

From the results shown in Table 2 the following conclusions may be drawn:—

(1) The treatment with 4N acid does not appreciably influence the structure of silica gel. Compare e.g. experiments A and B, F and G.

(2) Neither does the application of silicotungstic acid have an important effect. The measurements seem to permit of the conclusion that the pore diameter has slightly decreased. Compare experiment B with C, D and E.

Combining the data shown in Tables 1 and 2 it may be concluded that the catalyst based on gel I owes its favourable properties to its average pore diameter being largest, viz. 77 Å (gel 0, catalysts 55–59 Å, gel II, 50–55 Å).

It is not the gel with the largest specific surface area that provides the most active catalyst, but that with the largest pore diameter; for the specific surface area of gel I is some 100 m^2 smaller than that of gel II.

Continuous Experiments

1. *Method and results*

The influence of two variables, viz:— (a) the percentage of silicotungstic acid and (b) the particle size of the catalyst, has been established in continuous experiments, using catalysts prepared from gel I.

(*a*) *Influence of percentage of silicotungstic acid.* The influence of this variable has been studied in the alkylation of benzene with propene. For this purpose a liquid mixture of pure benzene (m.p. 5·45°–5·50°C) and propene (98% pure) was passed over a fixed catalyst bed (particle size 2·0–2·8 mm) in a tubular reactor. Operating conditions were as follows: temperature 85°C, liquid hourly space velocity (L.H.S.V.) 16 l. liquid feed/l. catalyst/hr, benzene/propene molar ratio 4; pressure 20 atm Abs.

The results are given in Table 3.

It is seen that, just as in the standard activity test, catalyst activity increases with silicotungstic acid content.

The experiments do not establish the extent to which it is possible to continue increasing the catalytic activity by increasing the acid concentration since under the reaction conditions applied total propene conversion was obtained with 20 per cent of acid. The activity test shows that with 33 per cent of acid the activity was still increasing. This was also found by Beneken, who used the same catalyst for the dehydration of ethyl alcohol [4].

(*b*) *Influence of particle size.* The influence of the particle size has not been studied from the alkylation of benzene with propene, for the following reason. Working conditions should be such that it is still possible for the propene conversion to increase and decrease, which means low temperatures and high throughputs. The experiments have shown that within a very narrow temperature range the propene conversion increases from 0–100 per cent. A very accurate temperature adjustment is therefore necessary. With the highly exothermic alkylation reactions, however, this requirement involved so many difficulties that another reaction was chosen to study the influence of the particle size, viz. the disproportionation of cumene:

VOL. 11 1959/

Table 3. Influence of the percentage of silicotungstic acid.

No. of experiment	*Silicotungstic acid* (% wt)	*Molar ratio of benzene/propene*	*Composition of reaction product and alkylate* (% wt)								*Conversion of propene* (%)
			Benzene		*Cumene*		*d.i.b**		*Residue†*		*Polymer*		
46	2	4·02	99·4	—	0·6	100	—	—	—	—	—	—	1·6
43	5	4·12 – 4·13	84·9	—	10·6	70·4	3·1	20·3	0·8	5·2	0·6	4·1	54
42	10	4·04 – 4·09	73·9	—	18·0	68·8	5·9	22·6	1·9	7·4	0·3	1·2	93
41	10	3·86 – 3·93	73·0	—	17·5	64·9	6·3	23·5	2·9	10·6	0·3	1·0	94
40	20	3·93 – 3·99	71·6	—	19·3	68·0	6·8	23·9	2·3	8·0	< 0·1	0·1	> 98

* d.i.b. = diisopropylbenzene

† residue = tri + tetraisopropylbenzene

2 cumene ⇄ benzene + di*iso*propylbenzene

This reaction has no appreciable thermal effect.

Cumene was passed over a fixed catalyst bed in a steel tubular reactor (internal diameter 3 cm). The reaction was performed in the liquid phase at a temperature of 230°C, a nitrogen pressure of 40 atm Abs. and various throughputs. Two catalyst sieve fractions, viz. 0·3–0·6 mm and 2·8–3·4 mm were employed.

The results given in Table 4 show that the disproportionation of cumene is attended by the formation of a small amount of tri*iso*propylbenzene according to the equations:—

2 di*iso*propylbenzene ⇄ cumene + tri*iso*propylbenzene and/or

cumene + di*iso*propylbenzene ⇄ benzene + tri*iso*propylbenzene.

Besides, low throughputs give maximum cumene conversion (46–48 per cent). This points to the establishment of a kind of equilibrium between the various *iso*propylbenzenes.

As regards the influence of the particle size it may be concluded that, just as in the activity test, the use of small particles results in a greater conversion. With a particle size of 2·8–3·4 mm, a cumene conversion of about 40 per cent can still be reached with a L.H.S.V. of 2–4 l/hr l.; with particles of 0·3–0·6 mm, the said conversion can even be reached at the very high L.H.S.V. of 40 l/hr.l.

2. *Discussions and conclusions*

When considering the catalyst particles as globules, with diameters of 3·1 and 0·45 mm, the total external surface area of a given weight of catalyst consisting of particles with a diameter

Table 4. *Influence of catalyst particle size on disproportionation of cumene.*

(*Temperature :* 230°C ; *pressure :* 40 atm Abs.)

Particle size 2·8–3·4 mm							*Particle size* 0·3–0·6 mm						
Experiment no.	*L.H.S.V.* (l/hr l.)	*Composition of reaction product* (% wt)				*Cumene conversion* (%)	*Experiment no.*	*L.H.S.V.* (l/hr l.(	*Composition of reaction product* (% wt)				*Cumene conversion* (%)
		Benzene	*Cumene*	*d.i.b.*	*tri i.b.*				*Benzene*	*Cumene*	*d.i.b.*	*tri i.b.*	
6	1	15·3	53·5	27·3	3·9	46·5	19	2	16·3	51·8	28·5	3·4	48·2
5	2	12·7	60·2	23·8	3·3	39·8	15	8	16·2	51·2	29·6	3·0	48·8
8	2	12·9	60·1	24·4	2·7	39·9	14	11	14·8	53·4	29·0	2·8	46·6
22	2	12·0	60·8	26·7	0·5	39·2	17	16	16·2	51·2	30·4	2·2	48·8
7	4	13·3	59·5	25·8	2·0	40·5	18	22	15·1	53·2	29·0	2·2	46·8
11	8	10·7	67·1	21·3	0·9	32·9	20	32	14·5	56·0	28·0	1·5	44·0
12	8	10·2	66·6	22·1	1·1	33·4	21	44	13·5	58·0	26·4	2·1	42·0
9	11	7·1	75·9	16·0	1·0	24·1							
10	11	8·4	73·4	17·4	0·8	26·6							

of 0·45 mm is 3·1/0·45 = approx. 7 times as large as that composed of particles 0·45 mm in diameter.

Although, in view of the possible influence of particle size on mass transport in the catalyst bed, only tentative conclusions can be drawn, it may be stated that the reaction occurs mainly at the surface or in a very thin layer on the outside of the catalyst particles. In this connexion it is pointed out that the external surface area of a porous globule of silica gel is very much larger than that of a non-porous glass bead of the same diameter.

The above shows that with the rapid reactions occurring under the influence of the very active silicotungstic acid on silica gel catalyst these reactions are diffusion limited. There are two possibilities of eliminating this inhibiting effect:

(a) by giving the carrier the largest possible pores and

(b) by giving the catalyst particles the smallest possible dimensions.

In the latter case the use of a fixed catalyst bed imposes restrictions, because the pressure drop across the reactor increases according as the particle size decreases. For this reason it may be desirable to change over to a suspended catalyst (so-called slurry process).

Acknowledgements—The authors wish to thank the management of the Koninklijke Shell Laboratory for the assistance rendered.

Appendix

Calculation of the diameter of a silicotungstic acid molecule and of the surface area that can be covered by a monomolecular layer of silicotungstic acid of 1 g.

Crystalline silicotungstic acid 5 aq. possesses a body-centred cubic lattice. The elementary cell contains two acid molecules and the length of the edges is 12·11 ± 0·01 Å (Signer and Gross [14]). The silicotungstic acid molecules are considered as spheres touching in the space lattice, then the length of the diagonal of the elementary cell through 0, 0, 0 and 1, 1, 1 = 2 × the diameter of the silicotungstic acid molecule = $12{\cdot}11\sqrt{3}$ Å; so the diameter of a silicotungstic acid molecule is 10·5 Å.

If the molecules are arranged as in the vertical plane through the diagonal mentioned above, the surface area of a monomolecular layer formed by 1 g of acid is:—

$$(1/M)\,N\,(12{\cdot}11)\,(12{\cdot}11\sqrt{2})\,1/2\ \text{Å}^2,$$

M = molecular weight of silicotungstic acid and
N = Avogadro's number.

By substituting the numerical values it is found that 1 g of silicotungstic acid can cover an area of 211 m².

In preparing a catalyst containing 20 per cent wt of acid, 1 g of silicotungstic acid is applied to 4 g of silica gel; 4 g of gel I have a surface area of about 1600 m²; this area has been determined with the aid of nitrogen molecules. Although silicotungstic acid molecules will be unable to penetrate into all places where during the determination of the surface area nitrogen molecules could be adsorbed, it seems justified to suppose that, if 20 per cent wt of silicotungstic acid is applied, the surface of silica gel is not yet fully occupied up by a monomolecular acid layer. This is in accordance with the observation that by applying a higher percentage of silicotungstic acid the activity of the catalyst further increased.

References

[1] Verstappen J. J. Thesis, Delft 1953; Verstappen J. J. and Waterman H. I. *J. Inst. Petrol.* 1955 **41** 343, 347.
[2] Klinkenberg J. W. Thesis, Delft 1956.
[3] Muller J. Thesis, Delft 1957; Muller J. and Waterman H. I. *BrennstChemie* 1957 **38** 321, 357.
[4] Beneken, genaamd Kolmer P. M. Thesis, Delft 1958.
[5] Oelderik J. M. Thesis, Delft 1958.
[6] Tamele M. W. *Disc. Faraday Soc.* 1950 **8** 270.
[7] Johnson O. *J. Phys. Chem.* 1955 **59** 827.
[8] Laidler K. H. *Catalysis* Vol. 1 Chap. 3. Reinhold, New York 1954.
[9] Hinshelwood C. N. and Prichard C. R. *J. Chem. Soc.* 1925 **127** 327.
[10] Booth H. W. *Inorganic Synthesis* Vol. 1 p. 129. McGraw-Hill, New York 1939.
[11] Jonassen H. B. and Kirschner S. *The Chemistry of the Co-ordination Compounds* Chap. 14. Reinhold, New York 1956.
[12] Iler R. K. *The Colloid Chemistry of Silica and Silicates.* Cornell University Press, Ithaca 1955.
[13] De Boer J. H. *Advances in Catalysis* Vol. 9 p. 131. Academic Press, New York 1957.
[14] Singer R. and Gross H. *Helv. Chim. Acta* 1934 **17** 1076.

Chemical Engineering Science, 1959, Vol. 11, pp. 35 to 52. Pergamon Press Ltd., London. Printed in Great Britain

Experimental investigation of horizontal liquid films

Wave formation, atomization, film thickness

J. J. VAN ROSSUM

Koninklijke/Shell-Laboratorium, Amsterdam*

(Bataafse Internationale Petroleum Maatschappy N.V.)

(*Received* 12 *January* 1959)

Abstract—The entrainment, wave formation and atomization of horizontal films of water, aqueous solutions and oils have been investigated.

The mean film thickness measured has been compared with the theoretical film thickness for laminar liquid flow and a smooth gas–liquid interface. Over a wide range of conditions the mean actual film thickness is about 0·6 times the theoretical one.

The critical velocities for the onset of waves and atomization were determined at different liquid flow rates. The critical conditions for atomization have been analysed in two ways, in a correlation involving the Weber number (which includes the film thickness), or in a correlation involving the Reynolds number for film flow (which includes the rate of liquid flow).

Résumé—Une étude a été faite de l'entraînement, de la formation d'ondes et de l'atomisation de films horizontaux d'eau, de solutions aqueuses et d'huiles.

L'épaisseur moyenne des films mesurée a été comparée avec la valeur théorique pour le cas d'un écoulement laminaire de liquide et une interface lisse gaz–liquide. Dans un grand intervalle de conditions l'épaisseur moyenne réelle des films est d'environ 0,6 fois la valeur théorique.

Les vitesses critiques pour le commencement de la formation d'ondes et de l'atomisation ont été déterminées à des vitesses différentes d'écoulement du liquide. Les conditions critiques d'atomisation ont été analysées de deux façons : dans une corrélation comprenant le nombre de Weber (qui implique l'épaisseur du film) ou dans une corrélation comprenant le nombre de Reynolds pour l'écoulement du liquide (qui implique la vitesse d'écoulement du liquide).

Zusammenfassung—Das Mitschleppen, die Wellenbildung und die Zerstäubung horizontaler Häutchen von Wasser, wässrigen Lösungen und Ölen wurden untersucht.

Die gemessene mittlere Schichtdicke wurde mit dem theoretischen Wert bei laminarer Strömung einer Flüssigkeit und flacher Grenzfläche zwischen Gas und Flüssigkeit verglichen. Unter weit verschiedenen Bedingungen ist die mittlere wirkliche Schichtdicke etwa 0,6 der theoretischen.

Die kritischen Geschwindigkeiten für den Beginn der Wellenbildung und Zerstäubung wurden bei verschiedenen Fliessgeschwindigkeiten der Flüssigkeit gemessen. Die kritischen Bedingungen der Zerstäubung wurden in zwei Weisen analysiert, und zwar in einer Beziehung mit der Weberzahl (die die Schichtdicke miteinbezieht) und in einer Beziehung mit der Reynoldszahl für Schichtströmung (die die Strömungsgeschwindigkeit der Flüssigkeit miteinbezieht).

1. INTRODUCTION

WHEN a gas flows over a liquid which is initially at rest or in slow motion three successive stages of the interface can be distinguished when the gas velocity is increased:

1. the interface is flat,
2. the interface is wavy,
3. the interface is wavy and liquid is atomized from the wave tops.

These three stages can easily be observed in nature on rivers or lakes (cf. Figs. 8 and 9).

The case where liquid at rest or in motion is in contact with a flowing gas or vapour occurs in various equipment in use in the field of chemical engineering, e.g. in furnace tubes, transfer lines, film evaporators, condensers, packed towers and gas–liquid separators. In most cases, atomization of liquid must be prevented in order to reduce

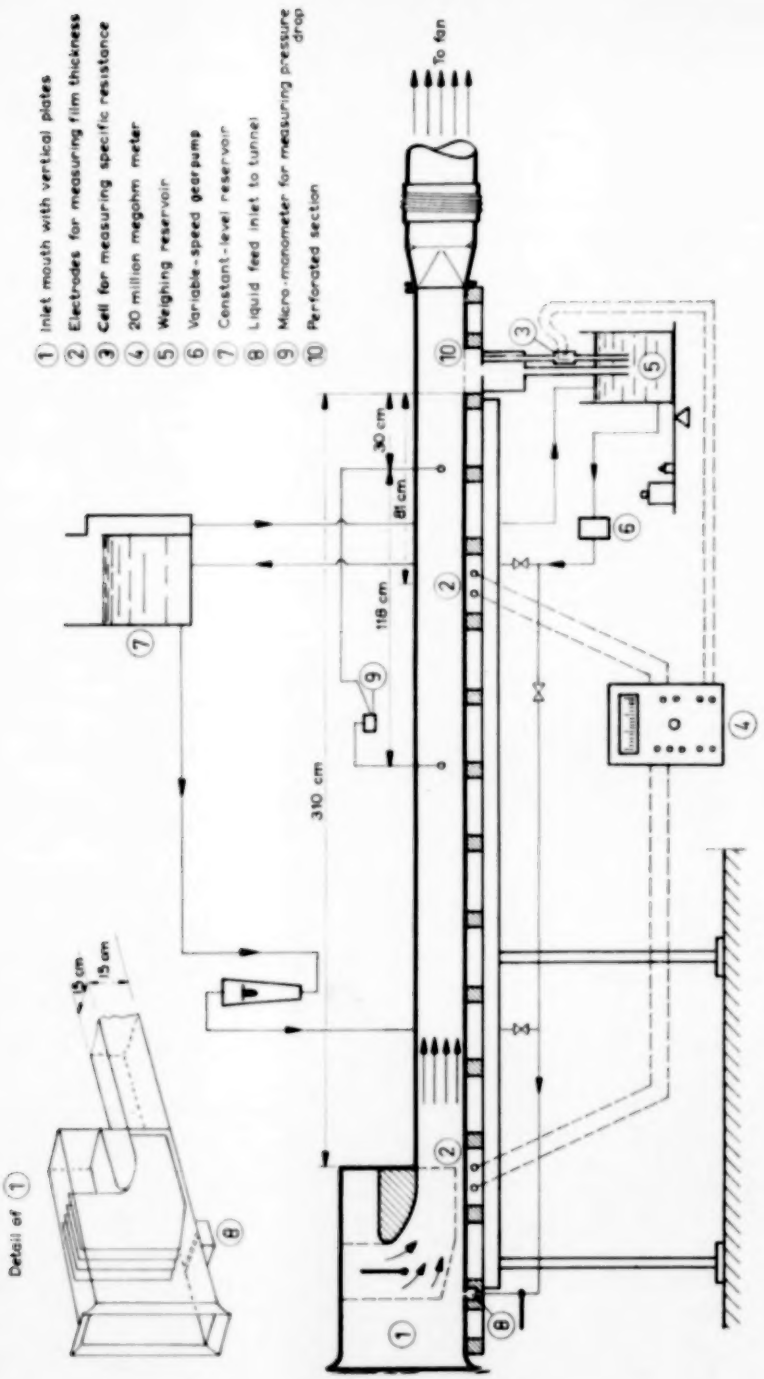

FIG. 1. Wind tunnel of transparent plastic.

liquid entrainment as much as possible. In literature, theoretical and experimental data on wave formation are scarce and no information at all could be found concerning the critical velocities at which atomization of a gas–liquid interface begins. In an attempt to fill this gap in our knowledge a number of experiments have been carried out.

II. Experimental Set-up

II. 1. *General*

A small wind tunnel was made of transparent plastic, 15 × 15 cm in cross-section and 310 cm long, see Fig. 1. In order to avoid vibrations, the tunnel was set on a heavy concrete foundation, and the connexion leading to the fan was made flexible. It was carefully placed horizontally. The upper wall was provided with a number of removable covers. Air was sucked through the tunnel at a velocity which could be varied from 2 to 65 m/sec by closing a by-pass valve. The air entered through a streamlined inlet mouth [(1) of Fig. 1], which had four vertical plates in order to free the inflowing air from large vortices. The flow of air was determined by means of a measuring orifice located between the tunnel and the fan. For the measurement of pressure drop, pressure taps were mounted in the second half of the tunnel with a distance of 118 cm between them.

Liquid was supplied through a slit (8) extending over the whole width of the bottom of the tunnel. The width of the slit was 1 mm, and, in some experiments where liquid flow rate was high, 12 mm. It was located in the inlet mouth where the mean air velocity was one third of that in the tunnel. The liquid was entrained and accelerated by the incoming air until it arrived at steady flow conditions in the tunnel. A constant head of liquid was ensured by means of a constant-level reservoir (7) with surplus surge. The liquid flow rate was measured by means of a rotameter which was regularly calibrated by weighing the flow over a given time. Total liquid flow rates were between 2·5 kg/hr and 1500 kg/hr. At the end of the tunnel the liquid was recovered through a perforated section (10) in the bottom of the tunnel; at low liquid flow rates the liquid simply drained through the perforations, but at high flow rates it was necessary to suck it through.

II. 2. *Device for measurement of film thickness*

The thickness δ of the liquid film is derived from the electrical resistance R of the liquid film between two thin platinum electrodes glued at some distance from each other on the bottom of the tunnel, see Fig. 2. By calibration of the device (see below) a certain resistance measured can be related directly to the liquid height above the electrodes. In order to eliminate temperature effects, the resistance R is compared with a reference resistance r of the liquid at the prevailing temperature. r is measured between two platinum plates in the draining liquid at the end of the tunnel [(3) in Fig. 1]. In all experiments the difference in temperature between the liquid at the measuring electrodes and that of the draining liquid was less than 1°C. The resistances were measured using a 20 million MΩ meter (Electronic Instruments Ltd.). During experiments with water a Philips conductivity measuring bridge was used. As the specific resistance of the oils used was too high for reliable measurements, it was lowered by doping. Thus the resistance was reduced from about 10^{13} to 10^{9}–10^{8} Ω cm depending on the viscosity of the oil. The effect of leakage-resistance was eliminated by a series of suitable measurements.

The calibration of the measuring device was carried out on stagnant liquid films over the measuring electrodes. The measuring section of the tunnel was for this purpose separated from the rest by means of dams so that a layer of liquid of varying thickness could be produced by introducing a variable amount of liquid between the dams. The film thickness was then measured with a micrometer as well as by the resistance method. To avoid disturbances in the electrical field it was necessary to locate the dams on both sides at a distance of at least 8 cm from the electrodes. It was checked that it made no difference to the results whether the liquid was stagnant or whether it was continually refreshed by a small overflow, thus approaching more or less the conditions of the actual film thickness measurements.

Calibrations were performed before and after

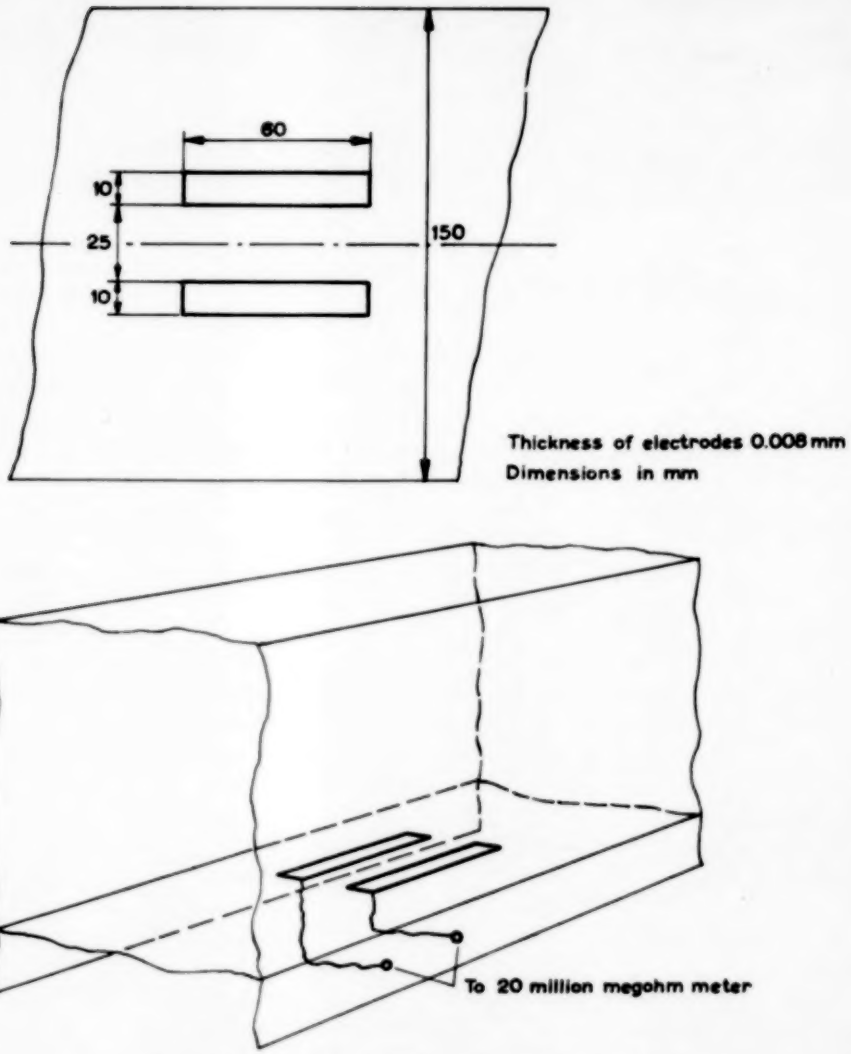

FIG. 2. Platinum electrodes for measuring film thickness.

each series of measurements. With the arrangement shown in Fig. 2 the film thickness was found to be: $\delta = \text{constant} \times r/R$, with the constant of the order of 0·4 for δ up to 0·3 cm. For $\delta > 0{\cdot}3$ cm the constant increased with increasing δ. By means of a plastic model of two-dimensional waves placed in the liquid at different heights above the electrodes it was checked that the real mean film thickness is measured, provided the wave crests are parallel to the direction of the electrical current. Using the method described, film thickness could be measured within $\pm$ 5 to 10 per cent, the largest deviations occurring at the smallest film thickness.

III. EXPERIMENTAL PROCEDURE AND PRELIMINARY MEASUREMENTS

Measurements were made using water, aqueous solutions and oils of various viscosity. During each run the liquid flow rate was kept constant. While the air flow rate was gradually increased,

the air mean velocity, the liquid flow rate and the liquid film thickness were determined. In all our measurements the slip between the air and the liquid was so large that the liquid velocity could be neglected with respect to the air velocity.

Attention was given to wave formation in a separate series of measurements on water and a mineral oil. At very low air velocities the air–liquid interface is flat or may show small irregular motions; the air velocity at which regular two-dimensional waves become distinctly visible was taken as the critical velocity for wave formation. With water two sets of measurements were carried out, one with a stagnant film retained between dams at both ends of the tunnel and one with the film entrained by the air stream.

At sufficiently high air velocity a situation is reached where atomization takes place. The onset of atomization could clearly be observed by looking through the air inlet mouth towards the end of the tunnel; with the film illuminated by a bright flood-light, the tearing-off of drops is easily seen against the dark background of the tunnel end. By illuminating different sections of the tunnel, it was found that, at a certain velocity, atomization starts near the inlet and, on increasing the velocity slightly, it spreads over the whole length. The velocities given in this paper for the onset of atomization refer to conditions where atomization was first observed over the whole tunnel length.

In order to check whether entrance conditions have an effect on the critical velocity for atomization, a venturi-like constriction was built in the wind tunnel having its throat at the location of the platinum electrodes for measuring film thickness (Fig. 3). The critical velocities for atomization in this constriction were found to be equal to those measured in the tunnel.

The film thickness was measured 81 cm from the end of the tunnel and in some experiments also in the throat of the air inlet. At air velocities lower than 20 m/sec the film thickness at the latter location was somewhat larger than that measured at the end of the tunnel. At higher velocities no difference was noticeable. The film thickness in the central part of the tunnel was found to be slightly larger than near the sides and it was observed that atomization always started in the central region. All δ-values were therefore measured in the central part of the tunnel.

In the experiments with oil, the bottom of the tunnel was cleaned with benzene and, since the plastic used is well wetted by oil, a continuous film was obtained down to the smallest film thickness. With water, however, dry spots appeared and the wettability of the plastic was increased by coating with a 5 per cent solution of polyvinyl-alcohol in water and subsequent hardening of this coating with a 4 per cent formalin solution in water.

A few additional experiments were made in which the bottom wall of the tunnel was roughened. In order to arrive at a well-defined roughness, plastic spheres of diameters between 0·5 and 0·75 mm were glued on the bottom, about 160 spheres per cm². The relative roughness (ϵ/D_H with $D_H = 15$ cm) so obtained is of the order of 0·004.

The shear stress τ_b at the bottom of the tunnel (with or without liquid film) was calculated from

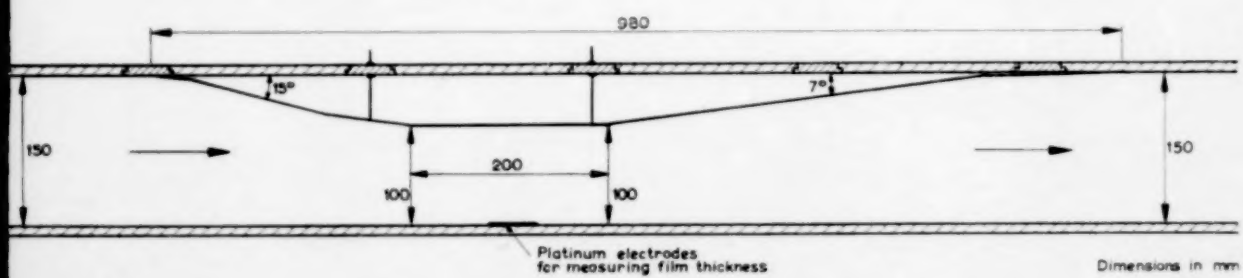

FIG. 3. Venturi-like constriction in wind tunnel.

the equilibrium of forces of that part of the tunnel over which the drop in pressure was measured; for the three smooth walls the shear stress according to that measured with four smooth walls (Fig. 10) was taken. From τ_b the coefficient of friction is obtained from the formula:

$$\lambda_b = 4 \cdot \frac{\tau_b}{\frac{1}{2}\rho_g V^2}.$$

This procedure gave for the dry rough tunnel bottom $\lambda_b = 0{\cdot}028$ at a Reynolds number of 2×10^5. This value compares well with $\lambda = 0{\cdot}029$ reported by NIKURADSE [1] for rough pipes with a relative sand roughness of 0·004.

In all experiments the total rate of liquid flow Q was measured. In view of a more general application it is desirable to know the rate of flow q per unit of width in the central part of the tunnel where the film thickness is measured. Since the variation of the liquid velocity distribution over the tunnel width is not known, the conversion factor qB/Q has been determined experimentally for several of the liquids used. To this end, plates were set on the perforated section at the end of the tunnel thus permitting separate measurement to be made of the rate of flow of liquid over a width of 4·5 cm in the central part of the tunnel where the distribution of liquid velocities is assumed to be constant. The result is shown in Fig. 4 as a function of the liquid's viscosity. All the values of q reported below have been obtained from the measured total rate of flow Q using the mean conversion curve of Fig. 4.

It was to be expected that qB/Q would be

VOL 11 1959/

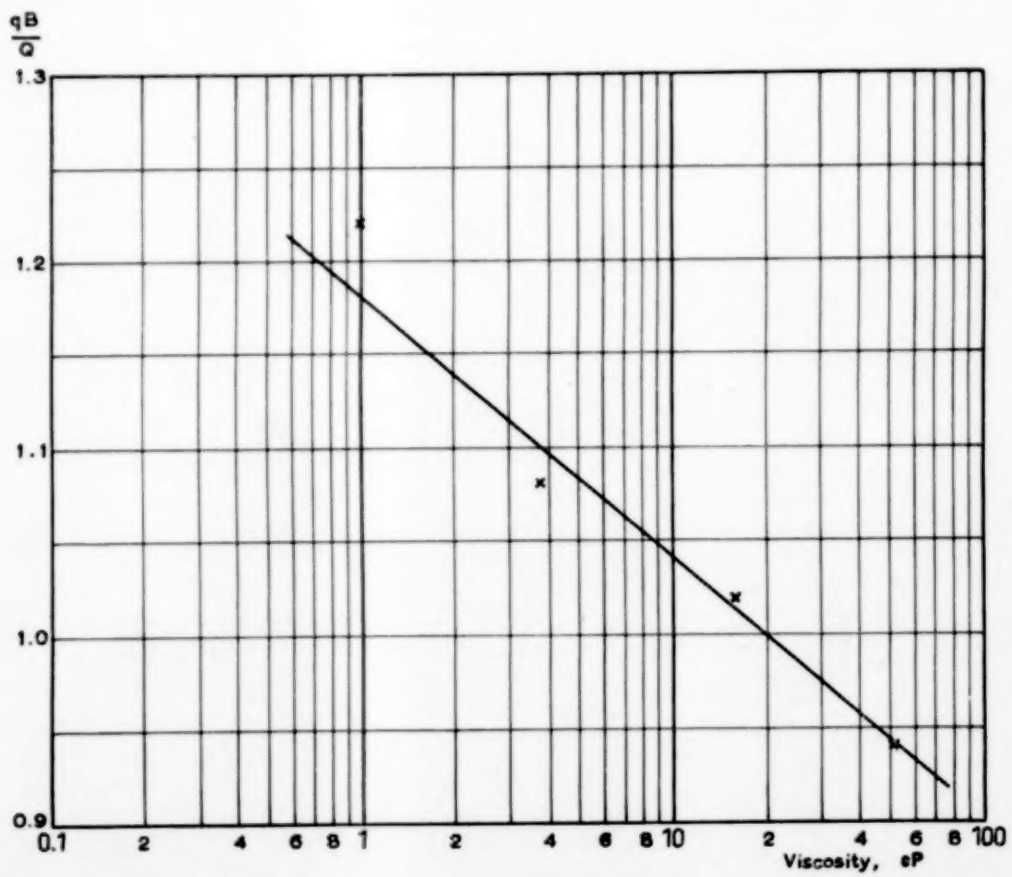

FIG. 4. Conversion factor for the rate of flow per unit of width as a function of liquid viscosity.

greater than unity ; we have no explanation for the value of 0·94 obtained with the most viscous liquid.

Finally, the distribution of air velocities in the vertical direction was determined at 270 cm from the tunnel inlet using a small pitot tube, in order to find out whether fully developed flow conditions are obtained. The results are shown in Fig. 5. For comparison the velocity distribution for fully turbulent flow along smooth walls according to VON KÁRMÁN has been added to Fig 5. The agreement is reasonable. This result is in accordance with the pressure drop results reported in section V.2, which agree with data given in literature for fully developed turbulent flow in pipes.

IV. LIQUIDS USED IN THE EXPERIMENTS

All the relevant physical properties of the liquids at the operating temperatures are collected in the following table. The oil resistance was lowered (see section II.2) by doping.

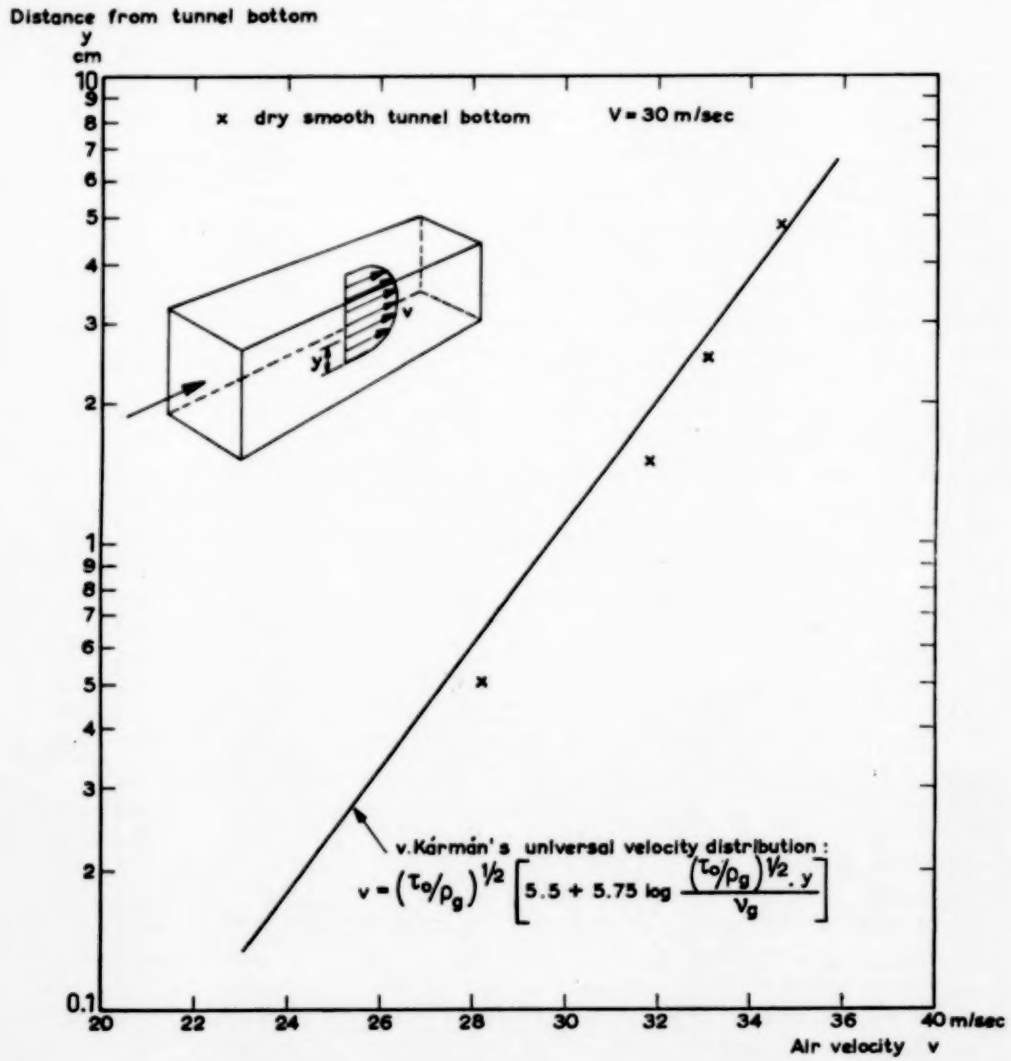

FIG. 5. Velocity distribution 270 cm from the inlet of the wind tunnel $Re_{tunnel} = 3 \cdot 10^5$ (smooth walls)

Table 1. *Physical properties of the liquids used*

Liquid	*Operating temp.* (°C)	*Density* (g/cm³)	*Surface tension* (dyne/cm)	*Viscosity* (*cP*)
Mineral oil 1	20	0·86	30	51
Mineral oil 2	17	0·87	30	28
Mineral oil 3	20	0·85	30	16
Gas oil	19	0·83	31	3·8
Kerosine	19	0·80	32	1·5
Water + 7 per cent butanol	18	0·99	31	1·4
Water + 3·7 per cent butanol	14	1·00	40	1·4
Water + 1·5 per cent butanol	15	1·00	50	1·3
Water	16	1·00	73	1·1

V. Discussion of the Experimental Results

V.1. *Wave formation and onset of atomization*

The critical air velocities for wave formation were determined with water and mineral oil 3, the liquid films being entrained by the air stream. The critical velocities for oil and water respectively, are shown in Figs. 6 and 7 as a function of film thickness. Examples of the wave patterns at velocities slightly above critical are shown in Fig. 8a and 9a. Measurements have also been carried out with a stagnant film of water (Fig. 7).

The critical air velocities for atomization of the liquid films and for the formation of waves, show similar trends, as can be seen from Figs. 6 and 7. The results obtained with mineral oil 3 and water and with the other liquids have been correlated in two different ways as shown in Figs. 10 and 11 and are discussed below (Section VI. 1).

Figs. 6 and 7 show that there is a wide gap between the critical air velocity for wave formation and the critical velocity at which atomization starts. It is seen that both critical velocities tend to a constant value for very thick films sometimes called "deep water." These "deep water" conditions are reached at a smaller film thickness for atomization than for wave formation. Jeffreys [2] developed a theory of the formation of waves under "deep water" conditions. The waves generated are of the gravity type and the effect of surface tension can then be ignored. Jeffreys found:

$$V_{\text{crit}} \left(g \nu_l \frac{\rho_l - \rho_g}{\rho_g} \right)^{-1/3} = \text{constant.}$$

The numerical value of the constant was determined from observations in nature and Jeffreys found 4·7 for it. Other investigators report velocities that are higher than those following from Jeffreys' relation; for a survey of the various data see Ursell [3].

The critical air velocities for wave formation calculated from Jeffreys' formula have been included in Figs. 6 and 7 for the purpose of reference. Jeffrey's formula is not applicable to our experiments, the waves generated on the shallow films being of much shorter length, so that surface tension must have an effect.

A few experiments were carried out to find the effect of surface-active agents on wave formation. With an entrained water film 0·6 mm thick V_{cr} was increased from 7 m/sec to 10 m/sec by adding 1 per cent of a synthetic wetting-agent, "TEEPOL 410" (cf. Keulegan [4]).

Measurements of wave formation on entrained water films by Hanratty and Engen [5] agree with our results as to the order of magnitude, but show a wide spread. The measurement of film thickness in Hanratty and Engen's experiments, however, was not completely satisfactory, as was already mentioned by the authors in their paper.

The effect of wall roughness on atomization was studied with mineral oil 2 at only one liquid flow rate of $q = 0{\cdot}655$ cm²/sec. Both with the smooth

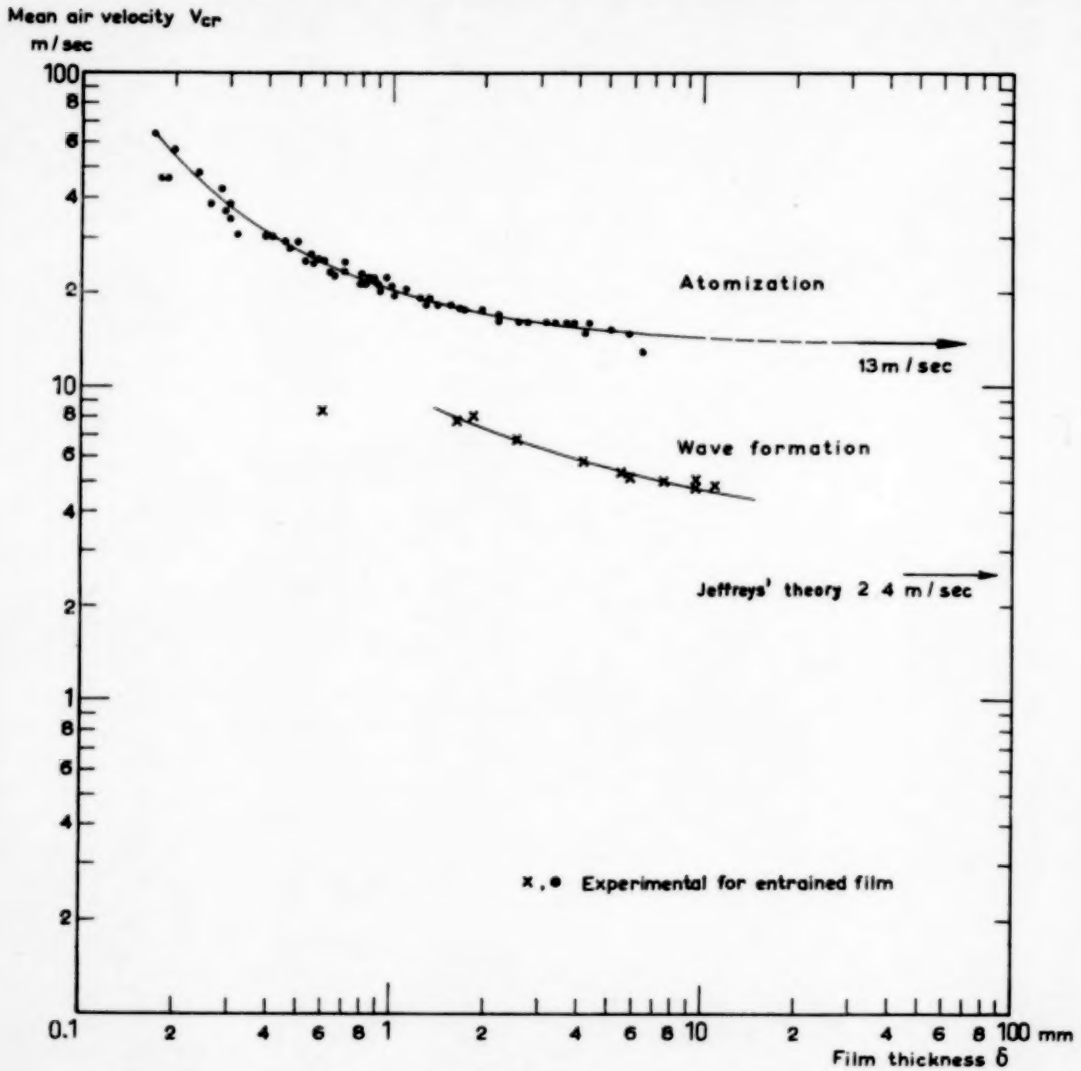

FIG. 6. Wave formation and onset of atomization for films of mineral oil 3; $\eta_l = 16\ cP$.

and with the rough tunnel atomization set in at $V = 25$ m/sec. In this case the film thickness above the plastic beads was 0·3 mm whereas for the smooth bottom the film thickness was 0·9 mm.

No measurements on wave formation were carried out with the rough tunnel bottom.

V.2. *Pressure drop measurements with smooth and rough tunnel wall*

Measurements on pressure drop with and without liquid film were carried out with a smooth tunnel bottom and with the bottom covered with plastic beads as described in section III. The results obtained with the dry, smooth tunnel

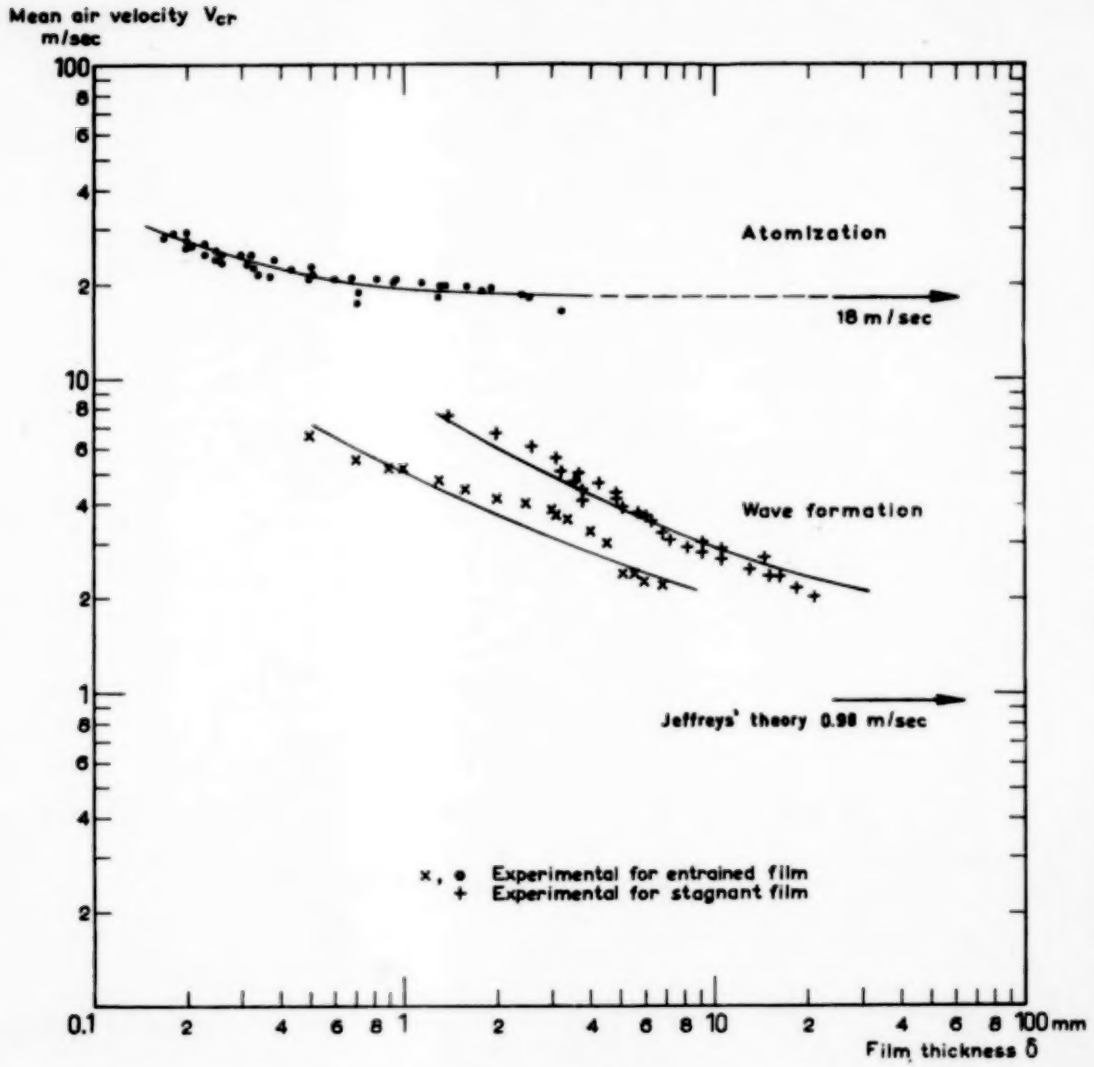

FIG. 7. Wave formation and onset of atomization for water films.

bottom have been plotted in Fig. 10 together with the line for smooth pipes as found in literature (e.g. MOODY [6]) showing very good agreement. From the pressure drops measured, the coefficient of friction for the tunnel bottom λ_b was calculated in the way explained in section III. Fig. 11a shows the values of λ_b obtained with smooth and rough bottom of the tunnel and various rates of flow of mineral oil 2. There was an appreciable spread of the results and in order to avoid confusion, only the mean curves are given. For the dry, rough tunnel bottom an increasing Re_{tunnel} gave an increasing λ_b (Fig. 11a), as was found by NIKURADSE [1] for this range of

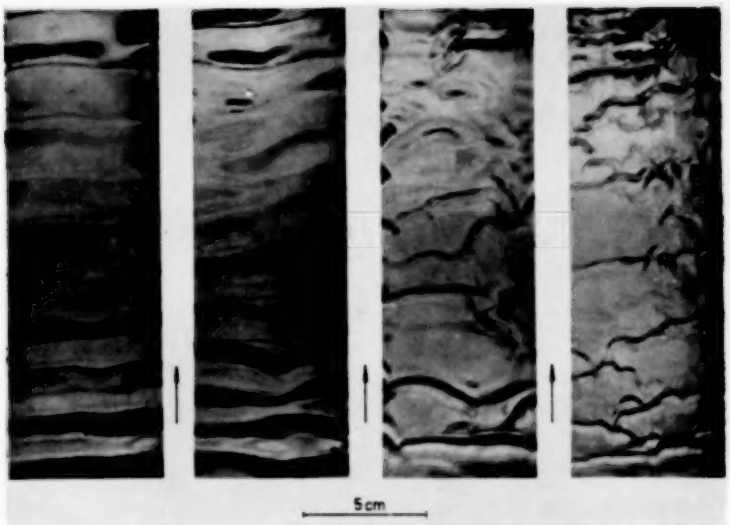

FIG. 8.

	(a)	(b)	(c)	(d)	
$q = 0{\cdot}57\ \mathrm{cm^2/sec}$	$V = 9{\cdot}5$	11·7	18·6	29·4	m/sec
mineral oil 3	$\delta = 2{\cdot}1$	1·08	0·66	0·34	mm

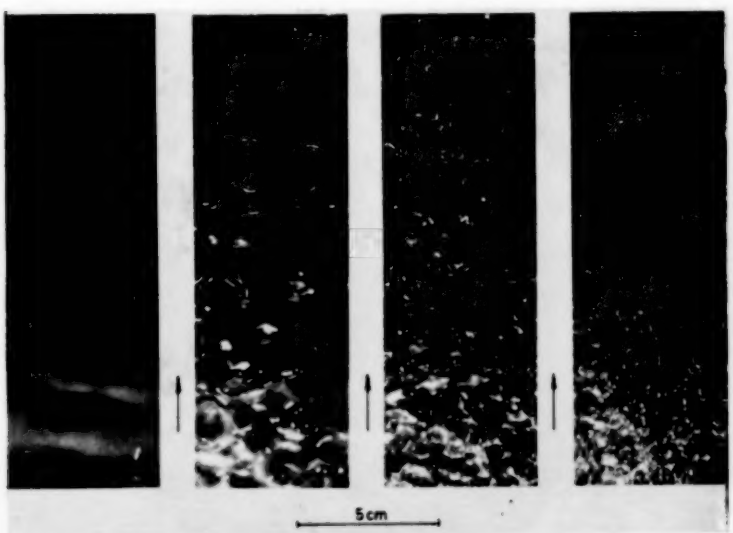

FIG. 9.

	(a)	(b)	(c)	(d)	
$q = 5{\cdot}87$	$V = 4{\cdot}2$	7·7	12·6	27·3	m/sec
water	$\delta = 7{\cdot}0$	5·0	4·0	3·0	mm

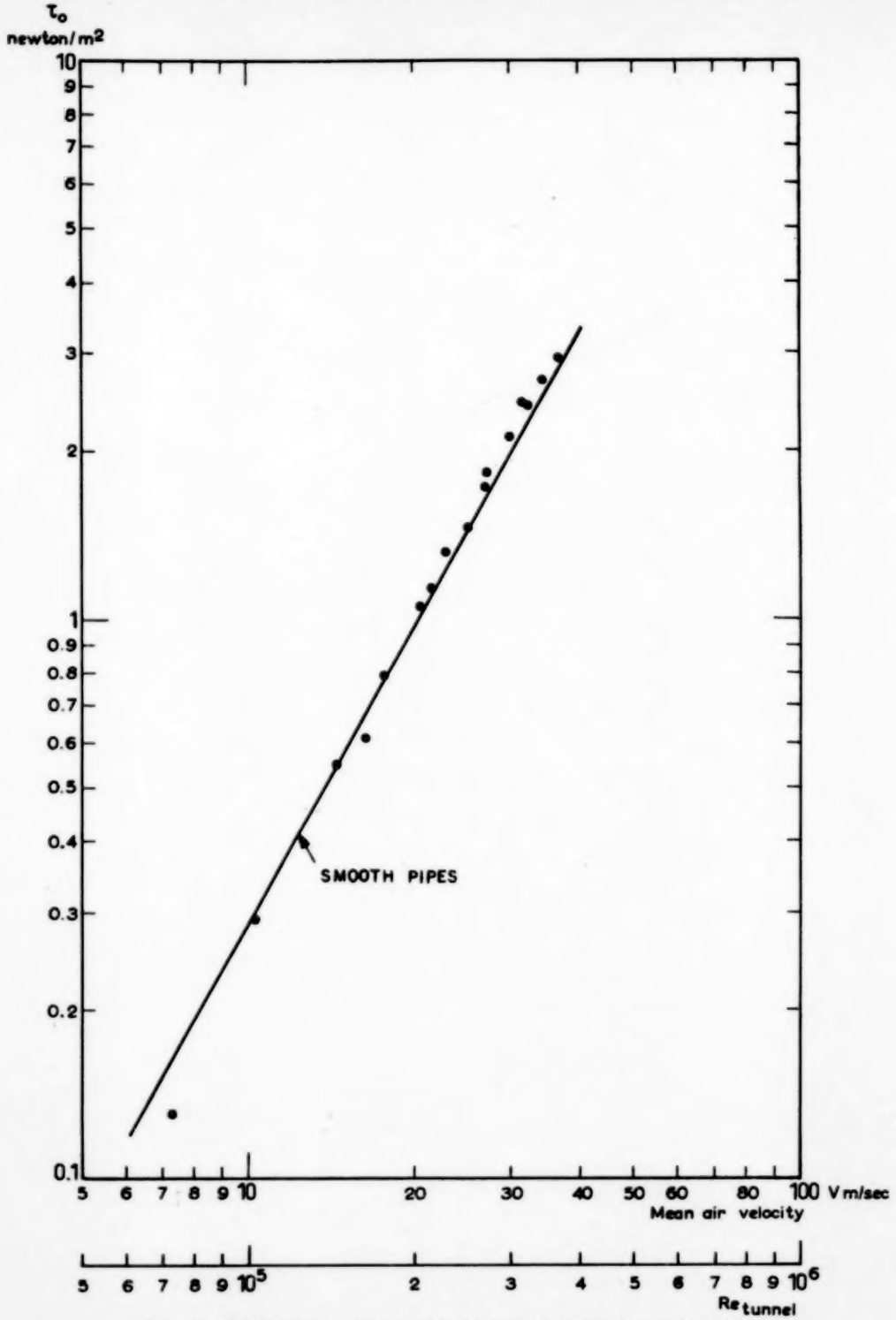

FIG. 10. Wall shearing stress as a function of air velocity (smooth wall).

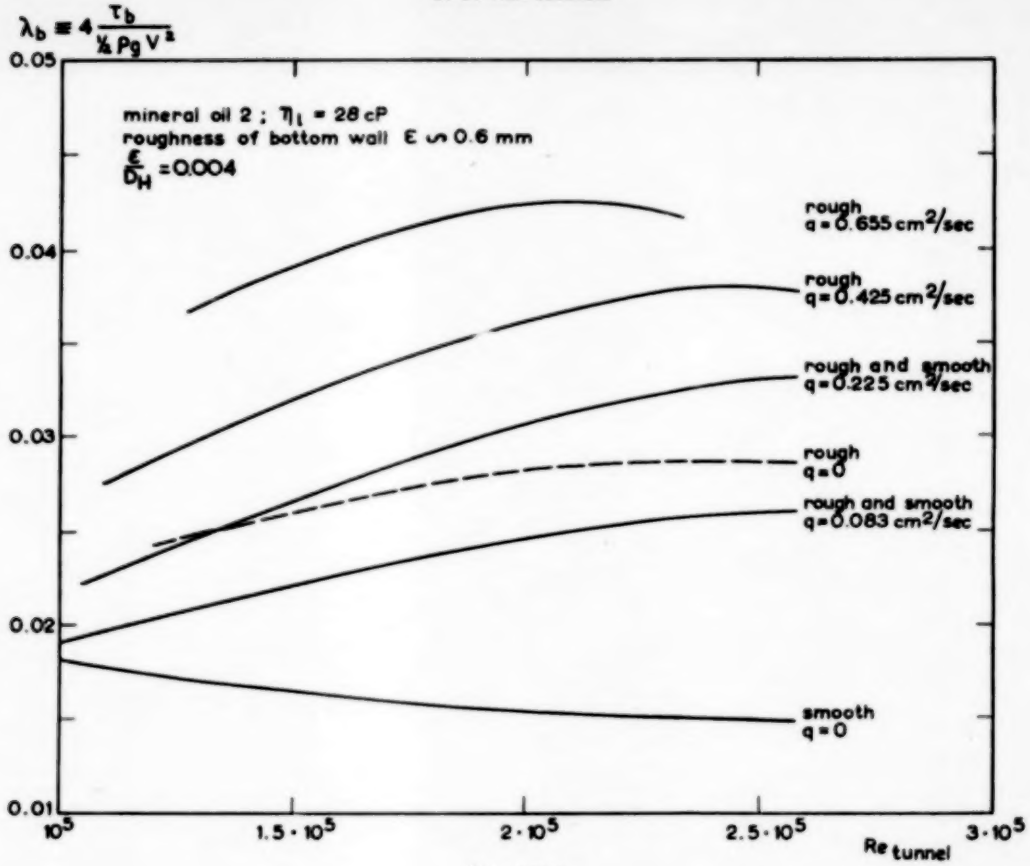

FIG. 11(a)

Reynolds number and uniform sand roughness. Fig. 11b shows λ_b as a function of q for $\mathrm{Re}_{\mathrm{tunnel}} = 2{\cdot}5 \times 10^5$. This figure demonstrates clearly that λ_b is no longer affected by the roughness of the wall above a certain rate of liquid flow. In the case considered this rate of flow is: $q = 0{\cdot}083$ cm²/sec or even less. The film thickness at this flow rate is 0·3 mm with smooth tunnel bottom; with rough tunnel bottom and the same conditions the oil extended about 0·1 mm above the plastic beads.

VI. Analysis of the Results on Atomization and Film Thickness

VI. 1. *Atomization*

No theory is available for the atomization of liquid films. The results have therefore tentatively been correlated by means of two dimensionless parameters. It was thought that some form of the Weber number, expressing the ratio between dynamic pressure of the air stream and pressure set-up in the film by surface tension, would be of importance.

The Weber number used was defined as:

$$\mathrm{We} \equiv \frac{\rho_g V^2 \delta}{\sigma}$$

for the other parameter $S \equiv V\eta_l/\sigma$ has been chosen. The correlation between these two parameters under the critical conditions where atomization is first observed is shown in Fig. 12. For the data pertaining to air velocities above 25 m/sec we may represent this correlation by a single curve. It appears that for $S > 5$, We_{cr} is practically constant (~ 17). For air velocities below 25 m/sec, We_{cr} increases beyond the correlation. For each liquid there is an air velocity (V_∞) below which no atomization occurs,

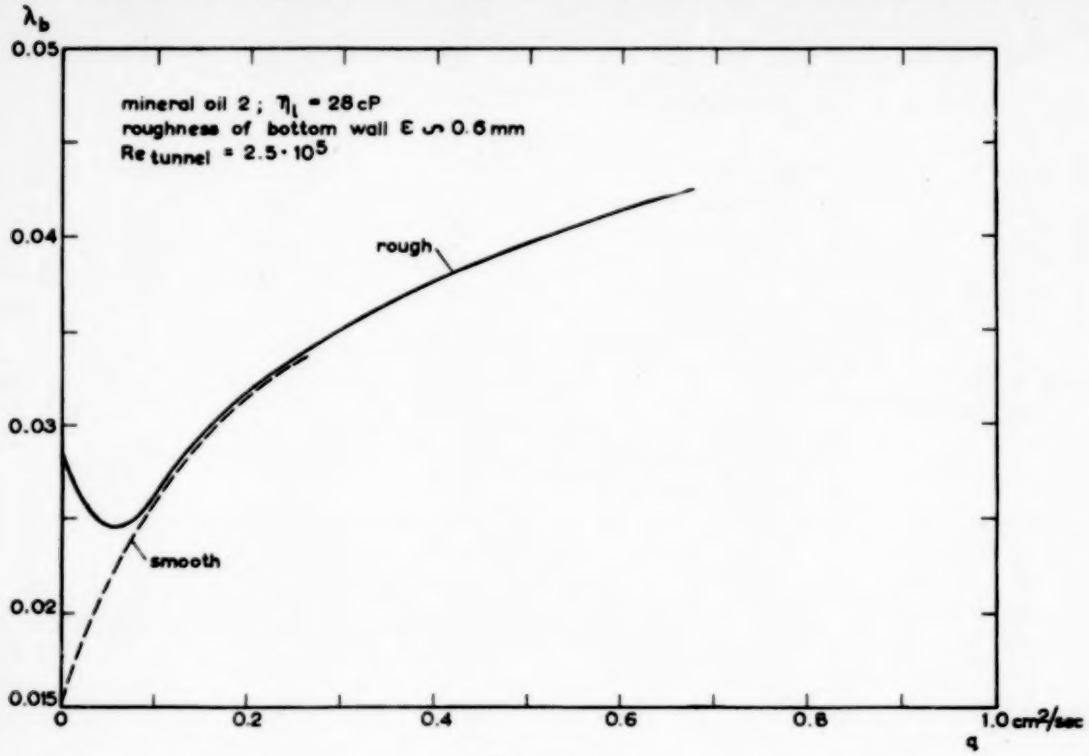

FIG. 11(b)

FIG. 11. Coefficient of friction at the tunnel bottom wall (smooth and rough wall)

whatever the film thickness. As a rule of thumb:

$$V_\infty \text{ (m/sec)} \sim \tfrac{1}{4}\,\sigma \text{ (dyne/cm)}.$$

This is translated in Fig. 12 by vertical asymptotes for each liquid.

A difficulty in applying the above correlation to practical cases is that usually the film thickness will be unknown. A rough estimate of the film thickness can be made from the film thickness correlation presented below (Section VI. 2).

A second analysis of the onset of atomization involves the tentative correlation of $S = V\eta_l/\sigma$ with the Reynolds number related to the liquid flow:

$$\mathrm{Re}_f = \frac{4q}{\nu_l}.$$

The result is shown in Fig. 13; it has the same features with respect to the data at air velocities below 25 m/sec as the Weber correlation. For applications of this second correlation the flow q per unit of width is required and this quantity is more easily obtainable than the film thickness.

The results obtained on atomization and pressure drop with a rough tunnel bottom (cf. section V.1 and V.2) suggest that the correlations can be applied to rough walls at least when the film thickness is greater than the height of the asperities.

The experimental data appeared to be insufficient to decide which of the two correlations has the most general significance. The correlations should therefore not be applied if conditions differ much from those of the experiments.

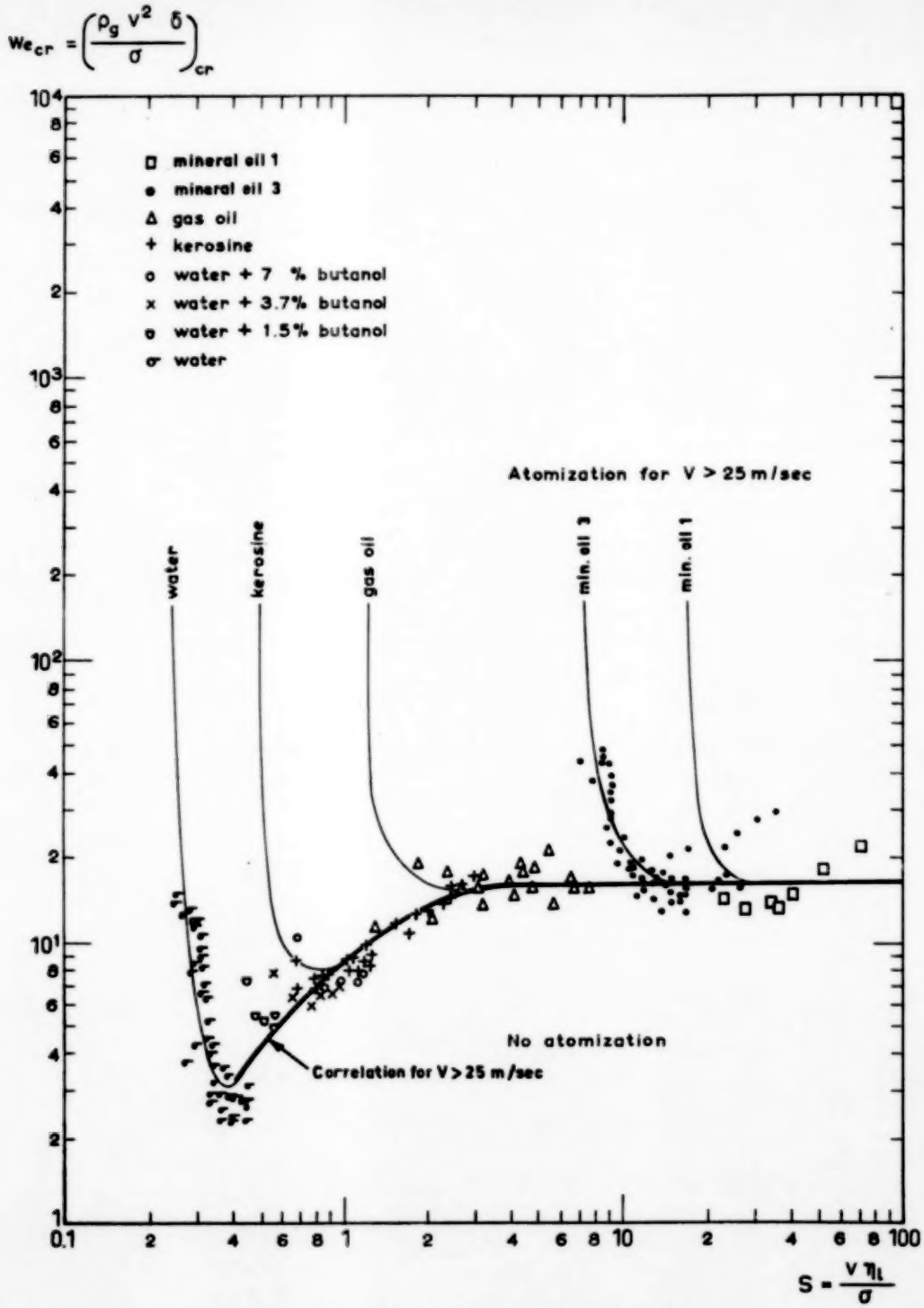

FIG. 12. Correlation for onset of atomization of liquid films.

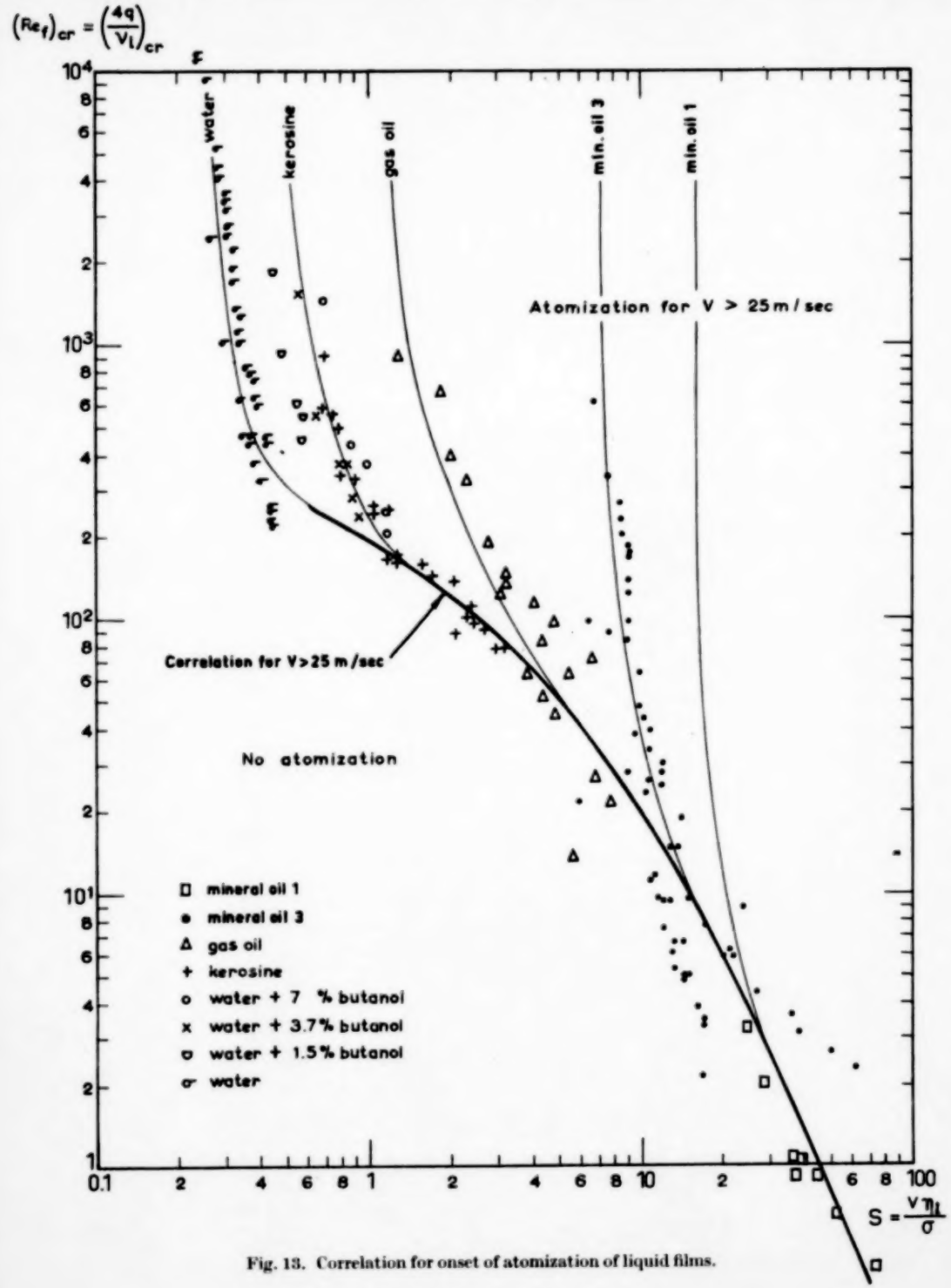

Fig. 13. Correlation for onset of atomization of liquid films.

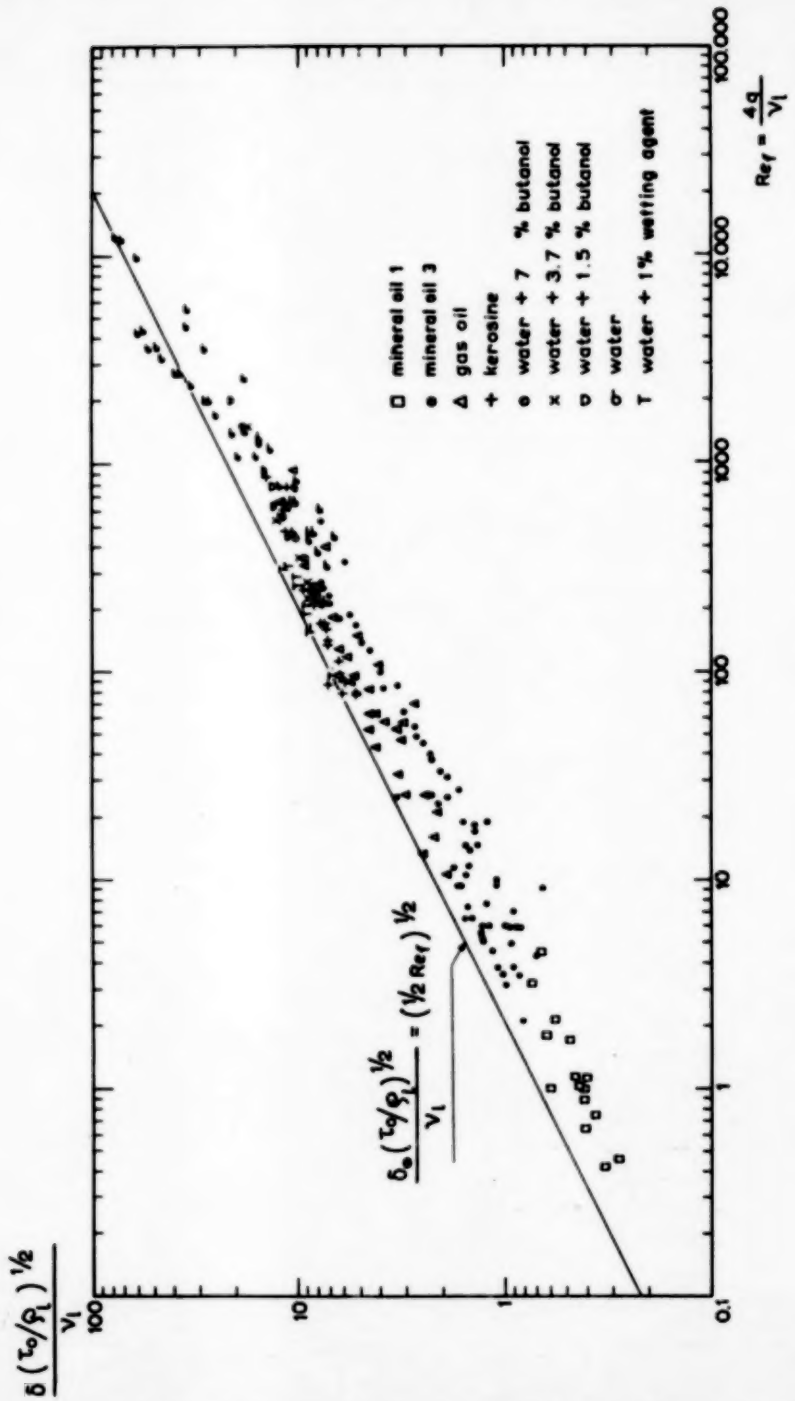

FIG. 14. Correlation for the thickness of horizontal liquid films entrained by an air stream. The experimental data have been plotted using for τ_0 the shear stress at the dry and smooth tunnel wall.

VI.2. *Film thickness*

The data obtained on film thickness are compared with those for an ideal case, viz. the case of a thin film in laminar flow with a flat and smooth gas-liquid interface. For this case it is easy to derive that:

$$q = \tfrac{1}{2}\,\frac{\tau_0\,\delta_0^2}{\eta_l}$$

or, written in a somewhat different form:

$$\frac{\delta_0\,(\tau_0/\rho_l)^{1/2}}{\nu_l} = (\tfrac{1}{2}\,\mathrm{Re}_f)^{1/2}.$$

This relationship is shown in Fig. 14 by a straight line. τ_0 is the shear stress at the (smooth) gas–liquid interface.

The actual film thicknesses δ measured have been correlated by means of the film-thickness parameter $\delta\,(\tau_0/\rho_l)^{1/2}/\nu_l$ and the Reynolds number for film flow Re_f in Fig. 14.

Since the shear stress at the gas–liquid interface involved in the first parameter was only measured in a few cases, the shear stress at the dry and smooth tunnel wall (Fig. 10) has been taken for it. Fig. 14 shows that for $0{\cdot}5 < \mathrm{Re}_f < 2000$ all points are below the straight line.

The results can also be presented as a correction factor on the film thickness δ_0 calculated for the ideal case mentioned. We then obtain:

$$\frac{\delta}{\delta_0} = 0{\cdot}6 \text{ for } 0{\cdot}5 < \mathrm{Re}_f < 2000.$$

Data obtained with the rough tunnel bottom all fall within the spread of the points of Fig. 14.

The fact that the actual film thickness is smaller than δ_0 may be explained by assuming that the transport of liquid mainly takes place in the tops of the waves moving at relatively high speeds and by a difference between the shear stress at the dry and smooth tunnel wall taken for the experimental data and τ_0.

In a few cases the actual values of τ_b were measured (Fig. 11). When using these values in the film thickness parameter, the resulting points in Fig. 14 would still remain below the straight line calculated for the ideal case mentioned above. However, since no further information about the actual values of τ_b than that given in Fig. 11 is available, we have based the correlation on the shear stress for a smooth wall which was measured in our experiments (Fig. 10) and in other cases can be calculated from correlations found in handbooks.

In the experiments with water + 1 per cent wetting agent the air–liquid interface was smooth or slightly wavy. It is seen in Fig. 14 that relevant points are very near to the theoretical line. For $\mathrm{Re}_f > 1500$ film flow becomes turbulent and the points in Fig. 14 are expected to come above the straight line in this region.

Acknowledgements—The author is much indebted to Prof. J. O. Hinze for his advice and stimulating interest during the investigation, to Mr. W. A. Welling, who developed the device for measurement of film thickness, and to Mr. A. Buitelaar, who carried out the experiments.

Notation

B = width of tunnel (= 15 cm)
D_H = hydraulic diameter of the tunnel (= 15 cm)
g = accelerating due to gravity, taken as 980 cm/sec^2
Q = total rate of liquid flow
q = rate of liquid flow per unit of tunnel width
R = resistance through the liquid film over the measuring electrodes
$\mathrm{Re}_f \equiv 4q/\nu_l$, Reynolds number for film flow
$\mathrm{Re}_{\mathrm{tunnel}} \equiv V\,D_H/\nu_g$, Reynolds number for air flow
r = reference electrical resistance
$S \equiv V\,\eta_l/\sigma$, correlation parameter
V = mean air velocity in tunnel
V_{cr} = critical velocity for wave formation or onset of atomization
V_∞ = critical velocity for onset of atomization for "deep water"
$\mathrm{We} \equiv \rho_g\,V^2\,\delta/\sigma$, Weber number
y = distance from the wall
δ = mean film thickness
δ_0 = film thickness for laminar flow with flat and smooth gas–liquid interface
ϵ = absolute roughness of tunnel bottom
η_l = dynamic viscosity of liquid
λ = coefficient of friction
λ_b = coefficient of friction at the tunnel bottom (with or without liquid film)
ν_g = kinematic viscosity of air
ν_l = kinematic viscosity of liquid
ρ_g = density of air
ρ_l = density of liquid
σ = surface tension
τ_0 = shear stress at the gas–liquid interface
τ_b = shear stress at the tunnel bottom (with or without liquid film)

REFERENCES

[1] NIKURADSE J. *Forschungsh. Ver. Dtsch. Ing.* 1933 No. 361.

[2] JEFFREYS H. *Proc. Roy. Soc.* 1925 **A107** 189.

[3] URSELL F. *Surverys of Mechanics* (Edited by G. K. Batchelor and R. M. Davies) p. 216. Cambridge University Press, 1956.

[4] KEULEGAN G. H. *J. Res. Nat. Bur. Stand.* 1951 **46** 358.

[5] HANRATTY T. J. and ENGEN J. M. *Amer. Inst. Chem. Engrs. J.* 1957 **3** 299.

[6] MOODY L. F. *Trans. Amer. Soc. Mech. Engrs.* 1944 **64** 671.

Chemical Engineering Science, 1959, Vol. 11, pp. 53 to 60. Pergamon Press Ltd., London. Printed in Great Britain

The stability of steady exothermic chemical reactions in simple non-adiabatic systems

D. B. SPALDING

Mechanical Engineering Department, Imperial College of Science and Technology, London

(*Received* 28*th January* 1959)

Abstract—The stirred homogeneous reactor, the solid catalytic surface and the solid fuel surface are shown to be governed by the same pair of algebraic equations, expressing energy and material conservation. A relation is derived between the temperature of the reaction region and two dimensionless controlling parameters, one representing the chemical loading, the other representing heat loss. The well-known phenomena of extinction, stable and unstable burning equilibria, and the existence of an upper permissible limit to the heat loss are then demonstrated. The paper does not present new physical insights, but aims at unifying, simplifying and clarifying this branch of reactor theory.

Résume—L'auteur montre qu'un réacteur homogène à agitation une surface catalytique solide et une surface combustible solide sont régis par la même paire d'équations algébriques exprimant la conservation de l'énergie et la conservation de la matière. Il en déduit une relation entre la température de la région réactionnelle et deux paramètres sans dimensions dont l'un représente la charge chimque, et l'autre la perte de chaleur. Les phénomènes bien connus d'extinction, d'équilibre stable et instable de combustion et d'existence d'un maximum de perte de chaleur sont ensuite démontrés. L'article n'apporte pas de nouvelles connaissances physiques mais a pour but d'unifier, simplifier et clarifier cette partie de la théorie des réacteurs.

Zusammenfassung—Der gerührte homogene Reaktor, die feste Katalysatoroberfläche und die feste Brennstoffoberfläche lassen sich durch das gleiche Paar algebraischer Gleichungen behandeln, in denen die Erhaltung der Energie und des Stoffes zum Ausdruck kommen. Zwischen der Temperatur der Reaktionszone und zwei dimensionslosen Einflussgrössen, von denen die eine die chemische "Aufladung," die andere den Wärmeverlust kennzeichnen, wird eine Beziehung abgeleitet. Die wohlbekannten Phänomene der Auslöschung, des stabilen und unstabilen Brennens und der Existenz einer oberen Grenze für den Wärmeverlust werden abgeleitet. Die Arbeit bringt keine neuen physikalischen Einsichten, sie hilft aber zur Vereinheitlichung, Vereinfachung und Klärung dieses Teils der Reaktortheorie.

1. INTRODUCTION

1.1 *Purpose*

NUMEROUS investigations [1–11] have been made of the theory of systems involving steady exothermic chemical reaction with heat loss to the surroundings. The present paper concerns those dealt with in the first ten reference papers. Its intention is to point out the formal similarity between the systems, to simplify and unify their treatment, and to present particular solutions of the equations in terms of dimensionless variables. The paper is a tidying-up operation, and does not disclose new physical phenomena.

1.2 *Systems considered*

The first system is the ideal stirred reactor. This is a vessel through which a combustible gas mixture flows steadily; mixing is supposed so intense that the gas state (temperature and composition) is uniform at all points within the vessel. Unlike the early treatments of [12, 13, 14, 15], but in accordance with those of [7, 9, 9a], heat transfer is supposed to occur from the gas to the reactor walls.

The second system is the solid catalyst surface, past which reactive gas flows steadily. The surface temperature, and the composition of the gas

immediately adjacent to it, are supposed to have taken up steady values controlled by the exothermic reaction at the surface and by heat loss from the surface; the latter might be by radiation to cold vessel walls. This system has already been studied in [1], which also contains references to other early work in the field of reaction stability.

The third system is the solid-fuel surface, for example carbon, which is suspended in a stream of oxidizing gas, for example air. Once again, heat transfer other than by convection between fuel and gas is allowed for. The first analysis of this system, but without heat loss, was by WAGNER [16]; analyses with heat loss have been made in [1, 2, 3, 4, 5, 6].

In the last two systems the reactive region is the solid surface. The gas composition and temperature adjacent to it are assumed uniform; this is often the case in practice over sufficiently large regions for the analysis to be valid.

The three systems must be distinguished from others which exhibit similar behaviour in some respects but which are rendered harder to analyse by non-uniformity of the reaction regions. Such other systems are the laminar flame in a premixed gas, in which the temperature is non-uniform [10, 11], and the gaseous diffusion flame in which the fuel-oxidant ratio is non-uniform as well [17, 18, 19].

It will be supposed below that in each case the reaction rate depends on gas temperature and composition in accordance with relatively simple laws, i.e. increasing according to a power law with temperature rise and linearly with fuel or oxidant concentration. The extension to other reaction-rate functions, for example those of the Arrhenius type, presents no special difficulty. It is in any case always possible to find an exponent for the power law which fits the experimental data over a restricted temperature range.

1.3 *Mathematical features*

It will appear that the mathematical problem reduces to the simultaneous solution of two *algebraic* equations, which may be reduced, for the composition-dependence assumed, to a single quadratic equation. Solution is therefore easy. Trial-and-error procedures may be necessary with other reaction-rate functions.

The laminar propagating flame and the diffusion flame on the other hand involve the solution of *differential* equations; it is for this reason that they are excluded from the present treatment.

In each case, the condition of the reaction zone will be shown to depend on the values of two dimensionless parameters. The first of these involves the ratio of the mass flow rate to the reaction zone divided by the maximum possible reaction rate for the system if operating adiabatically; it will be called the *loading parameter*, L. The second involves the ratio of the maximum possible heat transfer rate from the reaction zone to the same reference reaction rate; it will be called the *heat loss parameter*, Q.

The solution of the problem will be seen to have some striking characteristics. For fixed values of L and Q, in general three different reaction-zone conditions satisfy the equations. Only two of these represent physically stable conditions.

If L is too large or too small, two of the solutions become imaginary. If Q is too large, there is no real value of L for which three real solutions can be found.

2. THE EQUATIONS

2.1 *The stirred reactor*

It will be supposed that the volumetric reaction rate, $\dot{q}'''$ in, say, cal/cm³sec, can be expressed by the formula:

$$\dot{q}''' = K\dot{q}'''_{\mathrm{m}}\, v\, \alpha\, \tau^{n} \qquad (1)$$

where

$\dot{q}'''_{\mathrm{m}}$ is a constant of the fuel and oxidant streams and the reactor pressure;

v is the reactor volume;

α is the fraction of the initial fuel mass which is still unburned;

τ is the reactedness (dimensionless temperature rise above unburned state)

$K = (n+1)^{n+1}/n^{n}$, a constant which ensures that the maximum possible value of $\dot{q}'''$ is $\dot{q}'''_{\mathrm{m}}$, and n is a constant of the reaction, chosen so as to fit approximately the experimental data.

Equation (1) implies that the reaction is first order with respect to fuel. The temperature dependence of the reaction rate is measured by the value of n.

It is further assumed that the heat loss from the gas to the reactor walls in unit time, $\dot{Q}$ is given by

$$\dot{Q} = \dot{Q}_m \tau^m \qquad (2)$$

where m is a constant depending on the mode of heat transfer. Once again, the exponent is shown so as approximately to fit the experimental data over the important part of the temperature range.

For constant gas specific heat, c, the steady-flow energy equation for the reactor can then be written as

$$\dot{m} c (T_b - T_u) \tau = K \dot{q}'''_m v \alpha \tau^n - \dot{Q}_m \tau^m \qquad (3)$$

where

$\dot{m}$ = mass flow rate of entering mixture

$T_b - T_u$ = temperature rise of mixture in complete adiabatic steady-flow reaction.

The conservation-of-mass principle applied to the fuel or oxidant flowing through the reactor yields the equation :—

$$\dot{m} (1 - \alpha) = K \dot{q}'''_m v \alpha \tau^n / c (T_b - T_u) \qquad (4)$$

wherein the left-hand side represents the difference between the inflow and the outflow, while the right-hand side represents the rate of disappearacne of the reactant due to chemical reaction.

Dimensionless form of the equation. We now introduce the dimensionless loading and heat-loss parameters by the definition :—

$$L \equiv \dot{m} c (T_b - T_u) / \dot{q}'''_m v \qquad (5)$$

and $$Q \equiv \dot{Q}_m / \dot{q}'''_m v \qquad (6)$$

Introducing these definitions into (3) and (4), we obtain the pair of equations governing the behaviour of the stirred reactor. They are :—

$$L\tau = K \alpha \tau^n - Q \tau^m \qquad (7)$$

and $$L (1 - \alpha) = K \alpha \tau^n \qquad (8)$$

Here we leave the matter until the other systems have been dealt with. It will appear that they yield equations which are almost identical with (7) and (8).

2.2 *The solid catalyst surface*

It will be supposed that the reaction rate at the catalyst surface, $\dot{q}''$, in, say, cal/cm²sec, is given by

$$\dot{q}'' = K \dot{q}''_m \alpha \tau^n \qquad (9)$$

where

$\dot{q}''_m$ is the maximum possible of reaction rate at the catalyst surface, with the given gas stream, when non-convective heat loss is prevented and Reynolds Analogy holds (these conditions lead to $\alpha = 1 - \tau$). $\dot{q}''_m$ is a property of the catalyst, the reactants, and the stream temperature and pressure.

α is the concentration in the gas at the surface of the less plentiful reactant, divided by its concentration in the unreacted stream.

τ is the surface temperature minus the stream temperature divided by $T_b - T_u$, the temperature rise of the gas in adiabatic complete reaction.

Reaction in the gas phase is neglected.

Heat transfer from the catalyst to its non-gaseous surroundings, $\dot{Q}''$, is supposed to obey the equation

$$\dot{Q}'' = \dot{Q}''_m \tau^m \qquad (10)$$

where $\dot{Q}''_m$ is the heat transfer rate when the catalyst surface is at the temperature of the adiabatic combustion products.

The catalyst surface is supposed to be engaged in steady heat and mass transfer with the combustible stream obeying linear laws, such that the convective heat transfer rate per unit area is

$$g c (T_b - T_u)$$

and the reactant transfer rate per unit area is

$$\frac{g}{\sigma} m_{fu} (1 - \alpha) \qquad (11)$$

where

m_{fu} is the fuel concentration in the unreacted stream,

g is the mass of stream fluid reaching temperature equilibrium with unit area of catalyst surface in unit time,

g/σ is the mass of stream fluid reaching composition equilibrium with unit area of the catalyst surface in unit time, and

σ, according to the Chilton–Colburn analogy, is the Lewis No. (molecular diffusivity of fuel divided by thermal diffusivity of mixture) to the minus two-thirds power. When the Lewis No. equals unity, Reynolds Analogy holds for heat and mass transfer, though not necessarily for friction.

g is related to the more usual heat transfer coefficient h by

$$g = h/c \tag{12}$$

where c is the specific heat of the gas at constant pressure.

Conservation equations. The equations of conservation of energy and material can now be written for an element of the catalyst surface in the steady state. They are respectively:

$$gc\,(T_b - T_u)\,\tau = K\,\dot{q}''_m \,.\, \alpha\,\tau^n - \dot{Q}''_m\,\tau^m \tag{13}$$

and

$$\frac{g}{\sigma}\,m_{fu}\,(1-\alpha) = \frac{K\,\dot{q}''_m\,\alpha\,\tau^n}{c\,(T_b - T_u)/m_{fu}} \tag{14}$$

wherein it is recognized that $c\,(T_b - T_u)$ is equal to m_{fu} times the heat of reaction of the combustible.

Dimensionless form of equations. We now introduce the dimensionless loading and heat loss parameters in the form

$$L \equiv g\,c\,(T_b - T_u)/\dot{q}''_m \tag{15}$$

$$Q \equiv \dot{Q}''_m/\dot{q}''_m \tag{16}$$

which, substituted in (13) and (14), lead to

$$L\,\tau = K\,\alpha\,\tau^n - Q\,\tau^m \tag{17}$$

$$\frac{L\,(1-\alpha)}{\sigma} = K\,\alpha\,\tau^n \tag{18}$$

Comparison of (17) and (18) with (7) and (8) shows that the two pairs are identical except for the presence of σ in (18). This difference disappears if the Lewis Number is unity, i.e. when the Reynolds Analogy holds.

2.3 *The solid fuel surface*

We consider a solid fuel surface suspended in an oxidizing gas stream; it will be supposed, for simplicity, that only one oxide can be formed. The reaction will be be taken as first order in surface oxygen concentration, so that the reaction rate, $\dot{q}''$, in, say, cal/cm²sec is given by

$$\dot{q}'' = K\,\dot{q}''_m\,\alpha\,\tau^n \tag{19}$$

where

$\dot{q}''_m$ is the maximum possible of reaction rate at the fuel surface with the given gas stream, when non-convective heat transfer is absent and Reynolds Analogy holds (then $\alpha = 1 - \tau$). $\dot{q}''_m$ is a property of the fuel and of the gas stream composition, pressure and temperature;

α is m_{OS}/m_{OG}, the surface fractional mass oxygen concentration divided by that in the gas stream;

τ is defined as $(T_s - T_u)/(T_b - T_u)$ where T_s is the surface temperature, T_u is the temperature of the gas stream, and T_b is the temperature attained by a stoichiometric mixture of gas and fuel, the latter being supplied at T_b.

Equation (19) is formally identical with (9)* Similarly, equation (10) can be taken as representing the non-convective heat loss from the fuel surface, as well as that from the catalyst, while the convective term is again represented by, $gc\,(T_b - T_u)\,\tau$.

The rate of transfer of oxygen to the surface, $\dot{m}''$ per unit area, is given mass transfer theory (e g. [20]) as

$$\dot{m}''_O = \frac{g}{\sigma}\,\frac{m_{OG} - m_{OS}}{1 + m_{OS}/r} \tag{20}$$

where

g, σ, m_{OG}, and m_{OS} are as above,

r is the stoichiometric ratio, mass of oxygen required for unit mass of fuel.

This transfer rate, in the steady state, equals the rate of oxygen consumption, S_0

$$\dot{m}''_O = m_{OG}\,\dot{q}''/c\,(T_b - T_u) \tag{21}$$

where c is the mean specific heat of the gas stream or products at constant pressure, and it is recognised that $c\,(T_b - T_u)/m_{OG}$ is the heat of combustion per unit mass of oxygen.

Conservation equations. Since (19) is identical with (9), equation (13) expresses the conservation-of-energy principle for the solid fuel surface also.

The conservation of mass is represented by combining equations (20) and (21).

After introduction of the same dimensionless loading and heat loss parameters from (15) and (16), the dimensionless energy- and mass-conservation equations becomes

$$L\,\tau = K\,\alpha\,\tau^n - Q\,\tau^m \tag{22}$$

$$\frac{L}{\sigma}\cdot\frac{(1-\alpha)}{1+\alpha\,m_{OG}/r} = K\,\alpha\,\tau^n \tag{23}$$

The former equation is identical with (7) and (17), which hold for the stirred reactor and for the catalyst surface. Equation (23) differs slightly both from (8) and (18), through the presence of the σ and $(1+\alpha\,m_{OG}/r)$ terms.

2.4 *Comparison of three systems*

We shall consider, for simplicity, the case in which the Lewis Number is unity. Then σ disappears from equations (18) and (23). Further, we note that m_{OG}/r is of the order of 0·1 for many practical systems; since, in addition, α is considerably less than unity under most conditions of interest, the term $\alpha\,m_{OG}/r$ will be neglected.

These simplifications ensure that equations (7) and (8) now hold for each of the three physical systems; their solution therefore is also valid for the three systems. From now on, therefore, the stirred reactor, the catalytic surface and the solid fuel surface will all be simultaneously under discussion.

3. Solution of the Equations

3.1 *Analytical solution*

In practice, the operator of a combustion plant controls the mass flow to the reaction region, while the heat loss relations are fixed by the geometry; the interplay of mass flow, heat flow and reaction then settles what temperature the reaction region will take up.

Correspondingly, we shall want to use equations (7) and (8) to tell us what τ is when L and Q have fixed values. It is however easier to develop a formula for L in terms of τ and Q. This follows by noting that, by eliminating $K\,\alpha\,\tau^n$ between (7) and (8), we find

$$\alpha = 1 - \tau - Q\,\tau^m/L \tag{24}$$

After substitution of (24) in (7), there results a quadratic equation in L, with solution:

$$L = \frac{K}{2}\,\tau^{n-1}(1-\tau)\times \left\{1-(Q/K(1-\tau)\,\tau^{n-m}) \pm \sqrt{\left[1-(2Q(1+\tau)/K(1-\tau)^2\,\tau^{n-m}) + (Q^2/K^2(1-\tau)^2\,\tau^{2n-2m})\right]}\right\} \tag{25}$$

3.2 *Graphical representation*

Equation (25) has been evaluated for various values of Q. The temperature exponents used were: $n = 8$, $m = 4$. The results are represented graphically in Fig. 1, with L as independent variable, τ as dependent variable, and Q as parameter.

It is evident that, for fixed Q, the $L-\tau$ relation is a closed loop; so for each value of τ there are in general two L's [as is deducible at once from the $\pm$ sign in (25)]; but also, for each L, there are in general two τ's (or rather three, since $\tau = 0$ is a solution for all L and Q).

The area occupied by the loop diminishes as Q increases. At $Q = 0{\cdot}155$ the loop encloses a tiny area around the point $L = 0{\cdot}163$, $\tau = 0{\cdot}64$; for higher values of Q there are no real pairs of values of L and τ which satisfy the equation at all.

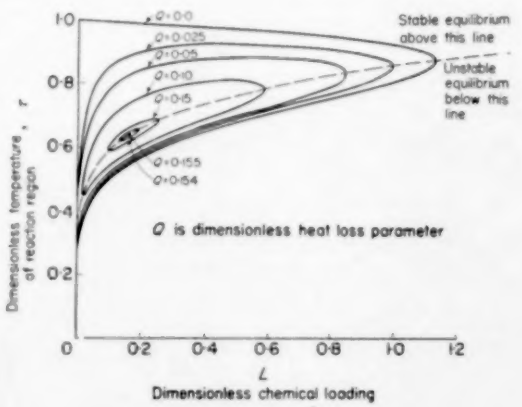

Fig. 1.

For a given Q the real range of L for which there is a real value of τ is bounded by the values for which the tangent to the loop is vertical. The corresponding points on the loops are joined by a broken line in Fig. 1.

The general shape of the curves of Fig. 1 is typical of those cases for which $n > m$, i.e. for which reaction rate depends more strongly on temperature than does heat loss, as is invariably the case in combustion practice.

4. Discussion of Solution

4.1 *Physical significance*

The loading parameter L, it will be recalled, is a dimensionless measure of the mass flow rate through the stirred reactor or of the mass transfer rate between the reacting surface and the gas stream. Inspection of Fig. 1 shows that, when L and the heat-loss parameter Q are fixed, the reaction region can have three possible temperatures, one of which is zero (i.e. equal to that of the gas stream).

Considering for a moment the highest of these three temperatures, (i.e. the upper half of a loop), we see that over a large part of the range an increase of L (blowing rate) causes the temperature to rise. This is a common phenomenon with burning carbon. Eventually however the temperature falls again, until, for an L value greater than that giving a vertical tangent, no real temperature can be found which satisfies the steady-burning equations: the flame has been extinguished.

For fixed heat-loss parameter Q, extinction also occurs when L is made very small. This phenomenon is also well-known: if the blowing rate is too low, heat losses become dominant and prevent continuance of steady reaction.

If Q exceeds a critical value (0·155 in the case considered) no reaction is possible at all. With fixed reactor geometry, this condition is often encountered when the pressure falls; for the reaction-rate usually falls off more rapidly than the heat loss rate as the pressure falls, and so their ratio Q decreases.

$Q = 0$ corresponds to the well-known adiabatic reactor studied by Wagner [16], van Heerden [12], Longwell [14] and others. The low-L extinction condition has now become $L = 0$, and so has ceased to be of practical importance.

4.2 *Stability*

It will now be demonstrated that the intermediate value of τ for fixed L and Q represents a condition which cannot be obtained in practice; for, although this condition satisfies the steady-state equations, the equilibrium is unstable.

Suppose that a reaction system is operating at such a condition, represented by U in Fig. 2. Now let the temperature of the system rise infinitesimally to U'. Will equilibrium be restored? The point U' lies on a steady-state curve which has a higher Q than that prevailing in the system. The system therefore cannot get rid of all the heat which is developed; its temperature correspondingly rises. So a small upward deviation from the steady-state point U causes the system to deviate still further upward.

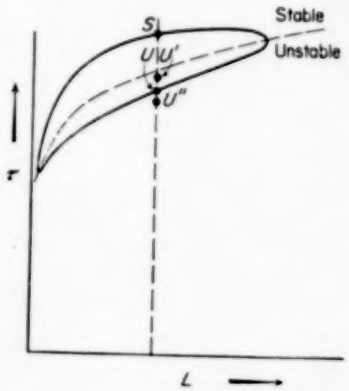

Fig. 2.

Similar arguments show that a downward deviation to U'' precipitates a further fall of temperature. The whole U branch of the loop is therefore unstable.

When points on the upper (S) branch of the loop are considered in this manner, it is easily seen that a small deviation from equilibrium so changes the heat development rate that the temperature tends to be restored to its equilibrium value for the L and Q in question. The S

branch therefore represents stable equilibrium states.

The trivial $\tau = 0$ solution is also stable.

4.3 *Remarks*

(*a*) *Influence of simplifying assumptions.* Equation (25) is only valid for all three systems when $\sigma = 1$ and $m_{OG}/r = 0$, and indeed when the reaction rate and heat loss depend exponentially on τ. In most practical cases these assumptions will not hold exactly. It should however be obvious that the insertion of more realistic functions into the equations will not fundamentally alter the character of the solution.

Extinction at the upper limit of L is caused by the reaction rate increasing more steeply than linearly with reactedness τ; extinction at the lower limit of L is caused by a steeper temperature dependence of reaction rate than that of heat loss. These conditions almost invariably prevail.

The actual run of the curves on Fig. 1, and in particular the upper limit of Q, naturally depend on the values of n and m or of other parameters (e.g. activation energy) describing the form of the reaction-rate and heat-loss functions. Each case has to be worked out as required. However the upper limit of Q is always likely to be less than unity.

Realistic reaction-rate functions differ from the exponential ones considered in not giving zero values at $\tau = 0$. This ensures that the $Q = 0$ curve, for example, does not quite touch the line $L = 0$ but sweeps round and becomes asymptotic to the line $\tau = 0$. Physically, this feature permits spontaneous ignition at low values of L.

Similar characteristics may appear where the temperature of the reservoir to which the reaction region loses heat is higher than that of the incoming stream. This is true of some furnace situations for example. Corresponding changes are easily made to the equations.

(*b*) "*Chemical resistance*" *to reaction.* In calculations of the rate of reaction at catalyst or solid fuel surfaces, it is common to suppose that mass transfer alone controls the rate, that is to say that the concentration of the gas-phase reactant is reduced to zero at the surface. We can use the present analysis to see whether this is true.

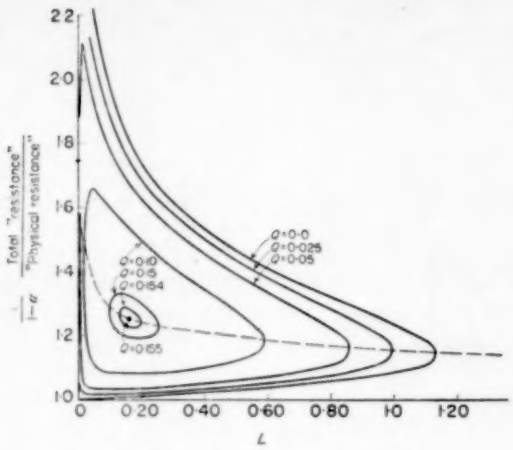

FIG. 3.

Figure 3 shows curves of $1/(1 - \alpha)$ versus L for various values of Q; the values $n = 8$, $m = 4$ have been used as for Fig. 1. Now it may easily be shown that $1/(1 - \alpha)$ is equal to the total "resistance" to reaction, divided by the "resistance" of the mass transfer process alone. "Resistance" is defined as stream reactant concentration divided by reaction rate at the surface.

Inspection of Fig. 2 shows that when heat loss is absent ($Q = 0$), $1/(1 - \alpha)$ has the value unity at low L and increases by 15 per cent over the whole range of stable reaction. This 15 per cent is the contribution of "chemical resistance."

When Q is finite, $1/(1 - \alpha)$ is always greater than unity, and can exceed 1·5 if L is very small. However, over most of the stable range of burning $1/(1 - \alpha)$ does not exceed 1·25. So a calculation of the burning rate which entirely ignores chemical influences will not usually over-estimate the rate by more than 25 per cent. A safe general rule, which will often give sufficient accuracy, would be always to reduce the rate calculated from the mass-transfer-control hypothesis by 10 per cent.

Of course different temperature dependences (n and m) of the chemical reaction and heat loss will modify the numbers in the above paragraphs. The larger n and m are, the smaller will be the amount by which $1/(1 - \alpha)$ exceeds unity. If the chemical reaction rate does not vanish at

$\tau = 0$, stable reaction is possible at much lower temperatures than in the present case; then $1/(1 - \alpha)$ greatly exceeds unity, and the main "resistance" to reaction is chemical. This matter has recently been discussed in connexion with ammonia synthesis by BOŠNJAKOVIĆ and others [21, 22].

5. CONCLUSIONS

(a) Systems involving steady flow, exothermic chemical reaction, and non-convective heat loss, take up a temperature which depends on two dimensionless quantities, a chemical loading and a heat-loss parameter.

(b) If the rate of increase of chemical reaction rate with temperature itself rises with temperature, reaction can be extinguished by increase of the loading parameter.

(c) If the rate of increase of the chemical reaction with temperature exceeds that of the non-convective heat loss, reaction can also be extinguished by reducing the loading.

(d) If the heat loss parameter exceeds a critical value, which depends on the temperature dependences of chemical reaction and of heat loss, reaction is not possible at any value of the loading, unless significant chemical reaction takes place at the gas stream temperature.

(e) For reactions at solid surfaces, the rate of reaction calculated by neglecting the "chemical resistance" may give an over-estimate of the order of 25 per cent. The exact amount of the over-estimate depends on the reaction and heat-loss functions, and on the loading and heat-loss parameters.

REFERENCES

[1] FRANK-KAMENETSKY D. A. *Diffusion and Heat Exchange in Chemical Kinetics.* Princeton University Press 1955. (Published in U.S.S.R., 1947).

[2] SMITH F. W. Mass. Inst. Tech. Meteor Report No. 6, 1947.

[3] SPALDING D. B. *J. Inst. Fuel* 1953 **26** 289.

[4] SILVER R. S. *Fuel* 1953 **32** 138.

[5] CANNON K. J. and DENBIGH K. G. *Chem. Engng. Sci.* 1957 **6** 155.

[6] GRIGULL U. *Chem.-Ing.-Tech.* 1958 **30** 40.

[7] SPALDING D. B. and TALL B. S. *Aero. Quart.* 1954 **5** 195.

[8] DE ZUBAY E. A. and WOODWARD E. C. Westinghouse Res. Lab. Sci. Pap. No. 1811, 1954; *Fifth Symp. Combustion* p. 329. Reinhold, New York 1955.

[9] SPALDING D. B. *Third AGARD Combustion and Propulsion Colloq. Pa'ermo, 1958.* p. 269. Pergamon Press 1959.

[9a] VAN HEERDEN C. *Chemical Reaction Engineering.* p. 133. Pergamon Press, London 1957.

[10] SPALDING, D. B. *Proc. Roy. Soc.* A **240** 1957 83.

[11] MAYER E. *Combustion and Flame* 1957 **1** 438.

[12] HEERDEN VAN C. *Industr. Engng. Chem.* 1953 **45** 1243.

[13] AVERY W. H. and HART R. W. *Industr. Engng. Chem.* 1953 **45** 1634.

[14] LONGWELL J. P., FROST E. E. and WEISS M. A. *Industr. Engng. Chem.* 1953 **45** 1629.

[15] BRAGG S. Unpublished work 1953. See also *Selected Combustion Problems* Vol. 2. Butterworth, London 1956.

[16] WAGNER C. *Tech. Berlin Chem.* 1945 **18** 28.

[17] ZELDOVICH Y. B. *Zh. Tekh. Fiz.* 1949 **19** 1199.

[18] SPALDING D. B. *Fuel* **33** 253.

[19] AGAFANOVA F. A., GUREVICH M. A. and PALEEV I. I. Theory of burning of a liquid fuel drop. *J. Sov. Phys. Techn. Phys.* 1958 **2** 1689.

[20] SPALDING D. B. *Some Fundamentals of Combustion.* Butterworth, London 1955.

[21] BOŠNJAKOVIĆ F. *Chem.-Ing.-Tech.* 1957 **29** 187.

[22] KOPPER H. H. *Chem.-Ing.-Tech.* 1958 **30** 40.

Chemical Engineering Science, 1959, Vol. 11, pp. 61 to 71. Pergamon Press Ltd., London. Printed in Great Britain

The rate of absorption of NO_2 in water

W. A. Dekker, E. Snoeck and H. Kramers

Laboratorium voor Fysische Technologie, Technische Hogeschool, Delft, Netherlands

(*Received* 4 *February* 1959)

Abstract—The mechanism of the absorption of nitrogen dioxide–nitrogen tetroxide gas mixtures from nitrogen into water was investigated. For this purpose a wetted wall column was used in which a concurrent flow of a laminar liquid film and a laminar gas core with a flat velocity profile could be established. These flow conditions were verified separately.

The NO_2 absorption experiments were analysed on the basis of the following model:

(a) in the gas phase, NO_2 and N_2O_4 are in continuous chemical equilibrium with each other and they are transported from the bulk to the gas–liquid interface by molecular diffusion;

(b) at the interface, only N_2O_4 is dissolved in the water;

(c) the diffusion of N_2O_4 into the water is accompanied by a rapid pseudo first-order reaction between N_2O_4 and water. The experimental results agreed fairly well with the proposed absorption mechanism, and from these, data were obtained on the liquid-side kinetics of the absorption process.

Résumé—On a étudié la vitesse de l'absorption de NO_2–N_2O_4 d'un mélange avec l'azote dans l'eau. Pour ce but on a utilisé une colonne à paroi mouillée, dans laquelle l'eau et le gaz confluent en écoulement laminaire. Les conditions hydro- et aerodynamiques ont été vérifiées séparément.

Les mesures sur l'absorption de NO_2 ont été analysées selon le mécanisme suivant:

(a) dans le gaz les espèces NO_2 et N_2O_4 sont transferées vers la paroi par diffusion moléculaire, toujours mutuellement en équilibre chimique;

(b) à la paroi seulement N_2O_4 est dissolu dans l'eau;

(c) la diffusion du N_2O_4 dans l'eau est accompagnée par une réaction rapide de premier ordre entre le N_2O_4 et l'eau. Il y a une correspondence satisfaisante entre le modèle proposé et les résultats expérimentales, dont on a pu déduire des données quantitatives sur la cinétique de l'absorption dans le liquide.

Zusammenfassung—Der Absorptionsmechanismus von NO_2–N_2O_4 in Wasser aus einer Mischung mit Stickstoff wurde untersucht. Hierzu wurde eine Kolonne mit berieselter Wand verwendet, in der ein laminarer Flüssigkeitsfilm im Gleichstrom mit einer laminaren Gasströmung mit flachem Geschwindigkeitsprofil eingestellt werden konnte. Diese Strömungsbedingungen wurden getrennt verwirklicht.

Die Versuche zur NO_2–Absorption wurden mit Hilfe folgender Modellvorstellung analysiert:

(a) in der Gasphase werden NO_2 und N_2O_4 aus dem Strömungskern zur Grenzfläche durch molekulare Diffusion transportiert und befinden sich ständig im chemischen Gleichgewicht miteinander;

(b) an der Grenzfläche wird nur N_2O_4 im Wasser gelöst;

(c) die Diffusion von N_2O_4 in Wasser ist von einer schnellen Reaktion erster Ordnung zwischen N_2O_4 und Wasser begleitet. Die Versuchsergebnisse stimmten ziemlich gut mit dem vorgeschlagenen Absorptionsmechanismus überein. Aus ihnen wurden Daten zur flüssigkeitsseitigen Kinetik des Absorptionsprozesses erhalten.

1. Introduction

The absorption rate of nitrogen dioxide–nitrogen tetroxide gas mixtures from nitrogen into water plays an important role in the industrial production of nitric acid and the removal of NO_2 from gaseous mixtures*.

The essential chemical reactions which accompany this absorption are:

$$2NO_2\,(N_2O_4) + H_2O \rightleftharpoons HNO_2 + HNO_3$$

$$4HNO_2 \rightleftharpoons 2NO + 2NO_2\,(N_2O_4) + 2H_2O$$

The resulting overall reaction is represented by the following equation:

$$3NO_2\,(3/2\,N_2O_4) + H_2O \rightleftharpoons 2HNO_3 + NO$$

The absorption of NO_2 in water is carried out in absorption towers which can be operated under various conditions. As a consequence, various designs of absorption towers are possible. An optimum design can only be realized, however, if the chemical and physical mechanisms of the absorption are thoroughly understood.

During the last forty years several investigators have studied this process but so far their views on this subject are rather conflicting as appears from a literature survey [1]. A summary of the most important conclusions from the studies by other investigators is given below.

Chambers and Sherwood [2] interpreted their results on the basis of the "two film theory" and found the gas film to be rate controlling. However, the absorption rate was lower than was expected from similar absorption experiments with other gases. According to these authors, this was due to the formation of mist in the gas phase. In addition, they found NO to be present in the gas phase when a NaOH solution was used as the absorbing liquid; this indicated that a chemical reaction between NO_2 and H_2O took place in the gas phase.

Denbigh and Prince [3] and Caudle and Denbigh [4] concluded from their experiments that the absorption rate was controlled by the chemical reaction between N_2O_4 and water in the liquid phase. These authors did not find an indication of gas phase reaction.

Peters *et al.* [5] stated that the reaction between N_2O_4 and H_2O in the gas phase close to the interface was rate controlling.

Wendel and Pigford [6] recently stated the controlling mechanism in the absorption to be the homogeneous liquid phase reaction of dissolved N_2O_4 with water. However, their data indicate that the gas phase resistance also plays an important role in the absorption rate.

Because of the apparent complexity of the problem we have especially aimed at carrying out the absorption experiments in an apparatus in which the flow conditions of both the gas and the liquid phase were well determined, so that a quantitative interpretation of the experimental results might be possible. In this respect, a favourable case would be the situation, in which gas and liquid, both in laminar flow, are brought into contact with each other for a specified period of time τ on their way through the absorption unit. If, moreover, there is no velocity gradient perpendicular to the interface in either phase, it is then possible to apply a rather simple form of the theory of diffusion to the transfer of NO_2 from the gas to the liquid. A wetted wall column seemed best suited to obtain the situation described above, because it has three attractive features:

(1) a sharp boundary between the gas and the liquid phase,
(2) a well-defined absorption area, and
(3) well-known hydrodynamic conditions of the falling liquid film.

In addition, special measures were taken in order to insure:

(4) cocurrent laminar flow of both gas and liquid,
(5) a flat velocity profile of the gas in the wetted tube,
(6) equal values of the surface velocity of the liquid film and the velocity of the gas,
(7) equal temperatures of gas and liquid.

*In the gas phase NO_2 is in continuous equilibrium with N_2O_4 according to the equation: $2NO_2 \rightleftharpoons N_2O_4$. This equilibrium, which is dependent on temperature and pressure, is reached very rapidly. In this paper NO_2 will be referred to as the mixture of NO_2 and N_2O_4, unless stated otherwise.

VOL 11 1959

Before the NO_2 absorption experiments were started, a check on the flow conditions of both liquid and gas was desired. The laminar flow behaviour of the falling *liquid film* was verified by measurement of the absorption rate of pure CO_2 gas into water. The flow conditions of the *gas* were tested separately by means of absorption of NH_3 from N_2 into water.

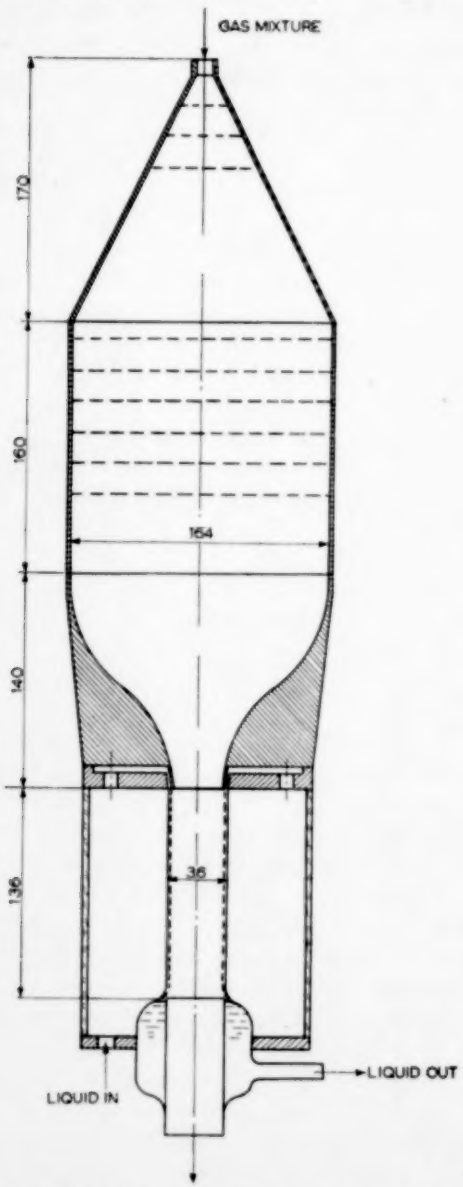

FIG. 1. Sketch of absorption apparatus ; dimensions in mm.

2. EXPERIMENTAL PART

2.1 *Absorption apparatus*

The absorption apparatus is shown in Fig. 1. It consists of a stainless steel upper section containing several gauzes in which the eddies in the gas are suppressed, and in which the gas is forced through a contracting section, into a flat velocity profile. The lower end of this section just fits into the top of the cylindrical absorption column (glass) in such a way that a slit of 0·4 mm width is left ; through this slit the liquid enters into the wetted wall tower.

The radial velocity distribution of the gas was measured at several distances downstream the entrance by means of a hot wire anemometer under conditions where the average gas velocity and the liquid film surface velocity were equal. Figure 2 shows for one example that the velocity profile was practically flat, except for a small boundary layer effect near the top, which was due to wall friction in the contracting section. This effect can not, in principle, be entirely eliminated. It was possible to fulfill the (arbitrary) requirement that the maximum deviation from the average gas velocity be reduced to 10 per cent within $\frac{1}{3}$ of the total height. (See Fig. 2).

The hot wire anemometer was also used to determine the degree of turbulence of the gas inside the wetted wall column. From these measurements it was verified that eddy diffusion could be entirely neglected with respect to molecular diffusion.

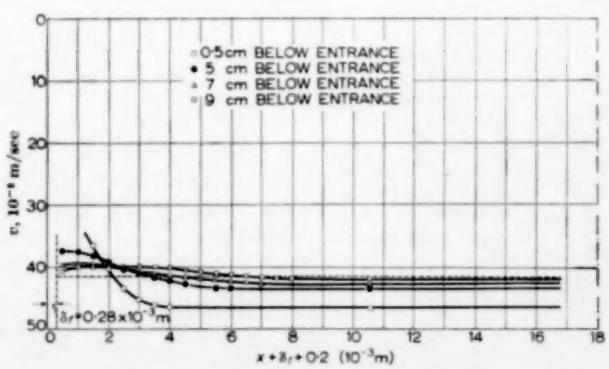

FIG. 2. Velocity distribution of the gas for $v_g = 41{\cdot}4$ cm/sec.

Whereas the height of the wetted wall column (13·6 cm) was fixed by the boundary layer entrance effect, the inside diameter of the absorption column was chosen such that a reasonably accurate interpretation of gas absorption results from gas analysis data alone would be possible. With a diameter of 3·6 cm the percentage of NH_3 absorbed by water could be expected to lie between 20 and 35, depending on the contact time between gas and liquid.

2.2 *Additional equipment*

CO_2 absorption—For the measurements of the absorption rate of CO_2 into the water film the pure CO_2 gas was saturated with water vapour at the temperature of the absorption experiments and was then led through the absorber. A very small amount of detergent had been added to the water in order to prevent surface rippling. The CO_2 absorption rate was found from the decrease of the CO_2 volume at constant pressure which was measured by means of the "soap bubble" method [7].

NH_3 absorption—The absorption experiments of NH_3 into water from nitrogen were carried out at 25°C. The gas flows of NH_3 and N_2 were measured separately by means of calibrated rotameters and then mixed and fed to the absorber. The incoming and outgoing gas streams could be sampled for NH_3 analysis. The NH_3 content of the outgoing liquid was determined by chemical analysis of a number of samples during a run. Thus a NH_3 mass balance could be set up around the absorber for every experiment.

Also the electrical conductivity of the outgoing liquid was recorded in order to verify the steady operation during an experimental run.

NO_2 absorption—A differential photometer was built for the accurate measurement of the NO_2 concentration in the gas mixtures. Its operation was based on the selective light absorption of NO_2. The value of the light absorption coefficient k_λ for $\lambda = 5461$ Å was determined to be 1·22 cm^{-1} atm^{-1} by chemical calibration [1]. With this photometer the NO_2 concentration of both inlet and outlet gas could be accurately measured at frequent intervals. Special precautions had to be taken in order to maintain the temperature and the pressure of the gas at constant known values because of the sensitivity of the dimerization equilibrium constant of the reaction $2NO_2 \rightleftharpoons N_2O_4$.

During a run liquid samples were taken for analysis of HNO_3 and HNO_2 in the outgoing liquid. In this way, a material balance could be set up around the absorber, expressed in equivalent moles of NO_2. Also in these experiments the electrical conductivity of the outgoing liquid was recorded.

3. Discussion of the Experimental Results

3.1 *The CO_2 absorption experiments*

The experimental absorption rates of pure CO_2 gas into the laminar falling water film were compared with the rates predicted from the "penetration" theory for physical absorption. According to this theory (see e.g. [7] and [8]), the amount of gas absorbed by the liquid with initial zero gas concentration will be, per unit surface area and after a contact time τ:

$$m(\tau) = \frac{\Phi_m}{\pi d^x v_s} = 2C_w \sqrt{\left(\frac{D}{\pi}\right)} \sqrt{\left(\frac{h - \Delta h}{v_s}\right)}$$

In a plot of $m(\tau)$ vs. $\sqrt{[(h - \Delta h)/v_s]}$ this relation would give a straight line through the origin with a slope of $2C_w \sqrt{(D/\pi)}$. In Fig. 3 such a a line has been drawn for $2C_w \sqrt{(D/\pi)} = 8{\cdot}04 \times 10^{-5}$ kg/m² $sec^{1/2}$, which was found by Nijsing [7] for absorption of CO_2 at 20°C and a CO_2 pressure of 760 mm Hg. The experimental points obtained in this investigation under the same conditions have also been indicated in Fig. 3, and it is seen that the agreement with Nijsing's results is very good.

Also in these experiments it proved necessary to reduce the total film height h by the amount Δh which is the height of the reflection wave formed above the liquid level of the collecting reservoir (1–2 cm in these experiments). In this part of the film practically no absorption occurs as has been shown in previous work [7, 8].

From the CO_2 absorption measurements it appears that the hydrodynamic conditions of the

falling liquid film agree well with the theoretical model.

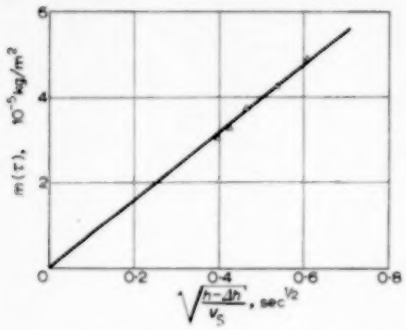

FIG. 3. CO_2 absorption: comparison between experimental results and theory.
△ experiment
— theory

3.2 *The NH_3 absorption experiments*

The flow conditions of the gas were separately investigated by absorbing NH_3 from N_2 into water. Since the solubility of NH_3 in water is high, the absorption rate is mainly determined by the diffusion of NH_3 in the gas phase. If one assumes the NH_3 concentration in the gas at the interface, c_w, to be constant the decrease of the NH_3 concentration can be mathematically predicted for laminar piston flow of the gas from the following formula [9]:

$$\frac{\bar{c} - c_w}{c_0 - c_w} = 4 \sum_{n=1}^{\infty} \frac{1}{\beta_n^2} e^{-\beta_n^2 D\tau/(R-\delta_f)^2} \qquad (2)$$

where β_n are the roots of the Bessel function of the first kind of order zero.

In applying this theory to the present case of NH_3 it had to be taken into account that the liquid-side resistance is not entirely negligible. The value of c_w at the interface can be calculated for the case where a stagnant gas with concentration c_0 and a stagnant liquid are suddenly brought into contact with each other. It is then found that $c_w = f c_0$, where f can be regarded as the fraction of the total diffusional resistance which is due to the liquid phase. In this way, f was calculated to be about 0·07 for the system N_2–HN_3 – water and under the conditions of these experiments.

Figure 4 shows a graphical representation of equation (2) for $f = 0$ and $f = 0{\cdot}07$. When the experimental results on the NH_3 absorption had to be plotted in this graph, a difficulty arose as to the correct value of the active film height and the contact time τ. Since the mass transfer is mainly determined by diffusion in the gas phase, it seems unlikely that the area of the reflection wave just above the liquid level would be entirely inactive as was the case with absorption of pure CO_2 into water. Therefore, the experimental values were calculated on the basis

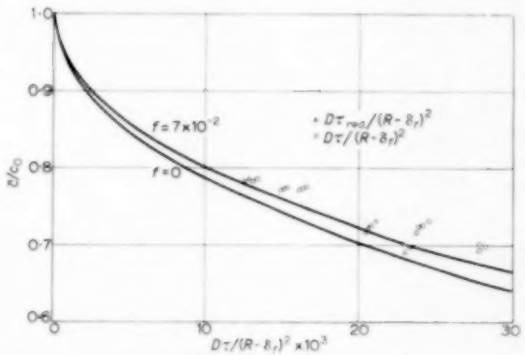

FIG. 4. NH_3 absorption; comparison between experimental results and theory.

of the total time of contact ($\tau = h/v_s$) as well as on the reduced time ($\tau_{red} = (h - \Delta h)/v_s$). Moreover, the accuracy of the results was limited by some uncertainty with respect to the molecular diffusivity of the system $NH_3 - N_2$*).

Nevertheless the results plotted in Fig. 4 fit the predicted data sufficiently well for the purpose of these experiments. It can be concluded that transport by turbulence in the gas flow was negligible and that the deviation from the flat velocity profile at the top of the column had no appreciable effect.

3.3 *The NO_2 absorption experiments*

The absorption rate of NO_2 into water was measured for various contact times (0·2–0·4 sec), inlet concentrations of the nitrous gases (3–15

*A value of $2{\cdot}5 \times 10^{-5}$ m²/sec was used for 25°C and 760 mm Hg.

Table 1. *Main results of the* NO_2 *absorption experiments*

Run	T (°C)	v_g (10^{-2} m/sec)	τ (sec)	$(p_e)_0$ (10^{-2} atm)	$\overline{p_{N_2O_4}}$ (10^{-2} atm)	$(\Phi_m)_e$ (m mole/min)	$(c/c_0)_e$
1	25	33·8	0·40	3·01	0·29	3·16	0·871
2	25	33·8	0·40	3·03	0·30	2·93	0·882
3	35	34·8	0·39	3·02	0·18	2·10	0·914
4	25	50·3	0·27	2·99	0·30	3·46	0·905
5	25	64·1	0·21	2·98	0·31	3·17	0·931
6	25	64·3	0·21	3·09	0·33	3·42	0·927
7	25	34·0	0·40	5·82	0·81	6·86	0·856
8	35	35·0	0·39	5·96	0·56	5·74	0·882
9	25	50·5	0·27	5·76	0·83	6·90	0·902
10	35	52·5	0·26	6·18	0·62	6·40	0·915
11	25	65·0	0·21	5·69	0·85	7·99	0·910
12	25	64·9	0·21	5·66	0·81	7·58	0·915
13	25	34·5	0·39	8·94	1·56	11·8	0·843
14	25	34·2	0·40	9·03	1·52	10·9	0·858
15	25	34·3	0·40	9·11	1·61	12·3	0·840
16	25	34·4	0·39	9·15	1·61	11·7	0·850
17	35	35·6	0·38	9·39	1·15	10·6	0·866
18	25	50·8	0·27	9·04	1·63	13·4	0·883
19	25	65·4	0·21	8·57	1·54	13·5	0·899
20	25	50·5	0·27	15·3	3·16	26·1	0·864
21	25	50·7	0·27	15·3	3·30	25·2	0·866

per cent) and operating temperatures (25–35°C). The main results have been collected in Table 1; these lead to the following general conclusions:

(a) the absorption rate $(\Phi_m)_e$, expressed in equivalent moles of NO_2, is proportional to the average partial pressure of N_2O_4 in the bulk of the gas (see Fig. 5);

(b) if the inlet concentration of the gas is kept constant the absorption rate only slightly depends on the contact time;

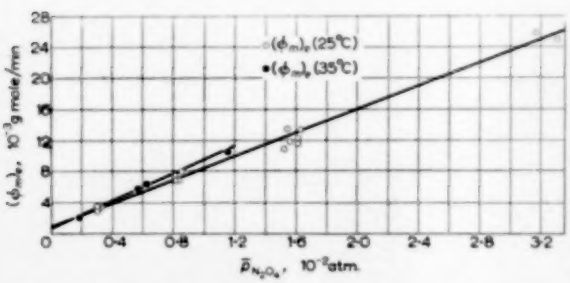

FIG. 5. NO_2 absorption rate as a function of the average N_2O_4 partial pressure in the gas.

(c) the absorption rates are considerably lower than would be the case if only the diffusion in the gas phase were controlling;

(d) the absorption rate, calculated from the photometric analysis, is always 30–60 per cent higher than that obtained from the chemical analysis of the liquid $[(\Phi_m)_e]$;

(e) a change of the operating temperature from 25°C to 35°C has only a small effect on the absorption rate;

(f) mist was observed in the gas outlet when the eNO_2 concentration exceeded about 9 per cent.

From this it can be concluded that N_2O_4 rather than NO_2 plays an important role in the absorption process. The deficit in the material balance, as mentioned under (d), can be explained by the occurrence of a reaction between NO_2 and/or N_2O_4 and water in the gas phase in the neighbourhood of wet surfaces. It was estimated that at least 93 per cent of this reaction occurred in the equipment (tubing and drying column) between the gas outlet of the absorber and the

photometer, and at the very most 7 per cent in the absorber itself. Therefore the photometric analysis of the outgoing gas could *not* be used for calculations and the experimental absorption rates were computed from the chemical analysis of the outgoing liquid.

The effect, described under (c) suggests that the liquid phase also presents a resistance to NO_2 transport. The small sensitivity towards the contact time mentioned under (b) might indicate that this diffusional resistance is accompanied by a rapid reaction between NO_2 and/or N_2O_4 and water.

4. Interpretation of the Measured Absorption Rates of NO_2 into Water

For the analysis of the experimental results we will use the following model, which is similar to that applied by Wendel and Pigford [6]:

(a) Below the entrance of the wetted wall tower NO_2 and N_2O_4—in continuous equilibrium with each other—diffuse from the bulk of the gas to the gas-liquid interface;

(b) N_2O_4 is the *only* species which dissolves in the liquid;

(c) the diffusion of N_2O_4 into the liquid is accompanied by a rapid pseudo-first-order reaction between N_2O_4 and water.

A number of NO_2 and/or N_2O_4 molecules will probably also react with evaporated H_2O molecules near the gas–liquid interface. However, it could be assumed that the influence of the gas phase reaction on the NO_2 absorption rate was sufficiently small to be neglected. Moreover, complications arising from the liberation of NO were assumed to be negligible for the conditions of these experiments because of the slow decomposition rate of HNO_2.

Because in particular the physical solubility of N_2O_4 in water and the rate constant of the reaction mentioned under (c) were not known the following calculations were made.

The diffusion of the $NO_2 - N_2O_4$ mixture in the gas phase was regarded as the diffusion of one fictitious component "eNO_2." A derivation of the diffusivity of this component as function of D_{NO_2} and $D_{N_2O_4}$* was obtained by assuming a steady state diffusion of NO_2 and N_2O_4 molecules through a stagnant gas film of N_2 (cp. Roberts [10]).

The following differential equation was then set up for the diffusion of "eNO_2" from the cylindrical gas space to the wetted wall:

$$\frac{v_z}{D_e}\frac{\partial c}{\partial z} = \frac{\partial^2 c}{\partial r^2} + \frac{1}{r}\frac{\partial c}{\partial r}, \tag{3}$$

or

$$\frac{\partial (c/c_0)}{\partial \phi} = \frac{\partial^2 (c/c_0)}{\partial \rho^2} + \frac{1}{\rho}\frac{\partial (c/c_0)}{\partial \rho} \tag{4}$$

where $\rho = r/R^x$, $R^x = R - \delta_f$ and $\phi = Dz/(R^x)^2 v^s$

Two of the three boundary conditions are:

$$c = c_0 \text{ at } \phi = 0 \text{ and } 0 < \rho < 1, \tag{5}$$

and

$$c \neq \infty \text{ at } \rho = 0 \text{ and } \phi \geqslant 0. \tag{6}$$

At the gas–liquid interface ($\rho = 1$) the third boundary condition has to account for the above hypothesis concerning the N_2O_4 dissolution and reaction. The penetration of N_2O_4 molecules in the liquid film accompanied by the rapid pseudo first order reaction

$$N_2O_4 + H_2O \xrightarrow{k'} HNO_2 + HNO_3$$

results in the following equation for the absorption rate at the interface:

$$(\Phi_m'')_e = 2\,(\Phi_m'')_{N_2O_4} = 2C_w\sqrt{(k'\,D_l)} \tag{7}$$

As was shown by Danckwerts [11] equation (7) is a good approximation as long as $k'\,z/v_z > 4$ which is the case for the greater part of the absorbing film in our experiments†.

At the interface the rate of transport of eNO_2 in the gas phase is given by:

$$(\Phi_m'')_e = -\,D_e\,(\partial c/\partial r)_{r=R^x}. \tag{8}$$

---

*D_{NO_2} and $D_{N_2O_4}$ were taken to be 1·40 and 0·98 $\times$ 10^{-5} m^2/sec respectively at 25°C and 760 mm Hg [2].

†Strictly speaking, Danckwerts' derivation is valid for a constant value of the interfacial concentration in the liquid C_w. In the present experiments C_w decreases somewhat with increasing z but detailed calculations have shown here that equation (7) still is applicable with good accuracy.

The combination of equations (7) and (8) gives the third boundary condition:

$$\frac{\partial (c/c_0)}{\partial \rho} = -\,2\,\frac{C_w R^x}{c_0 D_e}\sqrt{(k'\,D_l)} \qquad \text{for } \rho = 1 \text{ and } \phi > 0 \quad (9)$$

The relation between c_w (the eNO_2 concentration in the gas at the interface) and C_w (the saturation concentration of N_2O_4 in the liquid, which is in equilibrium with the gas) follows from Henry's law:

$$C_w = H\,(c_{N_2O_4})_w\,R_g\,T \qquad (10)$$

and the equilibrium between $c_{N_2O_4}$ and c:

$$c_{N_2O_4} = 1/2\,c - K_c/8\,[\sqrt{(1 + 8c/K_c)} - 1] = f(c) \qquad (11)$$

Substitution of (10) and (11) into (9) finally gives:

$$\left[\frac{\partial (c/c_0)}{\partial \rho}\right]_{\rho=1} = -\,\frac{1}{Q}\cdot\frac{f(c)}{c_0} \qquad (12)$$

where Q is a dimensionless parameter defined as:

$$Q = D_e/2R^x\,HR_gT\,\sqrt{(k'\,D_l)} \qquad (13)$$

Table 2. Results of the numerical solution of equation (4)

	$T = 25°C$				$T = 35°C$		
Series	I	II	III	IV	I	II	III
$10^3\,c_0$	1·23	2·34	3·69	6·25	1·19	2·40	3·72
$100\,\phi$	$\bar{c}/c_0$	$\bar{c}/c_0$	$\bar{c}/c_0$	$\bar{c}/c_0$	$\bar{c}/c_0$	$\bar{c}/c_0$	$\bar{c}/c_0$
			$Q = 0{\cdot}01$				
0·375	0·953	0·942	0·935	0·928	0·967	0·954	0·946
0·500	0·942	0·929	0·920	0·912	0·958	0·943	0·934
0·625	0·932	0·917	0·907	0·898	0·949	0·932	0·922
0·750	0·922	0·906	0·895	0·885	0·941	0·922	0·911
0·875	0·912	0·895	0·884	0·873	0·934	0·913	0·901
1·000	0·903	0·885	0·873	0·862	0·926	0·904	0·892
1·125	0·895	0·876	0·863	0·851	0·920	0·896	0·883
1·250	0·887	0·867	0·853	0·841	0·913	0·888	0·874
1·375	0·879	0·858	0·844	0·832	0·907	0·880	0·866
1·500	0·872	0·850	0·835	0·823	0·900	0·873	0·858
1·625	0·865	0·842	0·827	0·814	0·894	0·866	0·850
			$Q = 0{\cdot}02$				
0·375	0·970	0·961	0·955	0·949	0·980	0·970	0·964
0·500	0·962	0·951	0·944	0·936	0·974	0·962	0·954
0·625	0·954	0·942	0·933	0·924	0·968	0·954	0·945
0·750	0·947	0·933	0·923	0·913	0·963	0·947	0·937
0·875	0·940	0·924	0·914	0·903	0·957	0·940	0·929
1·000	0·932	0·916	0·905	0·893	0·952	0·934	0·921
1·125	0·926	0·908	0·896	0·884	0·947	0·927	0·914
1·250	0·920	0·900	0·888	0·875	0·943	0·921	0·907
1·375	0·914	0·893	0·880	0·866	0·938	0·915	0·900
1·500	0·908	0·886	0·872	0·858	0·933	0·909	0·893
1·625	0·902	0·879	0·865	0·850	0·929	0·903	0·887

Since the equilibrium relationship between the eNO_2 concentration in the gas and the N_2O_4 concentration in the liquid is non-linear, an analytical solution of equation (4) with the boundary conditions (5), (6) and (12) was nearly impossible. Solutions to the differential equation were obtained by numerical computation (Table 2) for two values of the parameter Q, which were chosen by previous trials.

In order to compare the theoretically computed values of $\bar{c}/c_0$ with the experimental results, the value of $\phi_\tau = D_e\,\tau/(R^x)^2$ had to be determined for each run. The contact time τ was calculated as h/v_s and the end effect of the falling film was not taken into account for lack of arguments for the application of a proper correction.

The experimental results were plotted as $\bar{c}/c_0$ vs. ϕ_τ and compared to the theoretical lines for $Q = 0{\cdot}01$ and $Q = 0{\cdot}02$. Figure 6 gives an example of such a comparison for one concentration series.

Then for every run the corresponding value of

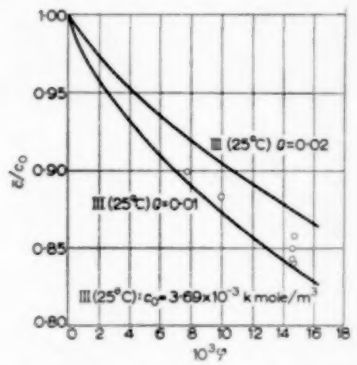

FIG. 6. Comparison between the eNO_2 depletion of the gas with computed results for $Q = 0{\cdot}01$ and $0{\cdot}02$ for one concentration series (runs 13, 14, 15, 16, 18 and 19).

Table 3. Values of Q *obtained from the measurements*

Run	T (°C)	$10^3\,c_0$ (kmole/m³)	$10^3\,\phi_\tau$ —	$10^2\,Q$ —	$10^2\,Q$ —	$H\sqrt{k'\,D_l}$ $\left(\frac{\text{kmole}}{\text{m}^3\,\text{atm}}\cdot\frac{\text{m}}{\text{sec}}\right)$	$H\sqrt{k'}$ $\left(\frac{\text{kmole}}{\text{m}^3\,\text{atm}\,\text{sec}^{1/2}}\right)$
1	25	1·23	15·8	1·1			
2	25	,,	15·8	1·4			
4	25	,,	10·7	1·2	1·4	$1{\cdot}03.10^{-3}$	28
5	25	,,	8·4	1·6			
6	25	,,	8·4	1·5			
7	25	2·34	15·1	1·2			
9	25	,,	10·2	1·6			
11	25	,,	8·0	1·3	1·4	$0{\cdot}99.10^{-3}$	27
12	25	,,	8·0	1·5			
13	25	3·69	14·5	1·1			
14	25	,,	14·7	1·5			
15	25	,,	14·6	1·1			
16	25	,,	14·6	1·3	1.3	$1{\cdot}04.10^{-3}$	28
18	25	,,	9·9	1·3			
19	25	,,	7·7	1·2			
20	25	6·25	9·6	1·0			
21	25	,,	9·6	1·0	1·0	$1{\cdot}30.10^{-3}$	35
3	35	1·10	16·9	1·6	1·6	$0{\cdot}97.10^{-3}$	23
8	35	2·40	16·2	1·4			
10	35	2·40	10·9	1·6	1·5	$0{\cdot}99.10^{-3}$	24
17	35	3·72	15·5	1·3	1·3	$1{\cdot}10.10^{-3}$	27

Q was found by linear interpolation between $Q = 0{\cdot}01$ and $0{\cdot}02$. The results of this interpolation are shown in Table 3. The Q-values have been subdivided into groups, each group representing one concentration series and one temperature. Reviewing the Q-values of each group given in Table 3, it appears that for one temperature no significant dependence of the contact time and the concentration can be observed. This would be expected on the basis of the working theory, since Q in equation (13) would only depend on the temperature except for a possible influence of the concentration on D_e and H.

The change of D_e with the concentration is, however, relatively small compared to the spread in the Q-values, whereas a constant value of H was more or less postulated.

So for each of the two temperatures a gross average for Q was deduced from the experiments:

$$T = 25°C \qquad Q = (1{\cdot}3 \pm 0{\cdot}2) \,.\, 10^{-2}$$
$$T = 35°C \qquad Q = (1{\cdot}5 \pm 0{\cdot}2) \,.\, 10^{-2}$$

By substituting the values of the known quantities* in equation (13) the corresponding values of the product $H\sqrt{k'}$ were obtained. The results are listed in Table 4.

For purpose of comparison, Table 5 contains a number of values for $H\sqrt{(k'\,D_l)}$ obtained from absorption experiments performed in different equipment. It is seen that the listed values all have the same order of magnitude as those found in this work.

Table 4. Final results on the liquid kinetics of N_2O_4 absorption

T	$H\sqrt{(k'\,D_l)}$	$H\sqrt{k'}$
(°C)	$\left(\frac{10^{-3}\ \text{kmole}}{\text{m}^3\ \text{atm}} \cdot \frac{\text{m}}{\text{sec}}\right)$	$\left(\frac{\text{kmole}}{\text{m}^3\ \text{atm sec}^{\frac{1}{2}}}\right)$
25	1·1	28 ± 5
35	1·0	24 ± 5

5. Conclusions

It may be concluded that the experimental results of this work are fairly well described by the proposed absorption mechanism. Also this theory explains that in general the gas phase resistance will be predominant at a high concentration of the nitrous gases; as the eNO_2 concentration in the gas decreases, the main resistance to mass transfer shifts towards the liquid phase.

In the light of these results it would have been more logical to set up a different kind of experiment in order to study the liquid phase kinetics of the NO_2 absorption and so to obtain more accurate values of $H\sqrt{(k'\,D_l)}$. As a consequence,

Table 5. Comparison with results of other investigations

Authors	*Temperature* (°C)	$H\sqrt{(k'\,D_l)}$ $\left(\frac{10^{-3}\ \text{kmole}}{\text{m}^3\ \text{atm}} \cdot \frac{\text{m}}{\text{sec}}\right)$
Caudle and Denbigh* [4]	25	1·10
Caudle and Denbigh [4]	35	2·50
Wendel and Pigford [6]	25	0·58
Wendel and Pigford [6]	40	0·54
Snoeck†	10	0·80
Snoeck	20	0·77
Snoeck	30	0·82

* For the diffusivity D_l of N_2O_4 in water at 25°C a value of $1{\cdot}40 \times 10^{-9}$ m²/sec was used [12].

*Calculated from their experiments for water as the absorbing liquid.

†These figures result from measurements by Snoeck in continuation of the work presented in this paper. Here, N_2O_4 was absorbed from $NO_2 - N_2O_4$ mixtures in a short laminar water jet. The data in Table 5 are preliminary only, the work still being in progress.

the NO_2 absorption experiments have been continued with an absorber where a low pressure $NO_2 - N_2O_4$ mixture is exposed to a laminar water jet. Preliminary results of this investigation have been included in Table 5.

In this paper we shall not deal with the calculation of the individual values of H and k'. As has been shown by WENDEL and PIGFORD [6] this can be done by combining $H\sqrt{k'}$ values with the kinetic studies in connexion with the decomposition of HNO_2 in aqueous solutions, which were carried out by ABEL and SCHMID [13]. The authors think that the treatment by WENDEL and PIGFORD can be improved by using more recent data. This would be worthwhile after more accurate values of $H\sqrt{k'}$ have been obtained from new experiments.

Acknowledgements—The authors gratefully acknowledge stimulating discussions with Dr. G. SCHMIDT (MEKOG, Ijmuiden), Professor D. W. VAN KREVELEN and P. J. HOFTIJZER (Central Laboratory State Mines, Geleen), and S. P. S. ANDREW (I.C.I. Billingham). In particular the authors thank MEKOG for their advice regarding the experimental set-up and for providing the NO_2 gas. The two first authors are indebted to the "Delfts Hogeschoolfonds" through which they obtained a fellowship from the Dow Chemical Company.

NOTATION

c = concentration of component to be absorbed in the gas phase — mole m^{-3} or kg m^{-3}
C = concentration of gas in the liquid — kg m^{-3}
d = internal diameter of the wetted wall tower (dry) — m
d^+ = diameter of the cylindrical film surface — m
D = coefficient of molecular diffusion — m^2 sec^{-1}
f = fraction
h = height of the film — m
Δh = height of the end effect — m
H = Henry coefficient — kmole m^{-3} atm^{-1}
k_λ = light absorption coefficient — e n^{-1} atm^{-1}
K_c = equilibrium constant of the reaction $2NO_2 \rightleftharpoons N_2O_4$ — kmole m^{-3}
$m(\tau)$ = quantity of gas absorbed per unit area after a contact time τ — kg m^{-2}
p = partial pressure — atm
Q = dimensionless parameter, defined in equation (13)
r = cylindrical co-ordinate — m
R = radius of the wetted wall tower (dry) — m
R^x = radius of the cylindrical film = $R - \delta_f$ — m
R_g = gas constant ($8{\cdot}316 \times 10^3$) — J $kmole^{-1}$ $°C^{-1}$
T = temperature — °C °K
v = velocity — m sec^{-1}
v_s = surface velocity of the liquid film — m sec^{-1}
z = co-ordinate in the direction of gas and liquid flow — m
δ_f = thickness of the liquid film — m
λ = wave length — Å
ρ = dimensionless radius r/R^x
τ = contact time ($= h/v_s$) — sec
$\tau_{red.}$ = contact time with correction for the end effect ($= (h - \Delta h)/v_s$) — sec
ϕ = dimensionless group $= Dz/(R^x)^2 v_s$
Φ_m'' = absorption rate per unit area — kg m^{-2} sec^{-1}
Φ_m = absorption rate — kg sec^{-1}

Subscripts

e = eNO_2 i.e. $c_e = c = c_{NO_2} + 2\,c_{N_2O_4}$
f = film
g = gas
l = liquid
w = wall or gas – liquid interface

REFERENCES

[1] DEKKER W. A. Ph.D. Thesis, Delft 1958.
[2] CHAMBERS F. S. and SHERWOOD T. K. *Industr. Engng. Chem.* 1937 **29** 1415.
[3] DENBIGH K. G. and PRINCE A. J. *J. Chem. Soc.* 1947 790.
[4] CAUDLE P. G. and DENBIGH K. G. *Trans. Faraday Soc.* 1953 **49** 39.
[5] PETERS M. S., ROSS C. P. and KLEIN S. J. E. *Amer. Inst. Chem. Engrs. J.* 1955 **1** 105.
[6] WENDEL M. M. and PIGFORD R. L. *Amer. Inst. Chem. Engrs. J.* 1958 **4** 249.
[7] NIJSING R. A. T. O., HENDRIKSZ R. H. and KRAMERS H. *Chem. Engng. Sci.* 1959 **10** 88.
[8] LYNN S., STRAATEMEIER J. R. and KRAMERS H. *Chem. Engng. Sci.* 1955 **4** 49.
[9] CARSLAW H. S. and JAEGER J. C. *Conduction of Heat in Solids* p. 199. Oxford University Press, 1959.
[10] ROBERTS J. B., Ph.D. Thesis, M.I.T. Cambridge 1936.
[11] DANCKWERTS P. V. *Trans. Faraday Soc.* 1950 **46** 300.
[12] WILKE C. R. and CHANG PIN *Amer. Inst. Chem. Engrs. J.* 1955 **1** 264.
[13] ABEL E. and SCHMID H. *Handbuch der Katalyse* Bd. 2 S. 3 1940.

SELECTION OF CURRENT PAPERS OF INTEREST TO CHEMICAL ENGINEERS

K. Rietema and H. J. Krajenbrink: Theoretical derivation of tangential velocity profiles in a flat vortex chamber – influence of turbulence and wall friction. (Part of a study of the hydrodynamics of a cyclone separator). *Appl. Sci. Res.* A 1959 **8** 177–197.

P. L. Slis, Th. W. Willemse and H. Kramers: The response of the level of a liquid fluidized bed to a sudden change in the fluidizing velocity. *Appl. Sci. Res.* A 1959, **8** 209–218.

W. Squire: A unified theory of turbulent flow. 1. Formulation of the theory. *Appl. Sci. Res.* A 1959 **8** 158–168.

H. J. Merk: Mass transfer in laminar boundary layers calculated by means of a perturbation method. *Appl. Sci. Res.* A 1959 **8** 237–260.

H. J. Merk: Mass transfer in the laminar boundary layer along a flat plate calculated by means of the integral method. *Appl. Sci. Res.* A 1959 **8** 261–277.

P. G. Saffman: Exact solutions for the growth of fingers from a flat interface between two fluids in a porous medium or Hele–Shaw cell. (Penetration of a viscous liquid by an inviscid liquid). *Quart. J. Mech. Appl. Math.* 1959 **12** 146–150.

D. R. Davies: On the calculation of eddy viscosity and heat transfer in a turbulent boundary layer near a rapidly rotating disk. *Quart. J. Mech. Appl. Math.* 1959 **12** 211–221.

D. E. Bourne, D. R. Davies and S. Wardle: A further note on the calculation of heat transfer through the axisymmetrical boundary layer on a circular cylinder. *Quart. J. Mech. Appl. Math.* 1959 **12** 257–260.

D. B. Concer: Heat flow towards a moving cavity. (Transfer of heat from surroundings of constant thermal conductivity to a moving cylinder whose surface temperature is constant). *Quart. J. Mech. Appl. Math.* 1959 **12** 222–231.

K. A. Wilde: Condensation in nozzles. *J. Appl. Phys.* 1959 **30** 577–580.

E. G. Bayley: Power law flow curves of dimethyl siloxane polymers. *J. Appl. Phys.* 1959 **30** 597.

A. J. Ede and O. A. Saunders: Heat transfer from a flat surface to a parallel stream of water. *Proc. Inst. Mech. Engrs.* 1958 **172** 743–758.

T. P. Newcomb: Flow of heat in a composite solid. (Conduction of heat generated by friction at interface between two slabs of solid). *Brit. J. Appl. Phys.* 1959 **10** 204–206.

D. G. Osborne and S. Thornton: Viscous properties of thixotropic materials. *Brit. J. Appl. Phys.* 1959 **10** 214–219.

J. F. Hutton: Flow properties of distillates at low temperatures: a review. *J. Inst. Petrol.* 1959 **45** 123–129.

S. R. M. Ellis and R. M. Contractor: Performance of the Oldershaw column at reduced pressures. *J. Inst. Petrol.* 1959 **45** 147–152.

J. A. Kitchener and C. F. Cooper: Current concepts in the theory of foaming. *Quart. Rev.* 1959 **13** 71–97.

A. W. Lawson, R. Lowell and A. L. Jain: Thermal conductivity of water at high pressures. *J. Chem. Phys.* 1959 **30** 643–647.

S. Broersma: Diffusion and viscosity in a spherical cavity. *J. Chem. Phys.* 1959 **30** 707–717.

A. G. Epprecht: Das wirkliche Fliessverhalten plastischer Substanzen. Schweiz. *Arch. angew. Wiss. Techn.* 1959 **25** 82–87.

R. Esche: Ultraschallanlagen in chemischen Produktionsprozessen. *Siemens-Z.* 1959 **33** 60–63.

A. Singewald: Über den Zusammenhang zwischen Flotation und Löslichkeit von Salzmineralien. *Z. Erzbergb. Metallhüttenw.* 1959 **12** 121–135.

Über die Evakuierungsgeschwindigkeit von Hochvakuumanlagen. *Vakuum-Techn.* 1959 **8** 39–43.

G. Zaeschmar: Wärmeübergang durch Konvektion und Strahlung. *Allg. Wärmetechn.* 1958/59 **9** 33–37.

H. Ziebland: Neuere Untersuchungen über die Wärmeleitfähigkeit von schwerem Wasser. *Allg. Wärmetechn.* 1958/59 **9** 37–39

E. Bodea: Die Temperaturwaage, ein MKSA-Normthermometer. *Acta Phys. Austr.* 1959 **12** 220–236.

SELECTION OF CURRENT SOVIET PAPERS OF INTEREST TO CHEMICAL ENGINEERS*

D. P. Dobychin and T. F. Tselinskaya: Effect of thermal ageing on porous structure and catalytic activity of synthetic alumino-silicates. *Zh. prikl. Khim.* 1959 **32** 486–494.

M. V. Tikhomirov and N. N. Tunitski: Separation of isotopes of carbon and oxygen by rectification of CO in a 12 m column. *Zh. prikl. Khim.* 1959 **32** 531–536.

L. N. Matusevich: Intensity of stirring of solutions and purity of produced crystals. *Zh. prikl. Khim.* 1959 **32** 536–542.

Fu Tsyu-Fu: Calculation of periodically operating distillation column. *Zh. prikl. Khim.* 1959 **32** 543–548.

L. N. Lambin and N. N. Ermolenko: Method of constructing diagrams of multicomponent systems. *Zh. prikl. Khim.* 1959 **32** 548–556.

N. I. Gelperin and A. I. Altikis: Effect of geometric parameters of a sorbent bed on the process of purification of solutions of corn sugar. *Zh. prikl. Khim.* 1959 **32** 599–603.

M. I. Bogdanov and E. P. Krushinskaya: Study of the process of separation of butylene–divinyl mixtures by chemisorption. *Zh. prikl. Khim.* 1959 **32** 603–608.

B. D. Kruzhalov and Kh. E. Khcheyan: Simultaneous production of phthalic acid and chloroform. *Khim. Prom.* 1959 **1** 48–54.

Ya. Beranek and D. Sokol: Theory of fluidized beds. *Khim. Prom.* 1959 **1** 62–68.

P. G. Romankov and P. A. Yablonski: On the influence of various internal structures on the effectiveness of classification of a separator with rotating blades. *Khim. Prom.* 1959 (**1**) 68–70.

L. V. Rashkovan, G. Z. Fain, A. A. Raisfeld and M. V. Shelyastin: Experimental automation of production of weak nitric acid. *Khim. Prom.* 1959 **1** 73–79.

E. L. Zorina and V. K. Semenchenko: Effect of *iso*amyl alcohol on critical phenomena in the system triethylamine–water. *Zh. fiz. Khim.* 1959 **33** 523–533. Effect of addition of the alcohol on the viscosity of the system.

A. B. Storonkin and N. P. Markuzin: Investigation of the total and partial vapour pressures of the ternary solution triethylamine–water–phenol separating at 15 and 35°C. *Zh. fiz. Khim.* 1959 **33** 581–588.

V. A. Zagoruchenko: Equations of state for propane, *iso*butane and *neo*pentane. *Zh. fiz. Khim.* 1959 **33** 607–609.

L. S. Aleksandrova, S. Z. Elovich and K. V. Chmutov: Dynamics of ionic sorption of various types of cation exchangers. *Zh. fiz. Khim.* 1959 **33** 627–635.

Ya. Z. Kazavchinski and V. A. Zagoruchenko: Equation of state and thermodynamic properties of propylene. *Zh. fiz. Khim.* 1959 **33** 662–664.

E. A. Gyunner: Equation for the density of binary aqueous solutions. *Zh. fiz. Khim.* 1959 **33** 683–687.

L. I. Kudryashev and A. Ya. Ipatenko: Influence of free convection on the heat transfer coefficient in flow around a sphere at low Reynolds numbers. *Zh. tekh. Fiz.* 1959 **29** 309–318.

A. N. Kozlova: Temperature distribution in an inclined air-filled pipe in the presence of free convection. *Zh. tekh. Fiz.* 1959 **29** 319–323.

I. A. Ioffe: Unsteady state problem of thermal conduction for a semi-infinite medium with internal cylindrical source of heat. *Zh. tekh. Fiz.* 1959 **29** 417–422.

*To assist readers, translations of any article appearing in the above list can be obtained at a reasonable charge. All orders should be addressed to the Administrative Secretary of the Pergamon Institute at either 4 Fitzroy Square, London W.1, or 1404 New York Avenue N.W, Washington 5, D.C. whichever is more convenient.

P. L. KAPITSA: Calculation of the helium liquifaction cycle. *Zh. tekh. Fiz.* 1959 **29** 427–432.

A. G. TEMKIN: Heat transfer in laminar flow in non-circular tubes. *Zh. tekh. Fiz.* 1959 **29** 433–449.

L. M. ZYSINA-MOLOZHEN: Investigation of the influence of longitudinal pressure gradient on the development of the boundary layer. *Zh. tekh. Fiz.* 1959 **29** 450–461.

M. B. SKOPETS: An approximate method of integration of the laminar boundary layer equations for an incompressible gas with superimposed heat transfer. *Zh. tekh. Fiz.* 1959 **29** 462–470.

L. S. ZAITSEVA: Experimental investigation of thermal conductivities of monoatomic gases over a wide temperature range. *Zh. tekh. Fiz.* 1959 **29** 497–505.

A. S. MONIN: On the theory of local isotropic turbulence. *Dokl. Akad. Nauk. SSSR* 1959 **125** 515–518.

K. I. MATVEEV, O. V. UVAROV and N. M. ZHAVORONKOV: Coefficients of separation of chlorine isotopes in equilibrium evaporation of HCl. *Dokl. Akad. Nauk SSSR* 1959 **125** 580–583.

G. V. SAMSONOV, V. V. VEDENEEVA and A. A. SELEZNEVA: Sorption of penicillin by polymeric sorbents. *Dokl. Akad. Nauk SSSR* 1959 **125** 591–594.

A. A. SERGYENKO and U. K. GRETSOV: Transition from turbulent to laminar boundary layer. *Dokl. Akad. Nauk SSSR* 1959 **125** 746–747.

S. I. KOSTERIN, I. A. KOZHINOV and A. I. LEONTYEV: Effect of pressure fluctuations in a gas flow upon convective heat transfer. *Teploenergetika* 1959 **6** (3) 66–72.

A. L. SHWARTS and V. A. LOKSHIN: Method of determining actual volumetric steam content and hydraulic resistance from experimental pressure drop data. *Teploenergetika* 1959 **6** (3) 72–75.

N. L. KAFENGAUZ and I. D. BOCHAROV: Effect of height of a flat projection on heat transfer to water. *Teploenergetika* 1959 **6** (3) 76–78.

Book Reviews

Advances in Chemical Engineering. Edited by T. B. Drew and J. W. Hoopes, Jr., Academic Press, New York, 1958, Vol. II, ix + 338 pp., $9.50.

Heterogeneity is an inevitable feature of an edition like Advances in Chemical Engineering, not only with respect to the subjects treated, but also regarding the approach by the different authors. Also in this volume it appears that the aim to present a "critical summary of recent work" (quoted from the editors' preface) may be interpreted rather freely.

Evidently, the task of the reviewer is to write a number of short reviews first and to sum them up, if possible, in the end.

J. W. Westwater finishes his monograph (the first part of which appeared in Advances of Chemical Engineering, Volume I) on the *Boiling of Liquids* (p. 1–3, 33 references) with chapters on transition boiling, film boiling, boiling of subcooled liquids and bumping during boiling. Except for the pure film boiling, these phenomena have not been successfully explained by theory and the experimental material is still very incomplete. This is reflected in the text which is clearly written and well illustrated, but has to be mostly descriptive.

Pages 33–80 contain a paper on *Automatic Process Control* (45 references) by E. F. Johnson. Control is introduced as a basic concept of chemical engineering and control problems are treated analytically, mostly by using the frequency response method. This paper has the character of an abridged textbook or university course; according to the reviewer's opinion its presentation in this volume would only be justified by the fact that the application of the servomechanism "language" to process control problems is still novel to many chemical engineers.

In *Treatment and Disposal of Wastes in Nuclear Chemical Technology* (p. 81–116, 37 references) by B. Manowitz, a survey is presented of the various methods which can be employed for the separation, confinement and disposal of radioactive wastes. Clearly, the author has considerable experience in the field and so the paper has become a useful guide for purposes of orientation.

G. A. Sofer and H. C. Weingartner have written *High Vacuum Technology* (p. 117–145, 16 references). After a short introduction on the history of the industrial application of pressures below 0·1 mm Hg, the authors treat the chemical engineering aspects of dilute gases (flow, heat and mass transfer, reaction equilibria) with their consequences to practical problems. The paper ends with a short description of vacuum pumps and gauges.

Separation by adsorption methods (p. 147–208, 99 references) by T. Vermeulen consists of a very valuable attempt to unify the theory of various fluid-solids transfer operations. Particular attention has been paid to adsorption and ion exchange, but application to fixed bed absorption or extraction, partition chromatography, leaching, drying and regenerative heat transfer are possible as well. In the reviewer's opinion, this monograph is an important step forward towards the general systematic treatment of these types of operation.

Finally, this volume contains thoroughly written monograph on the *Mixing of Solids* (p. 209–324, 73 references) by S. S. Weidenbaum. The first half is devoted to the statistical analysis of the state of mixedness and to the treatment of theoretical frequency distributions. Chapters on the rate of mixing and the performance of various types of dry mixers end this excellent review, which is the first of its kind.

Summarizing, the contributions by Westwater, Vermeulen and Weidenbaum in particular correspond to the aim set by the editors, whereas the other papers have more the character of handbook or textbook articles. The whole collection certainly deserves a place in every chemical engineering library.

The reviewer has been struck by the fact that on the total of about 310 literature references 250 are U.S. publications; of the remaining 60, 40 are in the English language and about 20 in foreign languages, including a reference to Poisuille (1838) and Knudsen (1909). One might wonder whether the contributions from the different parts of the world to advances in chemical engineering are in the same ratio.

H. Kramers

Second Symposium on Coal Preparation. Department of Mining, University of Leeds, 1958. xiii + 513 pp., 20s.

The Symposium was supported by the Coal Preparation Plant Association and held in October 1957 at the Department of Mining of the University of Leeds. Eighteen papers were given by authors from Britain, Holland, Germany, the U.S.A. and South Africa, and the papers are reproduced in the book with the discussion on each and summaries by *rapporteurs*.

The range of subjects is wide, from the attachment between bubbles and particles to the marshalling of railway wagons. An idea of the scope of the book may be given by dividing the papers into groups according to subject and approach. There are several accounts of practice in particular fields, including briquetting in the Ruhr, coal preparation in Australia, the choice of a material for use in suspensions in South African dense medium washers, and a general survey of present and future problems in Britain.

The subjects of the laboratory researches include the use of permeability and suction potential methods in a study of the retention of water by fine coal, the angle of contact between coal and air bubbles, and the attachment of bubbles to coal particles in froth flotation. An interesting discussion of the last paper showed some differences of opinion about the relative importance in practice of the two ways – collision and gas precipitation – in which bubbles become attached to particles. A better understanding of this question should lead to improvements in the design of flotation plant.

Three papers on coal preparation plant deal with jig and with dense medium methods, and cover the aspects of testing, prediction of performance and representation of results.

Other papers on practical aspects of the subject deal with the drying of coal, problems of sedimentation and filtration, and experience of interface-active chemicals. These last have interesting possibilities as flocculants, in spite of their high cost.

Most of the papers are devoted to the improvement of processes that are already well established in the coal industry rather than to new developments. The book will certainly be of interest to readers familiar with the coal industry. Though most of the processes and methods are familiar in other connexions, chemical engineers in general will no doubt find interest in their application in an industry which works on a large scale with processes that must be cheap. In general, the field of coal preparation offers to the chemical engineer great scope but perhaps rather less example.

M. J. G. Wilson

Automatic Measurement of Quality in Process Plants. Proceedings of a Conference sponsored by the Society of Instrument Technology, held at Swansea, Sept. 1957. Butterworths, London, 1958. xi + 320 pp., 50s.

The papers contained in this volume form the edited proceedings of the 1957 Summer Conference of the Society of Instrument Technology and they provide a broad survey of the various techniques available for the measurement and control of quality in process plants.

In all, twenty-five papers are presented and these are divided into six main sections. The first section deals with the adaptation of laboratory techniques to plant measurement, and a variety of instruments designed to perform repeated analytical measurements, such as titration and distillation, are described.

The techniques available for the analysis of gases are fully discussed in the second section and calorimetry, oxygen analysis and moisture content determination are included.

Continuous measurement of pH and dielectric constant are then discussed in the third section. The next two deal with spectrometric methods and new techniques for fluid stream analysis. Infra-red gas analysis, mass spectroscopy, vapour phase chromatography and the use of the property of nuclear magnetic resonance are all treated in some detail.

Various physical properties which can be used for the measurement and control of product quality, such as viscosity and density, are treated in the last section and instruments capable of continuously measuring and recording these properties are described.

Although many of the instruments described are capable of providing an accurate assessment of product quality it appears that many problems remain to be solved before they can be used as the measuring element in an automatic control loop. For successful control the response of the measuring unit has to be very fast compared with the response of the plant and the output from the unit should be in a form suitable for use with existing control equipment. These conditions are usually met by instruments which depend on the measurement of a physical property such as temperature, pressure and even less familiar properties such as dielectric constant, refractive index, viscosity and density, but where chemical methods are involved the response of the measuring unit is usually comparatively slow and often the output is intermittent. As an example we could quote the vapour phase chromatograph which does not give a continuous reading but a series of discrete records at intervals of about 10 min. This would require an elaborate control system incorporating a memory circuit to store information from one record to the next, assuming of course that plant is sufficiently stable so that the time interval of 10 minutes can be tolerated.

Although chemical methods are slow, the information they provide is much more complete than that provided by physical methods, especially for multi-component systems and in difficult or unusual circumstances their use is often unavoidable.

In summary this volume provides a complete survey of the latest techniques available for the measurement of product quality and should serve as a very useful reference book for process engineers and, to a lesser extent, for control engineers.

W. L. Wilkinson

F. S. Martin and G. L. Miles: **Chemical Processing of Nuclear Fuels.** Butterworths Scientific Publications, London and Academic Press, New York, 1958. x + 242 pp., 40s, $7.50.

The book gives a broad picture of the present state of knowledge in the nuclear processing field and of expected future developments. Particular emphasis is placed on the basic chemistry involved. Much useful information has been collected and summarized including that released at the 1955 Geneva Conference but not from the 1958 one nor the 1957 Brussels Symposium.

The aim of giving as broad a picture as possible and underlining the basic principles is an excellent one in itself, but inevitably means that less attention is paid to

the established processes. The book is commendably short but could have been lengthened to accommodate a more detailed account of current techniques, particularly in aqueous processing.

It is divided into five sections ; Nuclear Considerations, Aqueous Processes, Non-aqueous Processes, Effluent Disposal and Fission Product Recovery, and Trends in Nuclear Fuel Processing.

In the first and last of these a good introduction to nuclear fuel processing and much useful background knowledge is given. A discussion of the economics involved shows that fuel processing contributes a substantial part to the cost of nuclear power, and yet has no counterpart in conventional power production. There is little prospect of processing being completely avoided, as a high enough burn-up of the expensive fissile fuel cannot be achieved.

The section on aqueous processes is characterized by a detailed discussion of the chemistry involved. There is little information provided which would enable a plant for separating the constituents of irradiated fuel to be designed or its performance to be assessed. Solvent extraction has been the mainstay of the U.K.A.E.A.'s process for separating uranium, plutonium and fission products since its conception, and gives every indication of remaining so for many years to come. It has world-wide application in nuclear fuel processing and hence would have justified a more complete discussion.

An excellent survey of the possible non-aqueous processes, indicates the paucity of information available. They are usually high temperature processes giving partial removal of fission products. Although they are simple in concept and often leave the fuel in a form suitable for direct refabrication by remote handling, they possess technical difficulties. A possible application is to the reprocessing of fast reactor fuel elements of simple design.

The problem of radioactive effluent disposal is likely to become much more acute in the future. The possible ways of dealing with this are well summarized and placed in their proper perspective by a discussion of present practice and the basic techniques.

This is a book for the person wishing to acquire a broad outline of nuclear fuel processing who is particularly interested in the fundamental chemistry involved. It is a pleasure to see an English book join the American ones on nuclear fuel processing, since substantial contributions to this facet of atomic energy have been made by workers on both sides of the Atlantic, and anyway, like most English books it is more reasonably priced than its American counterparts.

S. Hartland

Scale-up in Practice. Edited by R. Fleming. Chapman and Hall, London, and Reinhold, New York, 1958. 134 pp., 36s.

There are examples in industry of processes which have been successfully taken straight from the test-tube scale on the laboratory bench to full size industrial production of hundreds of pounds. However, these examples are the exception rather than the rule, and more often the basic process is developed by a chemist or a physicist at the bench and then the chemical engineer steps in and says he must build one or even two intermediate scale pilot plants to study certain parts of the process before he can design full scale constant flow apparatus. This may be because the chemist has done a batch process, while the production engineer wants to operate a continuous process, but it is also very likely to be because of the inherent difficulties of scale-up which arise from the changing surface to volume ratio, and the fact that different parts of the process such as surface and volume chemical reaction, heat transfer by natural and forced convection, and radiation and turbulence and mixing in fluids have different scale-up similarity numbers which cannot all be satisfied. Sometimes scale-up even means that none of them can be satisfied because the pressure for output on the large plant is too great. The commonest difficulty however arises from the fact that the chemist says he wants equal time for his reaction on the small and the large scale, while the physicist wants equal Reynolds number.

This book is a series of papers presented at a Symposium of the American Institute of Chemical Engineers covering what might be called a study of the need for pilot plants : a not very mathematical treatment of scale-up theory, and its limitations based mainly on Damkohler's treatment, but including also Danckwerts' study of residence time distribution which is extremely important wherever reaction time comes in. The main conclusion from this section is, however, that we do not know enough about microscopic mixing which can often be the factor even when macroscopic mixing is similar. The next chapter deals with the use of analogue computors for solving the differential equations of scale-up by simulating them with voltage measurement on an electric circuit. A final answer has not been reached as to where an analogue computor is best used and a digital computor, but both of them suffer from the disadvantage that they are only accurate to the accuracy with which one knows the physical properties of the system and can represent its geometrical shape in some simple way. However, a good case is made for the use of the analogue approach in spite of the comparatively high cost. The next paper on pitfalls in scale-up gives some very interesting examples of cases where scale-up did not go according to plan, particularly in the petrochemical industry and petroleum refining, due to impurities and accumulation of impurities, and even incomplete communication between different departments. The next paper emphasizes the need for applying technical economics as early as possible in a research and development process and suggests ways of doing this. The sixth paper is more concerned with business economics by which is meant the factors which help a company to decide whether to build facilities for a new product or not. These are concerned with the prediction of the size and ground of the market, and the probable share of the market, plant

location, transport and distribution costs. One might consider this chapter a little outside the ordinary use of the word scale-up, but it is nevertheless clearly an important subject and the more these predictions can be made accurately, the better served the industry of a country will be. The last chapter deals with organizing for scale-up which might also be called administrative arrangements to ensure that the chemical industries continue to innovate.

The book covers a wide field, but obviously none of the authors of the chapters have been able to do more than give a few practical examples, since it is the record of a one-day Symposium. Within this limitation, however, it is worth reading by those in administrative posts in the chemical industries who are concerned in any way with the introduction of new processes and by the more junior people who are trying to see that processes promising on the laboratory bench have a fair chance of growing to commercial status.

M. W. THRING

E. HALA, J. PICK, V. FRIED and O. VILIM: **Vapour–Liquid Equilibrium.** (2nd Ed.) 1954. Translated into English by G. Standart. Pergamon Press, London, 1958. xviii + 402 pp., 90s.

THIS is an English translation of a book previously published in 1954 in Prague, but in preparing the translation the authors have brought their extensive index of published vapour–liquid equilibrium data up to date. The book is addressed primarily to "workers in the chemical industry who have to deal with problems of distillation and rectification." It summarizes a very large volume of data and many publications that pertain to the thermodynamic properties of solutions of non-electrolytes and their implications for phase equilibrium between vapour and liquid, and is probably the first book of this kind. While other catalogues of phase equilibrium data have been available, notably the two books by J. C. CHU (1950 and 1956) and his co-workers and the collections of azeotropic data by LECAT (1918) and HORSLEY (1947), no previous publications of which this reviewer is aware have brought together in a single volume as much of the important information derived from thermodynamic principles and developments in experimental technique, in addition to extensive references to modern sources of experimental data. American readers will be especially grateful for the many references to data in foreign journals such as *Chemicke Listy* and the *Collection of Czechoslovak Chemical Communications*, including important contributions from the Institute of Chemical Technology in Prague, where the authors and the translator are staff members.

The first part of the book contains four chapters devoted to general thermodynamic principles, properties of ideal and real solutions of non-electrolytes and the methods that have been found useful for representing equilibrium data for real solutions. A second part is composed of five chapters on various aspects of laboratory technique used in the measurement of vapour–liquid equilibria, such as criteria of purity of pure substances; measurement of temperature, pressure, vapour pressure, and boiling point; and direct determination of equilibrium compositions. Finally, an alphabetical list of references to over a thousand original sources of experimental equilibrium data is included, the authors' literature searches having extended to articles published by February, 1957. Many of the references probably have not been known to readers heretofore.

The sections on general thermodynamic relations, including the Gibbs-Duhem equation and its various uses for representing activity coefficients in non-ideal solutions, are based on material that will be very familiar to most readers, but it is nevertheless convenient to have such material readily available. This is especially true when it is associated with a very good summary of the rapidly expanding information on empirical equations for excess free energies of non-ideal mixtures, such as the polynomial equations of WOHL, VAN LAAR, MARGULES, REDLICH-KISTER and others. The authors point out that most of the equations in popular use can be derived from Wohl's general expressions by various assumptions about empirical constants. Several ways for evaluating the constants from experimental data are explained in detail and many instructive numerical examples are included. However, no clear expression of the possible superiority of one or another form of the general expansions is made — probably because no such statement is possible at the present stage of empirical knowledge. The treatment of methods for computing missing compositions from experimental observations of temperature-composition or pressure-composition relations for binary mixtures is especially well done and clearly reveals the value of such computational methods when experimental measurement of compositions is difficult or impossible.

The discussion of activity coefficients of components in multicomponent, non-ideal mixtures is also based primarily on the formulation of WOHL, but, unfortunately, the authors have employed equations from WOHL's early paper (1946) rather than his later one (1953), in which an important improvement was made. In WOHL's early work the excess free energy for a ternary mixture was represented by a polynomial function of the mole fractions which typically contained the term $x_1x_2x_3(A_{21} + A_{13} + A_{32} - C)$, in addition to terms representing contributions from the constituent binary systems. The A-constants are derived from the binary data but the ternary constant, C, has to be found from experimental ternary data if it cannot be estimated. The difficulty with this term in the excess free energy expansion is that it is ambiguous, for the expression is not invariant when the choice of numerical subscripts is changed. Thus, if a numerical value of C derived from a particular set of data is employed to reconstruct the data on the same system, but the subscripts 1 and 2 are interchanged (and A_{21} is replaced by A_{12}, for example), the true values of excess free energy and activity

coefficient will not be recovered. The numerical value of C in the early WOHL equations therefore depends on the *order* in which the pure components are numbered. With care in the use of C-values no errors will be made, but because of the ambiguity numerical values of C can hardly have any physical significance. In his later paper WOHL replaced the offending term in his equations by the alternative expression $x_1 x_2 x_3 [\frac{1}{2}(A_{12} + A_{21} + A_{23} + A_{32} + A_{31} + A_{13}) - C^*]$, which is obviously invariant to all interchanges in the subscripts. Equations derived from this modified form are therefore less likely to be misused and values of C^* can be expected to have some basic significance of their own. The same criticism apparently applies to many multicomponent equations of other forms, such as the VAN LAAR or SCATCHARD types, and it seems regrettable that the present authors have not called attention to the difficulties.

Preparation of a complete summary of vapour–liquid equilibrium information of all kinds would be an enormous task and would lead to a book at least twice the size of the present one. Arbitrary choices of what to include and what to omit are therefore inevitable, but it will be a disappointment to many chemical engineers that the authors have not found it possible to refer more than briefly to the technically important literature on K-values and the effects of high pressure on equilibria near the critical region. The subject is disposed of in two or three pages and not a single diagram illustrating critical phenomena and showing data for hydrocarbon systems is included. One must admit that the illogical division of the subject of vapour–liquid equilibrium into one branch dealing with low-pressure distillation of organic chemicals (and activity coefficients) and another branch dealing with hydrocarbons and gases under pressure (and K-factors) has become traditional. But a book that summarizes the whole subject ought to bring out the unity of the two fields rather than this difference. As it is, the information on hydrocarbons is included in the list of references to data but thermodynamic explanation of many of the associated equilibrium phenomena is missing.

Despite these criticisms the book is an outstanding contribution to chemical engineering literature and will doubtless be referred to frequently in future studies. One hopes that a third edition of the work will appear in a few years and will be even larger.

R. L. PIGFORD

Announcements

Annual Meeting of Verfahrens—Ingenieure

The 1959 meeting of Verfahrens-Ingenieure will take place from 4 to 7 October 1959 at Essen.

Some twenty papers will be presented and industrial visits will be arranged.

Further information can be obtained from:

Die Geschäftsstelle der VDI-Fachgruppe Verfahrenstechnik, Frankfurt/M., Rheingau Allee 25, Tel. 770481.

Second European Symposium on Chemical Reaction Engineering

On 27, 28 and 29 April 1960 the Second European Symposium on Chemical Reaction Engineering will be held in the "Koninklijk Instituut voor de Tropen" at Amsterdam, Holland. It is being organized by the two Dutch Societies "Koninklijke Nederlandse Chemische Vereniging" and "Koninklijk Instituut van Ingenieurs" under the auspices of the European Federation for Chemical Engineering.

Secretariat: P. J. Hoftyzer, A.M.I.Chem.E., Central Laboratory, Staatsmijnen in Limburg, Geleen (L), Netherlands.